30
12-8-82

I-6794

(1)

S-CUBED

FORMERLY

Systems, Science and Software

SSS-R-82-5516

DOE/ID/12067-13

INVERSION MODELING OF MULTIPLE GEOPHYSICAL DATA SETS FOR GEOTHERMAL EXPLORATION: APPLICATION TO ROOSEVELT HOT SPRINGS AREA

J. M. Savino

W. L. Rodi

J. F. Masso

MASTER

FINAL REPORT

DO NOT MICROFILM COVER

April 1982

Prepared for:

DEPARTMENT OF ENERGY
Idaho Operations Office
Under Contract No. DE-FC07-79ID12067

P. O. Box 1620
La Jolla, California
92038
(714) 453-0060

DISCLAIMER

DOE/ID/12067--13

DE83 003481

S-CUBED

FORMERLY

Systems, Science and Software

SSS-R-82-5516

DOE/ID/12067-13

INVERSION MODELING OF MULTIPLE GEOPHYSICAL DATA SETS FOR GEOTHERMAL EXPLORATION: APPLICATION TO ROOSEVELT HOT SPRINGS AREA

J. M. Savino

W. L. Rodi

J. F. Masso

FINAL REPORT

April 1982

Prepared for:

DEPARTMENT OF ENERGY
Idaho Operations Office
Under Contract No. DE-FC07-79ID12067

P. O. Box 1620
La Jolla, California
92038
(714)453-0060

TABLE OF CONTENTS

LIST OF ILLUSTRATIONS

LIST OF ILLUSTRATIONS (concluded)

LIST OF TABLES

I. INTRODUCTION

A geothermal area is often characterized by the anomalous behavior of several geophysical parameters at depth; such as density, seismic velocity, electrical conductivity and porosity. Thus, the goal of an ideal geothermal exploration method is to determine all of the relevant subsurface parameters based on an integrated interpretation of several geophysical data sets measured at the earth's surface. As a step toward this goal, several staff members at Systems, Science and Software (S^3) have been involved during the past several years in the development of a joint inversion modeling program that incorporates multiple geophysical data sets in order to produce a unified interpretation of the three-dimensional subsurface structure. Such a combined interpretation is an extremely cost-effective approach to geothermal exploration.

Our earliest joint inversion projects were funded by a combination of external (i.e., government and commercial) and internal (S^3) sources. The initial step taken was an S^3 funded internal research effort wherein Jordan (1975) formulated the generalized linear inverse problem and defined the inversion algorithms necessary for future modeling projects. Subsequently, under three externally funded projects we further developed the inversion modeling procedure, including the requisite forward modeling algorithms, and applied it to joint interpretations of teleseismic travel-time and Bouguer gravity data from three areas in the western United States: the Imperial Valley, California, in a Department of Energy (DOE) sponsored study (Savino, et al., 1977); Yellowstone National Park, in a study supported by the University of Utah (Evoy, 1978); and the Columbia Flood Basalts in eastern Washington, under a project supported by the Washington Public Power Supply System (WPPSS), reported by Savino, et al., 1979a and

1979b. As evidenced from the final inversion models obtained for each of these three study areas, both data sets, when jointly interpreted, were observed to be good indicators of deep seated structural features.

These early applications of the joint inversion modeling technique were for delineation of relatively large scale subsurface features. In each case, this was dictated by the inherent resolution of the particular data sets used rather than the modeling procedure iteself. In order to increase the modeling resolution, we next directed our efforts to developing the capability (i.e., forward modeling algorithms) for incorporating travel-time data from local seismic events in the joint inversion procedure. This effort was simultaneously performed under this DOE sponsored study and a project funded by WPPSS. Our first results from a joint inversion of local seismic travel-times (i.e., first arrival P waves) and Bouguer gravity data were obtained for the Columbia Flood Basalts region in eastern Washington (Rodi, et al., 1980a and 1980b).

In the following section of this report, Section II, we describe the theoretical basis for modeling the arrival times of local earthquake P waves at a network of seismic stations. Of particular importance is a description of a technique for separating the dependence of network arrival times on velocity structure from the dependence on the earthquake location parameters. Commented computer listings of the forward modeling algorithms developed in part under DOE support are given in Appendix A.

In Section III we describe the local earthquake arrival time and Bouguer gravity data sets that we acquired for the Roosevelt and Leach Hot Springs areas. As noted in this section, the seismic data from Leach Hot Springs, Nevada were found to be inadequate (i.e., in terms of numbers of events, stations and ray paths) for inversion modeling. Thus, the emphasis in Section III is on the editing and processing of the Roosevelt Hot Springs data sets prior to inversion.

Finally, in Section IV we describe the inversion model for the Roosevelt Hot Springs area obtained from a joint inversion of seismic and gravity data. The more robust features of the final model are discussed in light of the known geology and geophysics of the area and are compared to results obtained from related studies (e.g., Robinson and Iyer, 1981).

II. THEORETICAL DEVELOPMENT FOR LOCAL EARTHQUAKE ARRIVAL-TIME INVERSION

2.1 INTRODUCTION

In this section we describe the theoretical basis for the modeling of the arrival times of local earthquake P waves at a network of seismic stations. Using geometrical ray theory we establish the relationship among the P wave arrival time at a station, the origin time and location of the earthquake, and the P velocity distribution within the earth. This relationship defines the arrival time "data functional." The linearization of this functional, required for the application of linear inversion, is then described and the relevant formulae for a one-dimensional initial model with constant gradient layers are presented. Finally, we describe the application of linear inverse theory to the inversion of local earthquake arrival times. The joint inversion of arrival time and gravity data is described in a DOE report by Savino, et al. (1977).

2.2 ARRIVAL-TIME DATA FUNCTIONALS

According to geometrical ray theory, a seismic wave travels along a path — the geometrical raypath — which minimizes the source-receiver travel time. The travel time along a raypath is defined as the integral of the medium slowness (reciprocal velocity) along the path. This is the high frequency approximation in which the raypath is taken to have infinitesimal width. Geometrical ray theory thus predicts that the arrival time t^a of a seismic wave traveling from an earthquake to a station is the following functional of the medium slowness u and earthquake origin time t^0:

$$t^a = t^0 + \int_\Gamma ds\ u \qquad (1)$$

where s is distance along the raypath, and Γ symbolizes integration along the raypath trajectory (see Figure 1).

We gain mathematical precision later if we parameterize the raypath in terms of a nondimensional dummy variable η defined on the unit interval. Denoting the raypath as $\vec{r}(\eta)$, $0 \leq \eta \leq 1$, we can rewrite Equation (1) as

$$t^a = t^0 + \int_0^1 d\eta \left|\frac{d\vec{r}}{d\eta}\right| u(\vec{r}(\eta)) \quad . \tag{2}$$

We have used

$$ds = d\eta \left|\frac{d\vec{r}}{d\eta}\right| \quad . \tag{3}$$

The earthquake location (hypocenter) is $\vec{r}(0)$ and the station location is $\vec{r}(1)$. Therefore, Equation (2) implicitly defines the dependence of arrival time on the endpoints of the raypath.

The geometrical ray $\vec{r}$ obeys the differential equation

$$\frac{d}{d\eta}[u\vec{\ell}] = \left|\frac{d\vec{r}}{d\eta}\right| \nabla u \quad . \tag{4}$$

Here $\vec{\ell}$ is the unit vector tangent to the ray:

$$\vec{\ell} = \frac{d\vec{r}}{d\eta} / \left|\frac{d\vec{r}}{d\eta}\right| \quad . \tag{5}$$

Equation (4) is equivalent to

$$\int_0^1 d\eta \left|\frac{d\vec{r}}{d\eta}\right| u(\vec{r}) = \text{minimum w.r.t. } \vec{r}(\eta) \quad ,$$

given that the endpoints of the ray are fixed. This is Fermat's principle.

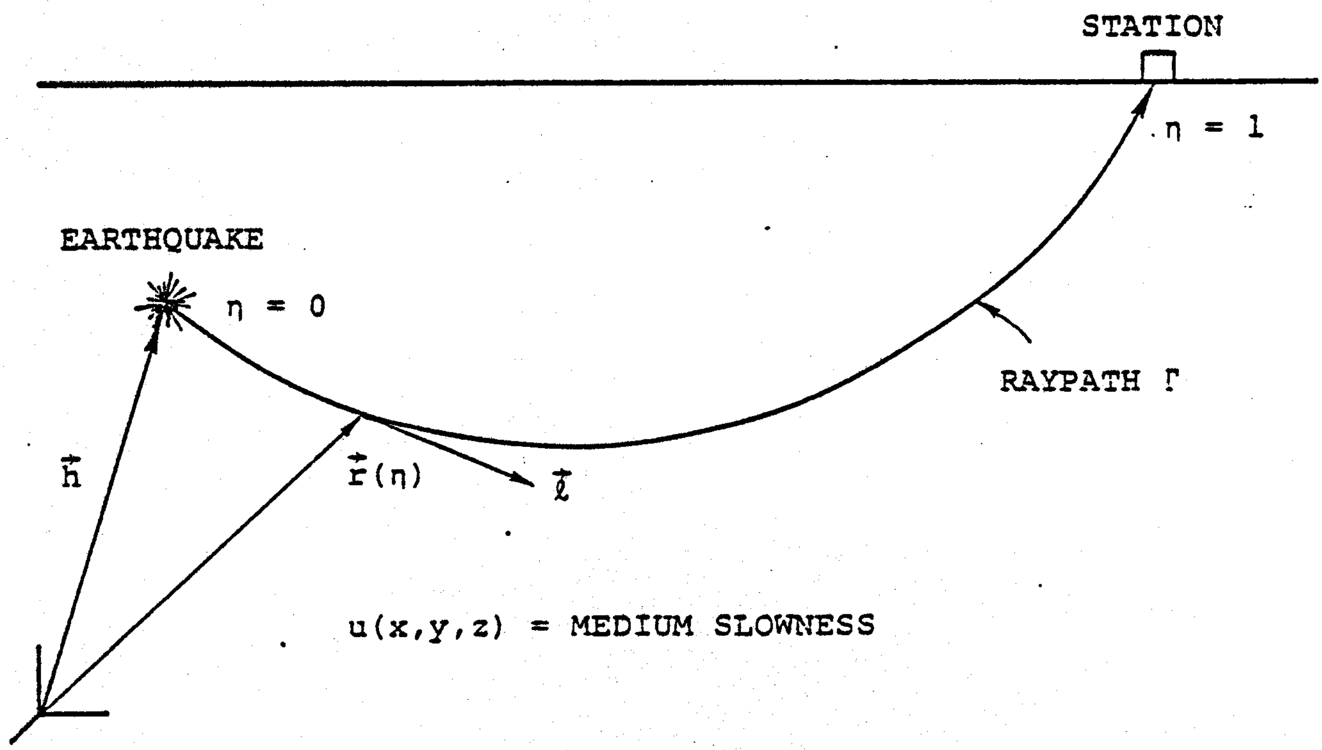

Figure 1. Raypath notation.

2.3 LINEARIZATION OF DATA FUNCTIONALS

The arrival-time functional in Equation (1) is nonlinear with respect to the slowness distribution u, by virtue of the dependence of the raypath on u through Equation (4). It must be expanded to first order about an initial slowness model u_0 for linear inverse theory to be applicable.

We shall consider u and $r(\eta)$ to be perturbed from initial values u_0 and $r_0(\eta)$:

$$u = u_0 + \delta u$$

$$\vec{r} = \vec{r}_0 + \delta\vec{r} \quad . \tag{6}$$

It is assumed that $\vec{r}_0$ is the least time geometrical raypath through u_0; i.e., u_0 and $\vec{r}_0$ obey Equation (4).

To first order in δu and $\delta\vec{r}$, the travel time along the perturbed ray is given by

$$\int_{\Gamma} ds\, u = \int_{\Gamma_0} ds\, u_0 + u_0(\vec{r}_0(1))\ \vec{\ell}_0(1) \cdot \delta\vec{r}(1) - u_0(\vec{r}_0(0))\ \vec{\ell}_0(0) \cdot \delta\vec{r}(0) \quad . \tag{7}$$

where Γ_0 symbolizes the unperturbed raypath, $\vec{r}_0(\eta)$. The first term is the integral of the slowness along the unperturbed raypath $\vec{r}_0$. The second and third terms, respectively, represent the effects of perturbing the endpoints of the ray.

Let $\vec{h}$ denote the hypocenter and $\vec{p}$ the slowness vector of the ray:

$$\vec{h} = \vec{r}(0)$$

$$\vec{p} = u(\vec{r}(0))\ \vec{\ell}(0) \quad . \tag{8}$$

The direction of the slowness vector is the ray takeoff direction and its magnitude is the medium slowness at the hypocenter. If we ignore perturbations to the station location (i.e., $\delta\vec{r}(1) = 0$), then Equations (1), (7) and (8) imply (to first order)

$$t^a = \int_{\Gamma_0} ds\ u - \vec{p}_0 \cdot \delta\vec{h} + t^0 \qquad (9)$$

where $\vec{p}_0$ is the slowness vector for the unperturbed raypath and $\delta\vec{h}$ denotes the perturbation of $\vec{h}$ from the initial hypocenter $\vec{h}_0 = \vec{r}_0(0)$.

From Equation (9) we see that the Frechet kernel (continuous partial derivative of a functional) of arrival time with respect to slowness is a singular function concentrated along the unperturbed raypath. Therefore, the partial derivatives with respect to the velocities of homogeneous blocks in the earth are found by tracing rays through the initial model and calculating the length of the raypath segment intersecting each block. The partial derivatives of the arrival time with respect to the hypocenter components are the components of the unperturbed slowness vector. Of course, t^a is a linear function of the origin time t^0.

Letting t^a be an observed arrival time and t_0^0 be an initial estimate of the earthquake origin time, we define an observed travel-time residual as

$$\delta t = t^a - t_0^0 - \int_{\Gamma_0} ds\ u_0 \quad . \qquad (10)$$

Equations (6), (9) and (10) imply

$$\delta t = \int_{\Gamma_0} ds\ \delta u - \vec{p}_0 \cdot \delta\vec{h} + \delta t^0 + e \qquad (11)$$

where e is the observational error and δt^0 is the error in the initial origin time ($\delta t^0 = t^0 - t_0^0$).

2.4 RAY TRACING IN GRADIENT LAYER MODELS

We restrict the initial velocity model to be a one-dimensional model with depth dependent velocity but no lateral variations. We lack sufficient prior knowledge of the lateral velocity variations in our study region to justify the development and production costs of two- or three-dimensional ray tracing.

Our ray tracing algorithm is designed for a rather general one-dimensional velocity model. The velocity function is assumed continuous with depth and consists of L segments or layers, each having a constant velocity gradient with depth. The gradient may be negative, zero, or positive. Thus, the model is specified by L+1 values of velocity and depth, v_ℓ, z_ℓ, $\ell = 1..L+1$, where $z_1 = 0$ (the surface) and z_{L+1} is the deepest point in the model (see Figure 2). The model is taken to be a "flat earth" model in which the earth's curvature is ignored. This is adequate for the source-receiver distances of concern (< 500 km).

The geometrical raypath through a medium of constant velocity gradient describes an arc of a circle. Let us write the velocity-depth function as

$$v = v_a + g(z - z_a) \quad . \tag{12}$$

This makes the velocity at a depth z_a equal to v_a and makes $dv/dz = g$. We will consider the raypath for the case $g \neq 0$. With little loss of generality, we assume the ray is confined to the plane $y = 0$. Let (x_a, z_a) be its starting point and θ_a

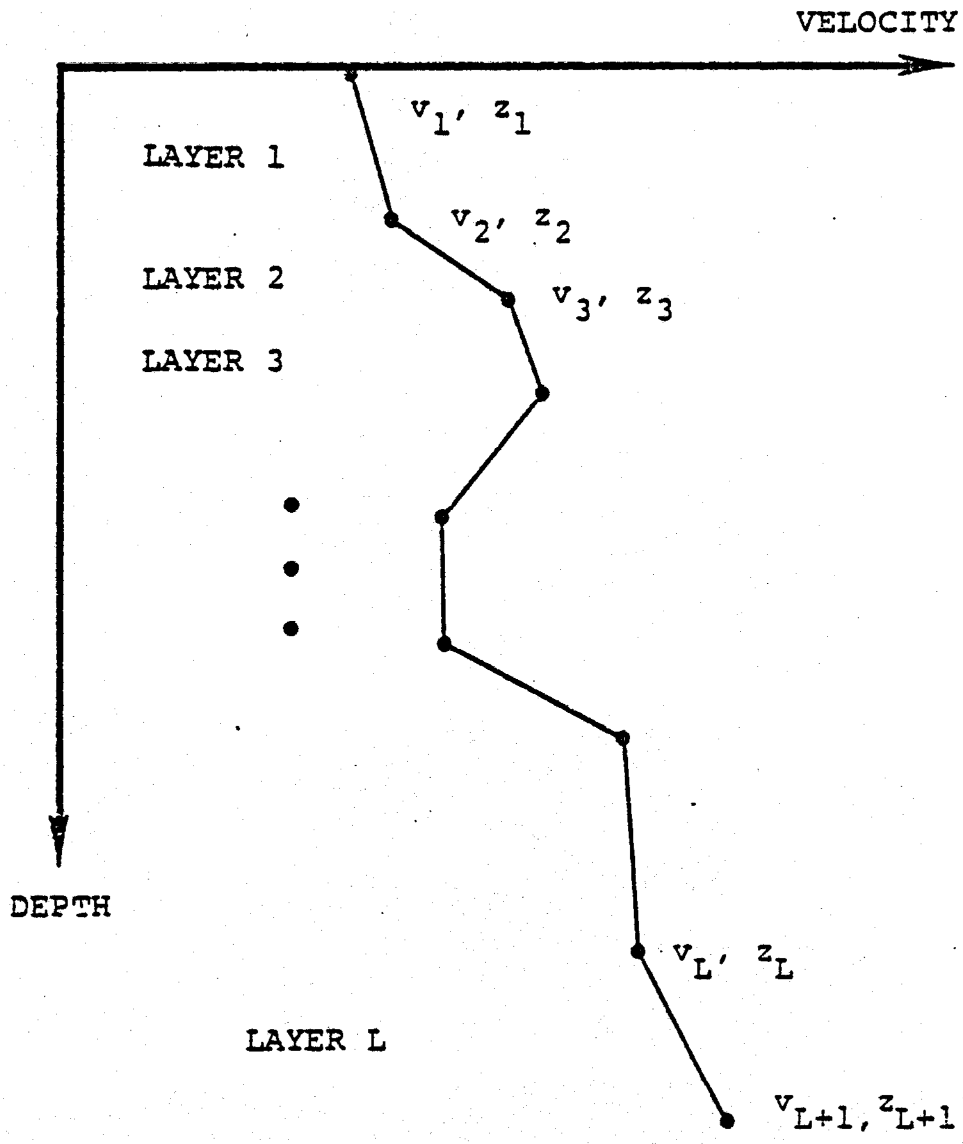

Figure 2. Schematic of initial velocity model.

its starting direction, measured as the angle from vertically down. Then the trajectory of the ray (x,z) is given by

$$p = \frac{\sin \theta_a}{v_a} = \frac{\sin \theta}{v} \qquad (13)$$

$$x = x_a - (pg)^{-1} (\cos \theta - \cos \theta_a)$$

$$z = z_a + (pg)^{-1} (\sin \theta - \sin \theta_a) \quad . \qquad (14)$$

Here v and θ are the velocity and tangent angle at any point on the ray. The constant p is the ray parameter and is the x component of the slowness vector used earlier. We note that Equations (13) and (14) are a solution of Equation (4). This can be verified after making the substitution $\eta = \theta \text{ sgn } (g)$.

Figure 3 illustrates the geometry of the raypath implied by Equation (14). The raypath is concave upward for $g > 0$ and concave downward for $g < 0$. (For $g = 0$, the path degenerates to a straight line.) The radius of the circular path is $(p|g|)^{-1}$. For the case $g > 0$, the path "bottoms" or turns at the depth where $v = p^{-1}$.

From Equations (12) through (14) one can derive the following formulae for the horizontal distance traveled (Δx), travel time (Δt), and length (Δs) of a ray traveling from the depth z_a to a depth z_b:

$$\Delta x = (pg)^{-1} (\cos \theta_a - \cos \theta_b)$$

$$\Delta t = g^{-1} \log \left[\frac{v_b \ (1 + \cos \theta_a)}{v_a \ (1 + \cos \theta_b)} \right]$$

$$\Delta s = (pg)^{-1} (\theta_b - \theta_a) \qquad (15)$$

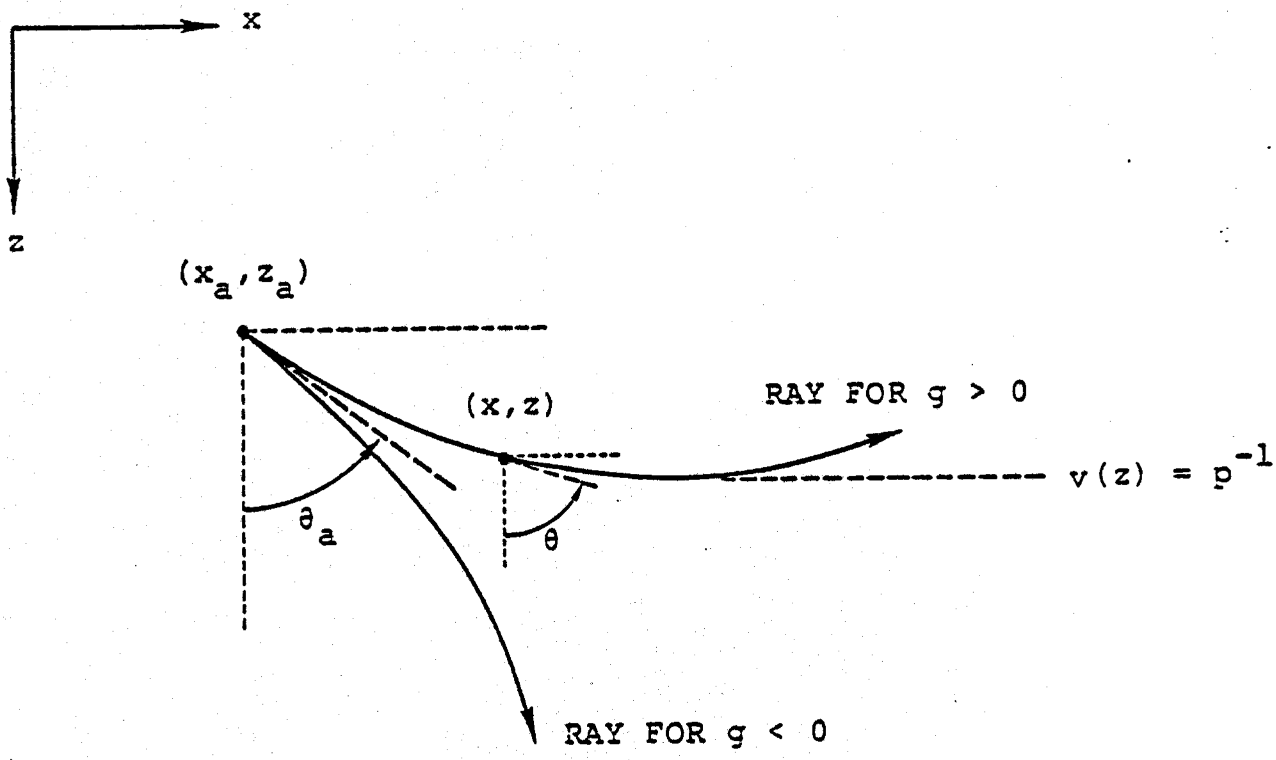

Figure 3. Circular raypaths through a medium of constant velocity gradient g.

where θ_b is determined from Equation (13) as

$$\theta_b = \sin^{-1} (p\ v_b) \quad . \tag{16}$$

The expressions for the case $g = 0$, in which case the raypath is a straight line, are very simple and not shown.

One can apply Equations (14) and (15) layer by layer in a multilayered gradient model to obtain the entire ray trajectory, horizontal distance, and total travel time from an event hypocenter at depth to a station at the surface. One can thus evaluate for the initial velocity model the predicted travel time for each event-station path and, by determining the length of the raypath segment that traverses each block in the inversion model grid, the partial derivatives of the travel-time with respect to the block slowness perturbations.

The ray tracing equations we have developed assume that the takeoff angle (θ) at the hypocenter is known. Equivalently, one may specify the ray parameter p and the sense of takeoff: diving ($\theta < 90°$) or "emerging" ($\theta > 90°$). However, it is required that the ray be traced between fixed endpoints, representing the station location and an initial estimate of the event hypocenter. Therefore, p must be determined indirectly.

To determine the ray parameter of a given path, we first generate tables of distance (X) and travel time (T) versus ray parameter appropriate to the event focal depth. Tables are generated for both diving and emerging rays: $X_d(p)$, $T_d(p)$ and $X_e(p)$, $T_e(p)$. They are sampled at closely spaced values of p spanning the range of possible values determined from the velocities in the ray tracing model. The tables are used to estimate the ray parameters predicting the known event-station distance. The estimate or estimates are then refined by an iterative root-finding procedure. Either a single emerging ray or a possible multiplicity of diving rays arrive at a given distance. The multiplicity results from triplications caused by large velocity gradients in the model. In this case, we choose the first-arrival ray parameter; i.e., the ray with the earliest travel time.

2.5 LINEAR INVERSE FORMULATION

Given travel-time residuals (δt) from several stations and events, and a three-dimensional block model representation of the slowness perturbation $\delta u(x,y,z)$, we can express Equation (11) as a discrete linear inverse problem of the form (E denotes expectation and Var denotes variance)

$$E[d] = Am + Bn$$

$$\mathrm{Var}[d] = \Sigma \qquad (17)$$

where d is the data vector containing the observed travel-time residuals, m a model parameter vector containing the block values of δu, and n a "nuisance" parameter vector containing the hypocenter mislocations ($\delta \vec{h}$) and origin time errors (δt^0) of the events. The Matrix Σ is the covariance matrix of the observational errors (e), which are assumed to have zero mean.

The separation of the unknown parameters into two vectors is done to distinguish the parameters of primary interest (slowness perturbations) from those of ancillary interest (event location parameters). The Matrices A and B, respectively, contain the partial derivatives of the travel-time residuals with respect to the block slownesses and event parameters. From Equation (11) we see that the derivative of a residual with respect to the slowness of a block is the length of the raypath segment intersecting the block. A given raypath intersects very few of the blocks so most elements in A are zero. Also from Equation (11), we see that B contains ones, zeroes and the slowness vectors from the various initial raypaths. A given residual depends on the parameters of only one event, so with a proper ordering of the data in d, B has a block diagonal structure.

We should mention that in setting up the problem in this form, there is no requirement that the data set be complete; i.e., that a residual exist for every event-station pair. Nonetheless, the system represented by Equation (17) is quite large in the present study. After data culling the data set consists of 601 residuals observed from 93 events. The model grid we designed (Section IV) contains 1050 blocks. Therefore, the system contains 601 equations and 1422 unknowns (1050 in m and 372 in n). The 372 event locations parameters, however, are not of interest.

Instead of applying generalized linear inverse techniques directly to a system this large, we first employed a technique that reduces the system to a simpler and smaller one; i.e., a "denuisancing" technique, which eliminates the nuisance vector n from the system by constructing an equivalent inverse problem involving only m. Before describing this technique and the inversion algorithm itself, let us define the optimality criterion we use to obtain a solution to Equation (17).

We define a solution to Equation (17) as estimates $\tilde{m}$ and $\tilde{n}$ which satisfy the damped least squares criterion

$$(d-A\tilde{m}-B\tilde{n})^T \Sigma^{-1} (d-A\tilde{m}-B\tilde{n}) + \theta\, \tilde{m}^T W^{-1} \tilde{m} + \phi\, \tilde{n}^T Z^{-1} \tilde{n}$$

$$\text{is minimum} \qquad (18)$$

where θ and ϕ are scalar trade-off parameters and W and Z are specified parameter weighting matrices, both assumed positive definite. This criterion is equivalent to the optimality criteria defined by Backus and Gilbert (1970) and Jordan (1973), but we have expressed it in terms of two parameter vectors instead of the usual one.

The first term in Equation (18) is a measure of the "misfit" between the observed data, d, and the data predicted by the solution $(\tilde{m},\tilde{n})$. The second and third terms are norms of $\tilde{m}$ and $\tilde{n}$, respectively. These terms stabilize the solution by damping components of $\tilde{m}$ and $\tilde{n}$ that do not contribute much to fitting the data, but which may cause the solution to become physically implausible.

In the travel-time problem, it is useful to interpret the product $\phi^{-1}Z$ as a prior variance assigned to n:

$$\mathrm{Var}[n] = \phi^{-1}Z \quad . \tag{19}$$

Thus, ϕ and Z assign an uncertainty to the initial origin times and error ellipsoids to the initial hypocenters. Making the prior variance sufficiently large allows $\tilde{n}$ to adjust freely to fit the data.

In selecting θ and W for the damping of $\tilde{m}$, the prior variance interpretation is not very useful. Instead, we set up the model norm to be a measure of the roughness of the velocity structure. That is, we construct W^{-1} as a non-diagonal matrix such that the model norm is a discrete approximation to the following integral:

$$\tilde{m}^T W^{-1} \tilde{m} \doteq \int dx \int dy \int dz \; [(\partial_x \delta\tilde{v})^2 + (\partial_y \delta\tilde{v})^2 + \lambda^{-2}(\delta\tilde{v})^2] \, . \tag{20}$$

where $\delta\tilde{v}$ is the velocity perturbation ($\delta\tilde{v} = -u_0^2\,\delta\tilde{u}$). With this definition, $\tilde{m}^T W^{-1}\tilde{m}$ is sensitive to lateral gradients in

$\delta\tilde{v}$ of a scale smaller than λ, which we set to a large value (200 km). In this way, θ allows us to control a trade-off between the smoothness of the velocity model and the fit it provides to the data. The best value of θ cannot be determined in advance. Rather, it must be selected on the basis of examining models and their predicted data computed with several values of θ.

In the following developments, we will use some abbreviations to simplify expressions. We will use a circumflex above symbols to denote that quantities have been normalized by the factor $\Sigma^{-\frac{1}{2}}$. Thus,

$$\hat{d} = \Sigma^{-\frac{1}{2}} d$$

$$\hat{A} = \Sigma^{-\frac{1}{2}} A \quad .$$

$$\hat{B} = \Sigma^{-\frac{1}{2}} B \quad . \tag{21}$$

We will also apply this notation to quantities defined later, without further explanation.

2.6 DENUISANCING

An example of denuisancing is the zero-meaning of teleseismic travel-time residuals and their partial derivatives, derived by Aki, et al. (1977) as a way to eliminate the effects of baseline errors from the inverse problem. This basic denuisancing technique has been extended and generalized by Savino, et al. (1977), Pavlis and Booker (1980), Spencer and Gubbins (1980) and Minster, et al. (1981). Here we summarize the algorithm of Minster, et al. (1981) in the context of solving Equations (17) and (18).

To begin, we note that Equation (18) is equivalent to the coupled normal equations:

$$(\hat{A}^T\hat{A} + \theta W^{-1})\tilde{m} + \hat{A}^T\hat{B}\tilde{n} = \hat{A}^T\hat{d} \tag{22a}$$

$$\hat{B}^T\hat{A}\tilde{m} + (\hat{B}^T\hat{B} + \phi Z^{-1})\tilde{n} = \hat{B}^T\hat{d} \quad . \tag{22b}$$

Solving Equation (22a) for $\tilde{n}$ we obtain

$$\tilde{n} = \hat{B}^- (\hat{d} - \hat{A}\tilde{m}) \tag{23}$$

where

$$\hat{B}^- = (\hat{B}^T\hat{B} + \phi Z^{-1})^{-1} \hat{B}^T \quad . \tag{24}$$

The matrix $\hat{B}^-$ is a damped generalized inverse of $\hat{B}$. Now we define the symmetric matrix Q_B by

$$Q_B = I - \hat{B}\hat{B}^- \quad . \tag{25}$$

Then substituting $\tilde{n}$ in Equation (23) into Equation (22a) gives

$$(\hat{A}^T Q_B \hat{A} + \theta W^{-1})\tilde{m} = \hat{A}^T Q_B \hat{d} \quad . \tag{26}$$

We can simplify this with the following substitutions:

$$\hat{A}_\nu = Q_B^{\frac{1}{2}} \hat{A} \equiv \Sigma^{-\frac{1}{2}} A_\nu \tag{27a}$$

$$\hat{d}_\nu = Q_B^{\frac{1}{2}} \hat{d} \equiv \Sigma^{-\frac{1}{2}} d_\nu \quad . \tag{27b}$$

Then Equation (26) becomes

$$(A_\nu^T \Sigma^{-1} A_\nu + \theta W^{-1})\tilde{m} = A_\nu^T \Sigma^{-1} d_\nu \quad . \tag{28}$$

Equation (28) is the normal equation that results from the minimization condition

$$(d_\nu - A_\nu \tilde{m})^T \; \Sigma^{-1} \; (d_\nu - A_\nu \tilde{m}) \; + \; \theta \tilde{m}^T W^{-1} \tilde{m} \text{ is minimum} . \qquad (29)$$

Comparing to Equations (17) and (18), we see that $\tilde{m}$ is a solution to an equivalent inverse problem that does not involve the nuisance vector $\tilde{n}$; namely,

$$E[d_\nu] = A_\nu m$$

$$\mathrm{Var}[d_\nu] = \Sigma \quad . \qquad (30)$$

Equations (29) and (30) are a standard linear inverse problem and we discuss its solution in Section 2.7.

We call the operator $Q_B^{\frac{1}{2}}$ in Equation (27) a denuisancing operator, and d_ν and A_ν denuisanced data and partial derivatives, respectively. It is convenient for computation to evaluate $Q_B^{\frac{1}{2}}$, and the damped generalized inverse $\hat{B}^-$, in terms of the singular value decomposition (SVD) of $\hat{B}$ (Lanczos, 1961; Wiggins, 1972). Let

$$\hat{B} Z^{\frac{1}{2}} = S \Gamma T^T \qquad (31)$$

where the columns of S and T are orthonormal eigenvectors and Γ is a diagonal matrix of positive eigenvalues:

$$S^T S = T^T T = I$$

$$\Gamma = \mathrm{diag}\,(\gamma_1, \gamma_2, \ldots) > 0 \; . \qquad (32)$$

Then we have

$$\hat{B}^{-} = Z^{\frac{1}{2}} T\Gamma(\Gamma^2 + \phi I)^{-1} S^T$$

$$Q_B = I - S\Gamma^2(\Gamma^2 + \phi I)^{-1} S^T$$

$$Q_B^{\frac{1}{2}} = I - S[I - \phi^{\frac{1}{2}} (\Gamma^2 + \phi I)^{-\frac{1}{2}}] S^T \qquad (33)$$

When $\phi << \gamma_k^2$, which is the case for the value of ϕ we selected for the Roosevelt Hot Springs inversion, $Q_B^{\frac{1}{2}}$ approximates an orthogonal projection operator:

$$Q_B^{\frac{1}{2}} \underset{\phi=0}{\simeq} I - SS^T \quad . \qquad (34)$$

Denuisancing then removes the projections of d and A onto the range space of B.

In the local travel-time residual problem, B has a block diagonal structure. The denuisancing operator $Q_B^{\frac{1}{2}}$ then reduces to a block diagonal matrix, and the denuisancing algorithm becomes particularly efficient.

2.7 LINEAR INVERSE ALGORITHM

We have reduced the teleseismic residual problem to a standard linear inverse problem of the form:

$$E[\hat{d}] = \hat{A}\, m$$

$$\mathrm{Var}[\hat{d}] = I \qquad (35)$$

where m represents the slowness perturbation δu and $\hat{d}$ represents the (denuisanced) travel-time residuals. A solution $\tilde{m}$ to Equation (35) has been defined by

$$(\hat{d} - \hat{A}\tilde{m})^T (\hat{d} - \hat{A}m) + \theta\, \tilde{m}^T W^{-1} \tilde{m} = \text{minimum} \quad . \tag{36}$$

This defines $\tilde{m}$ as a linear estimator of the form

$$\tilde{m} = \hat{A}^{-} \hat{d} \tag{37}$$

where $\hat{A}^{-}$ is the damped generalized inverse of $\hat{A}$.

The algorithm we use to obtain $\hat{A}^{-}$ is very similar to the algorithm described in Section 2.6 for obtaining $\hat{B}^{-}$. In this case, we factor the weighting matrix as

$$W^{-1} = H^T H \tag{38}$$

where H is a square nonsingular matrix. (We actually specify H instead of W^{-1}.) Then we obtain the SVD

$$\hat{A}\, H^{-1} = U \Lambda V^T \quad , \tag{39}$$

where

$$U^T U = V^T V = I$$

$$\Lambda = \text{diag}\,(\lambda_1, \lambda_2, \ldots, \lambda_K) > 0 \quad . \tag{40}$$

Even after denuisancing, $\hat{A}$ is a very large matrix (601 by 1050) so the SVD requires a core-to-disk computer algorithm. The inverse $\hat{A}^{-}$ is then obtained as

$$\hat{A}^{-} = H^{-1}\, V \Lambda (\Lambda^2 + \theta I)^{-1}\, U^T \quad . \tag{41}$$

Since Λ is diagonal this expression is readily evaluated for varying θ.

Equations (35) and (37) imply

$$E[\tilde{m}] = \mathscr{R} m$$

$$\mathrm{Var}[\tilde{m}] = \mathscr{V} \tag{42}$$

where

$$\mathscr{R} = \hat{A}^{-} \hat{A} = H^{-1} V\Lambda^{2} (\Lambda^{2} + \theta I)^{-1} V^{T} H$$

$$\mathscr{V} = \hat{A}^{-} \hat{A}^{-T} = H^{-1} V\Lambda^{2} (\Lambda^{2} + \theta I)^{-2} V^{T} (H^{-1})^{T} \tag{43}$$

$\mathscr{R}$ is the resolution matrix and $\mathscr{V}$ the covariance matrix of the model $\tilde{m}$. These matrices provide a means for assessing the uniqueness of $\tilde{m}$. Equation (43) states that $\tilde{m}$ is an estimate of m "filtered" by $\mathscr{R}$, and not of m itself. With $\tilde{m}$ as a three-dimensional block model of the earth, each component $\tilde{m}_i$ estimates a spatial average of the true structure; the i'th row of $\mathscr{R}$ is a discrete three-dimensional function which shows the spatial extent of the averaging or filtering. In addition to the filtering, $\tilde{m}$ is also contaminated by a random error whose variance is $\mathscr{V}$.

The quantities $\mathscr{R}$ and $\mathscr{V}$ aid in selecting a "best" single model among the family of models $\tilde{m}(\theta)$ defined over $0 < \theta < \infty$. Backus and Gilbert (1970) showed that as θ increases $(I-\mathscr{R})$ increases (resolution degrades) and $\mathscr{V}$ decreases, thus giving a trade-off between resolution and variance. One should attempt to choose θ such that $(I-\mathscr{R})$ and $\mathscr{V}$ are both acceptably small.

The parameter θ also controls a trade-off between model roughness and data misfit, as one can see from the minimization criterion, Equation (36). The quantity ε, given by

$$\varepsilon^2 = \frac{1}{N} (d - A\,\tilde{m})^T \Sigma^{-1} (d - A\,\tilde{m}) \quad , \tag{44}$$

where N is the number of data, is the r.m.s. misfit between the observed (denuisanced) data and the data predicted by $\tilde{m}$, A $\tilde{m}$. The squared model norm, $\tilde{m}^T W^{-1} \tilde{m}$, measures the total "roughness" of the model. As a function of increasing θ, ε increases and the model norm decreases. While these scalar quantities are useful, it is desirable to visually examine the smoothness of the entire model and to compare the full observed and predicted data sets, in selecting and assessing a final model.

It is convenient to convert the trade-off parameter to a dimensionless quantity which is the effective number of degrees of freedom (NDF) in the model $\tilde{m}(\theta)$. NDF is defined as

$$\text{NDF} = \sum_{k=1}^{K} \lambda_k^2 / (\lambda_k^2 + \theta) \tag{45}$$

and equals the rank of $\mathscr{R}$.

III. SEISMIC AND GRAVITY DATA

3.1 LOCAL SEISMIC DATA-ROOSEVELT HOT SPRINGS

The local seismic data set for the Roosevelt Hot Springs (RHS) area was obtained from Dr. Robert Smith at the University of Utah. This data set consisted of 870 arrival time estimates of P-waves recorded at a network of up to 20 seismographs from 163 events. Figure 4 shows the locations of the seismograph stations and Figure 5 the seismic events recorded during surveys conducted in 1974 and 1975 by Olson and Smith (1976). In Table 1 we list the locations of the 20 seismograph stations depicted in Figure 4. The last column in this table gives estimates of the average velocity of intervening material beneath the station and the common datum plane, which in this study was taken at 2 km above sea level. These estimates are based on station elevation-correction velocities determined by Robinson and Iyer (1981) for a set of stations located throughout the region of interest in this study. Hypocentral information for the 163 events plotted in Figure 5 is given in Table 2.

Some general comments based on Figures 4 and 5 are the following:

1. The actual number of seismograph stations operating during any one time period, and thus for a particular event, is less than 20.

2. The distribution of stations is quite inhomogeneous with a concentration of sites in the Cove Fort area.

3. The spatial distribution of seismic events is also inhomogeneous with concentrations of activity in a few areas of the study region.

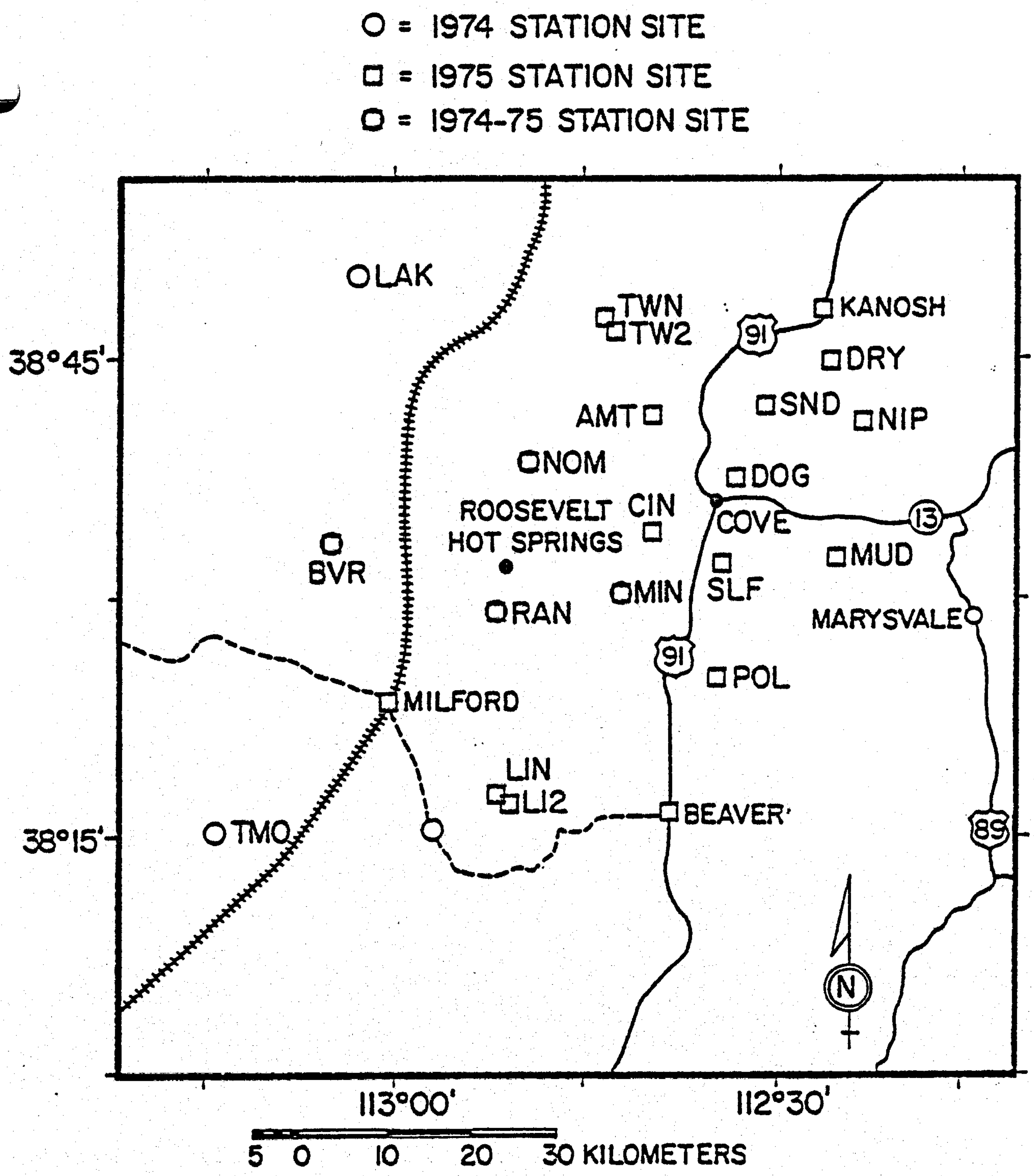

Figure 4. Station locations for 1974 through 1975 surveys in the Roosevelt Hot Springs area.

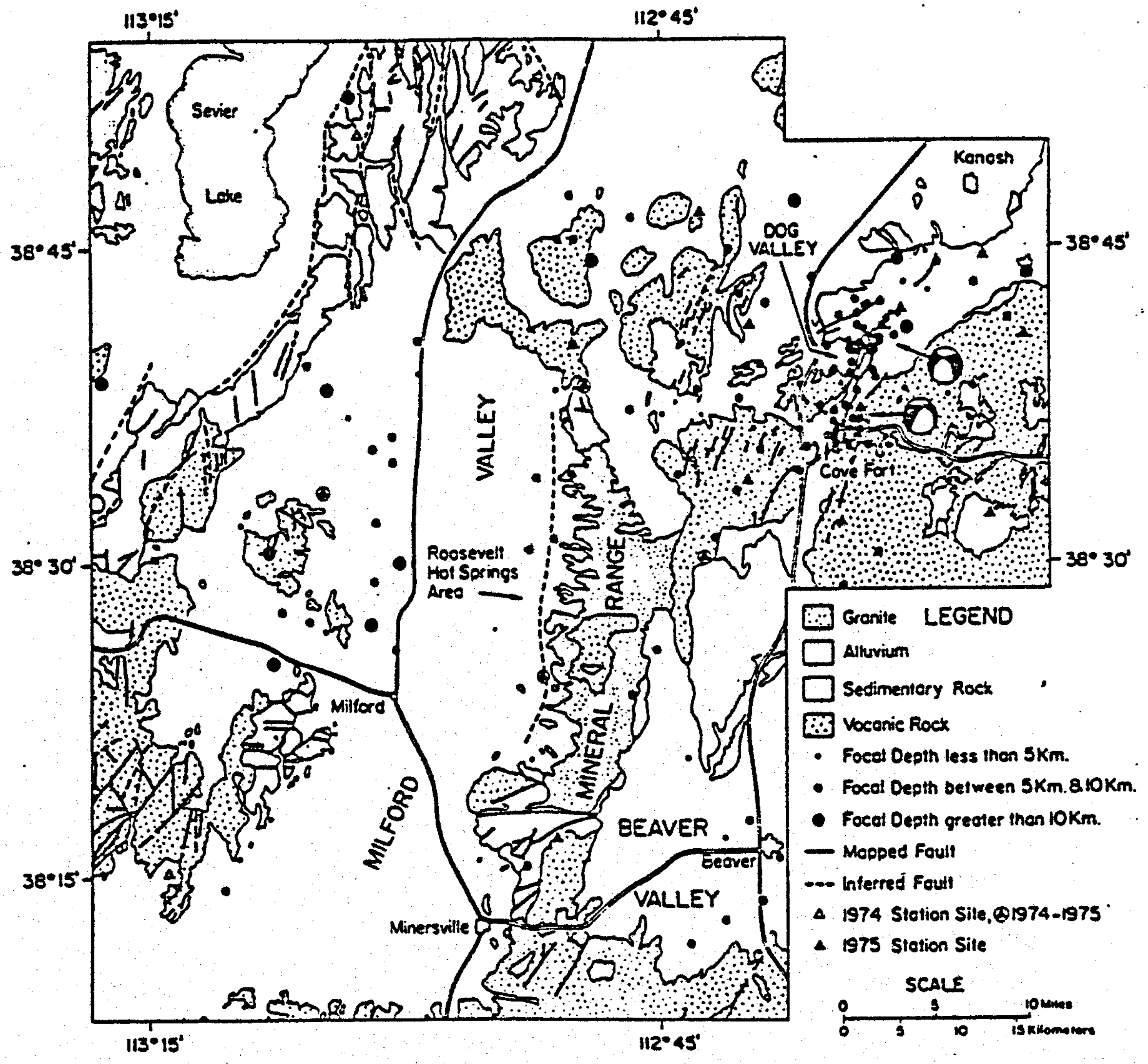

Figure 5. Epicenter map of the Roosevelt Hot Springs-Cove Fort, Utah area from earthquake surveys in 1974 and 1975.

TABLE 1

STATION LOCATIONS

Station Name (Code)	Longitude	Latitude	Elevation (meters)	Elevation Correction Velocity (km/s)
Antelope Valley (ANT)	112°38.36'	38°39.12'	1871.9	3.0
Beaver Lake Mountains (BVR)	113°04.66'	38°31.89'	1658.5	2.0
Cinder Crater (CIN)	112°38.27'	38°34.39'	1973.2	3.0
Dog Valley (DOG)	112°33.36'	38°38.43'	1964.0	3.0
Dry Wash (DRY)	112°28.06'	38°45.16'	1707.8	3.0
Lincoln Gulch (LIN)	112°52.22'	38°16.57'	2098.2	4.5
Linoln II (LI2)	112°51.62'	38°16.59'	2147.0	4.5
Mine (MIN)	112°41.27'	38°29.75'	2055.5	3.0
Mud Springs (MUD)	112°24.58'	38°32.08'	2214.1	3.0
Mary's Nipple (NIP)	112°25.69'	38°40.95'	2217.1	3.0
North Mineral (NOM)	112°49.71'	38°37.91'	1762.7	4.5
North Mineral II (NM2)	112°50.23'	38°37.64'	1834.0	4.5
Pole Canyon (POL)	112°32.54'	38°25.03'	2409.3	3.0
Ranch Canyon (RAN)	112°50.85'	38°25.65'	1982.3	4.5
Sandstone (SND)	112°31.72'	38°40.75'	1970.1	3.0
Sevier Lake (LAK)	113°02.44'	38°52.90'	1590.0	—
Sulphur Creek (SLF)	112°33.85'	38°32.69'	2098.2	3.0
Thermo (TMO)	113°17.62'	38°15.27'	1590.0	—
Twin Peaks (TWN)	112°44.35'	38°46.89'	1622.5	4.5
Twin Peaks II (TW2)	112°44.63'	38°44.96'	1616.4	4.5

TABLE 2

EARTHQUAKE LOCATION INFORMATION

Event	Date YrMoDy	O-Time HrMn	Sec	Lat(N) DgMnSec	Long(W) DgMnSec	Depth* (km)	m_b
*0098	750626	1230	44.88	3830 4.8	113 0 2.4	16.57	4.19
*0010	740913	1541	39.98	3838 9.6	1125042.6	1.16	1.75
*0036	750612	2044	41.32	384418.0	1124829.4	12.94	2.18
*0037	750612	2258	36.97	383510.2	1123834.2	8.06	1.44
*0070	750617	0729	31.89	381645.6	11241 1.2	2.57	1.59
*0073	750619	1300	42.26	382523.4	113 732.4	14.33	3.93
*0075	750620	2055	19.40	384021.0	11243 3.6	1.96	2.16
*0101	750628	0748	20.77	3836 1.8	113 025.8	8.42	3.19
*0113	750630	1948	24.65	381546.2	1123747.4	5.00	2.02
*0001	740907	1932	19.69	3834 3.6	1124333.0	5.00	1.55
*0002	740907	2055	39.26	383525.2	113 133.0	5.00	1.81
*0005	740911	1605	11.58	3834 4.8	1124948.6	5.00	1.12
*0006	740912	2053	36.10	383359.4	1125157.6	5.00	.98
*0007	740912	2128	59.74	382035.4	1124310.8	.88	1.63
*0009	740913	0808	16.79	3831 2.4	1124122.2	5.00	1.46
*0011	740913	1819	33.69	382651.0	113 433.0	.67	1.34
*0012	740913	1854	27.64	383712.0	1124623.4	5.00	.94
*0013	740913	1715	47.86	381146.8	11243 7.8	5.00	1.60
*0014	740913	2020	27.98	3839 9.0	1123918.0	5.00	1.60
*0015	740913	2049	8.45	382336.0	1124624.0	5.00	1.27
*0016	740913	2158	55.40	3837 1.2	113 3 1.8	1.90	1.24
*0017	740913	2159	20.09	382552.8	113 026.4	5.00	1.29
*0018	740914	0010	54.58	382545.0	1124455.8	7.91	1.42
*0021	740915	1747	57.16	3827 9.6	113 145.6	25.58	1.08
*0022	740915	1824	13.50	381436.0	1131034.8	5.00	2.43
*0024	740916	1523	7.99	3837 3.6	1125853.4	.71	1.14
*0025	740916	2252	28.96	3831 6.6	1125057.0	5.00	1.21
*0026	740916	2349	14.80	382912.0	113 132.4	5.00	1.37
*0028	740919	1937	3.76	3838 3.6	1124217.4	5.00	1.28
*0030	740920	2340	57.64	382717.4	113 526.4	5.00	1.42
*0031	740922	1012	53.51	38 655.2	1125330.0	5.00	1.69
*0032	740923	1309	34.86	383738.4	1123948.6	5.00	1.76
*0033	740923	2004	50.75	382746.2	113 7 3.0	8.37	1.59
*0034	740924	0014	20.54	383037.2	113 744.4	14.50	1.71
*0035	750611	2158	25.81	383822.2	113 419.8	21.13	1.68
*0038	750613	0255	54.89	383857.0	1131714.4	18.06	2.29
*0040	750613	0824	48.20	384620.8	1124612.0	5.00	1.95
*0041	750613	0827	36.36	381731.2	1123735.4	5.00	1.31
*0055	750614	2214	17.08	381251.6	11241 2.4	5.00	2.50
*0056	750615	0819	18.46	381345.0	1123850.4	5.00	1.75
*0065	750617	0006	27.04	381531.8	1125234.2	5.00	1.26
*0072	750617	1437	8.27	3738 8.4	1124157.0	7.45	2.44
*0077	750621	1639	57.44	384520.4	1124931.8	5.00	1.42
*0079	750621	2156	21.36	383928.8	113 525.2	5.00	2.10
*0080	750622	0351	45.00	383715.0	1123729.4	3.43	.96
*0083	750622	0624	9.26	385216.8	113 245.6	40.15	3.57
*0087	750622	1918	10.62	384445.0	1124017.4	5.00	1.16
*0096	750625	2313	57.50	384036.0	1125855.2	5.00	2.25
*0124	750703	0245	3.03	383158.8	113 127.0	5.00	1.45
*0150	750706	1332	42.85	383610.8	1123857.0	3.82	.82
*0106	750630	0417	22.24	3836 7.0	1123321.0	4.75	1.43
*0027	740917	2006	11.41	384725.2	1123647.4	10.00	1.95
*0053	750614	1247	47.78	383713.2	1123427.0	9.58	1.11
*0078	750621	2023	6.54	383831.8	11234 1.8	4.32	1.24
*0091	750623	1817	23.56	383538.4	11234 9.0	3.16	1.17
*0093	750625	0409	10.23	383913.2	1123427.0	9.15	1.12
*0107	750630	0425	39.73	3836 4.8	1123217.4	3.02	1.68
*0110	750630	0431	43.99	3836 4.8	1123336.0	4.70	1.25
*0111	750630	0436	13.31	3836 3.0	1123327.6	4.79	1.39
*0114	750630	2211	6.45	384237.8	11233 6.6	6.55	1.22
*0135	750704	0803	31.03	383627.0	1123343.8	1.69	1.33
*0145	750706	0106	12.61	383617.4	1123350.4	3.96	1.89
*0152	750706	1639	16.10	384220.4	1123222.8	8.01	1.74
*0157	750707	0747	37.32	384434.8	1123032.4	6.28	1.27
*0162	750708	1545	15.02	383554.0	1123333.6	5.63	1.38
*0003	740909	1718	22.61	384345.0	1122240.8	10.00	1.10
*0029	740920	1454	39.46	3835 9.0	1121639.6	10.00	2.27
*0039	750613	0350	57.66	3837 5.4	1123457.6	4.76	.77
*0043	750613	2034	59.45	383618.6	1123635.4	.39	1.40
*0046	750614	0457	7.46	383740.2	1123028.2	1.02	1.13
*0047	750614	0559	39.97	384043.2	1123217.0	5.00	.93
*0048	750614	0743	57.97	3843 1.2	1122840.2	1.02	.59
*0049	750614	1031	32.00	383615.0	1123421.0	5.00	1.95
*0051	750614	1029	46.48	383640.8	1123224.6	3.42	.88
*0052	750614	1116	29.34	383618.6	11234 6.0	2.29	.88
*0054	750614	1446	57.54	384157.0	1122057.6	.03	.85

*Measured from datum plane at 2 km above sea level.

TABLE 2 (continued)

Event	Date YrMoDy	O-Time HrMn	Sec	Lat(N) DgMnSec	Long(W) DgMnSec	Depth (km)	m_b
*0057	750615	0940	5.17	383638.4	11233 3.0	3.38	1.31
*0058	750615	0940	26.26	383629.4	11234 6.0	5.00	1.92
*0059	750616	0033	53.96	384545.0	1123110.2	1.65	.31
*0060	750616	0843	47.69	384037.8	1123331.2	.53	.55
*0061	750616	1042	49.18	3840 8.4	1123224.0	.60	.55
*0062	750616	1313	50.42	3838 9.6	11233 3.6	4.48	.91
*0064	750616	2331	38.07	383021.6	1123149.2	5.99	3.35
*0066	750617	0324	48.38	384141.4	1122354.0	5.00	1.70
*0067	750617	0330	4.00	384411.0	11228 6.0	5.00	1.14
*0068	750617	0337	44.27	384326.4	1123010.2	1.06	1.33
*0069	750617	0439	39.17	384452.8	1122849.2	4.08	1.03
*0071	750617	1339	39.40	38 746.8	11235 1.2	1.17	2.06
*0074	750619	1320	59.43	384342.6	1123548.0	5.00	1.47
*0076	750621	0825	57.85	383533.0	1123227.0	5.00	1.32
*0082	750622	0554	36.85	384039.6	1123145.0	.46	1.14
*0084	750622	0811	3.20	383649.8	1123251.0	5.00	.93
*0086	750622	1620	22.28	384237.2	1123940.8	5.00	1.81
*0088	750622	1934	44.11	382737.2	1122637.2	5.00	1.52
*0089	750623	0655	32.50	383737.8	11236 6.0	1.20	.73
*0090	750623	1645	31.48	383755.8	1122731.8	2.14	.82
*0094	750625	0758	1.65	384319.8	1122555.2	5.00	1.85
*0095	750625	1938	28.64	385019.6	11228 9.6	5.00	1.70
*0097	750626	1210	15.11	383846.2	11233 2.4	.30	.85
*0100	750628	0158	32.45	384110.2	1123237.2	6.64	.77
*0102	750628	1603	52.94	383619.2	1123253.4	5.00	1.34
*0103	750629	0213	15.39	381946.8	1121811.4	5.90	1.29
*0104	750629	1246	6.75	384139.0	1123113.2	8.57	.96
*0105	750629	1445	44.77	3839 6.6	1123436.6	.40	.74
*0108	750630	0429	20.70	383548.6	1123316.8	1.70	.75
*0109	750630	0427	42.45	383617.4	1123314.4	2.90	1.16
*0112	750630	0646	48.67	3836 3.0	1123335.4	2.72	.75
*0115	750701	0036	16.76	383530.6	1123334.8	5.00	1.40
*0116	750701	0515	44.60	383528.8	11231 6.0	1.73	.56
*0117	750701	0921	36.42	384116.8	1122958.8	11.07	1.05
*0118	750701	1717	46.45	383560.0	1123249.8	3.63	1.20
*0119	750701	1720	16.20	383616.8	1123325.2	5.00	1.51
*0120	750702	0115	59.92	383418.0	1123639.0	9.66	1.10
*0121	750702	0201	2.04	3836 9.0	1123327.6	.06	1.03
*0122	750702	0517	36.96	383639.0	1123352.8	.53	.79
*0123	750702	0633	14.61	382628.2	1121648.6	5.71	1.80
*0125	750703	0430	2.13	383542.6	1123424.6	5.00	.41
*0126	750703	0901	39.61	383622.2	1123342.0	5.00	1.17
*0127	750703	0949	9.90	384051.0	1123045.6	6.02	.63
*0128	750703	0949	22.78	383815.6	11230 8.4	2.92	.43
*0129	750703	0949	47.12	383530.0	11236 7.8	5.57	.78
*0131	750703	1305	49.98	393859.4	1123327.6	.21	.61
*0132	750703	2046	19.13	39 457.6	11232 7.2	5.00	2.08
*0133	750704	0404	34.04	383617.4	1123258.2	.38	.97
*0134	750704	0650	1.90	382831.2	1123633.6	8.12	.39
*0136	750704	1110	40.07	383628.8	1123337.0	1.00	.79
*0137	750704	1124	27.72	383748.0	1123617.4	3.49	.83
*0138	750704	1250	31.71	384117.4	1123129.4	7.55	.40
*0140	750704	1336	37.32	383620.4	1123336.6	2.73	1.17
*0141	750704	2202	43.38	384157.6	11233 2.4	5.00	.72
*0142	750705	0458	49.96	383617.4	1123257.0	4.44	.25
*0143	750705	0812	52.67	384122.2	11233 1.2	5.46	.61
*0144	750705	2107	3.53	392151.0	11245 9.6	.69	2.16
*0146	750706	0107	40.61	383612.6	1123342.6	3.43	1.11
*0147	750706	0246	27.34	383620.4	1123413.2	3.89	1.02
*0149	750706	0617	4.46	384217.4	1123230.6	5.00	.76
*0151	750706	1621	41.84	384439.0	1123351.6	6.72	1.06
*0153	750707	0110	19.62	383643.2	1123430.0	5.00	1.18
*0154	750707	0120	[illegible]	3836 4.2	11233 1.8	5.00	.71
*0155	750707	0256	36.21	382850.4	1121951.0	1.13	1.06
*0156	750707	0422	32.39	3836 4.8	1123250.4	5.00	.68
*0158	750707	1114	51.30	383727.6	1123516.8	6.43	.79
*0161	750708	0756	4.27	383558.8	1123327.6	2.50	1.14
*0163	750708	1730	.39	383535.4	1123537.8	4.15	.68
*0004	740907	2132	32.76	383034.2	1125224.6	5.00	1.84
*0008	740913	0148	22.25	382951.0	1122033.6	10.00	.55
*0019	740914	0113	42.45	38 457.0	1124758.2	10.00	2.23
*0020	740914	1843	31.76	384726.4	1124948.6	5.00	1.27
*0023	740915	2039	46.40	384021.6	1124940.8	5.00	1.36
*0042	750613	1744	43.73	384517.2	1125030.0	5.00	2.24
*0044	750613	2115	26.62	383449.2	[illegible]	5.00	2.30
*0045	750614	0343	11.25	383849.8	1123152.0	5.00	.91
*0050	750614	1034	[illegible]	3839 9.0	11232 4.2	5.00	.76
*0063	750616	[illegible]	[illegible]	[illegible]	[illegible]	5.00	[illegible]
*0081	750622	0545	14.25	383927.6	11233 1.8	5.00	1.05
*0085	750622	1043	17.57	383729.4	1123347.4	5.00	.76
*0092	750624	0029	4.94	383913.2	1123827.6	5.00	1.59
*0099	750627	0141	20.64	3836 2.4	1123327.6	5.00	.51
*0130	750703	1016	55.54	383315.6	11240 .6	5.00	.13
*0139	750704	1303	20.61	382845.6	1123357.0	5.00	1.03
*0148	750706	0304	16.09	383617.4	1123327.6	5.00	.63
*0157	750707	2323	23.73	383825.2	11226 .6	5.00	1.41
*0160	750708	0737	29.98	384148.0	11234 7.2	5.00	.70

As we will note in more detail in the following section of this report, the particular station and event distributions in the intended study region impacts the final inversion model in very specific and, in fact, negative ways. This situation is typical of most of our modeling projects conducted to date and mainly reflects the lack of seismic networks dedicated (i.e., more dense, evenly spaced stations) to the type of study we are interested in.

3.1.1 RHS Seismic Data Culling

The first step in the RHS data culling procedure was to delete poorly recorded events from the data base. To accomplish this, we adopted the following rejection criteria:

1. For an event in any part of the general study region, reject it if there are less than five stations reporting a P-wave arrival time and no stations reporting an S-wave arrival time, or if there are less than four stations reporting P times in the case where one or more report S times.

2. For an event in the Cove Fort area, where there is an abundance of events, reject it if less than six stations report P times and no stations report an S time, or if there are less than five stations reporting P times in the case where one or more report S times.

3. Reject any events located north of 38.9°N or south of 38.0°N. Such events, in addition to being outside the intended model region, are located well outside the local network and, thus, are very poorly located.

4. Reject events with reported focal depths greater than 25 km.

Application of these four rejection criteria resulted in a reduction of the original 163 events to 99 events (i.e., 64 events rejected). The breakdown by criterion is: 49 events by Criterion 1; 11 events by Criterion 2; 3 events by Criterion 3; and 1 event by Criterion 4. In addition, after applying these rejection criteria to the data base we found that two stations, LAK and TMO (refer to Figure 4, Table 1), located well outside the central portion of the intended model region, contributed a very small number of arrival time data. In view of these circumstances we deleted stations LAK and TMO from the station set. Thus, at the conclusion of this culling step the resultant data base consisted of 620 P-wave arrival times for 99 events recorded at a subset of 18 stations.

The final step in the culling procedure was to compare observed and predicted travel times corresponding to the remaining 620 station-event ray paths and reject obvious outliers (i.e., observed travel times that differ by more than ten percent from predicted values). Application of this culling procedure required the adoption of a plane-layered initial velocity model for the general study region shown in Figure 1. To accomplish this, we started with the velocity model used in HYPO 71 by Olson and Smith (1976; Figure 4b, Page 15) to locate the 163 earthquakes listed in Table 2. While this model, which consisted of three layers over a half-space, provides a good fit to the travel time versus distance data (as expected since it was used for the location of the events in question), the particular layering adopted by Olson and Smith (1976) does not provide an adequate parameterization for an inversion modeling procedure. More specifically, the Olson and Smith (1976) model does not yield an adequate distribution of ray paths in the different layers. An additional consideration is the fact that we used different station elevation correction velocities determined, as mentioned previously, from the work of Robinson and Iyer (1981). The initial velocity model that we arrived at by trial and error is given in Table 3.

Based on the velocity model in Table 3, we calculated travel-times for the 620 event-station ray paths in the seismic data set and used these results for final screening of the data, invoking the ten percent rule mentioned previously. The final data set consists of 601 P-wave travel times from 93 of the original 163 earthquakes. The location information for these 93 earthquakes is given in Table 4.

Figures 6a through 6e are plots of the observed reduced travel times (symbols), after all screening, for events with focal depths reported within the respective layers (e.g., events with focal depths between 0 and 1 km are plotted in Figure 6a). The observed times in each figure are corrected to be for a common focal depth, taken to be the depth of the midpoint of the respective layers, except Layer 1 which is taken at 0 km. The data are also corrected to a common station elevation of 2 km above sea level. The theoretical travel-time curves shown in Figures 6a through 6e were computed from the initial velocity model in Table 3 for event focal depths equal to the appropriate common depths for the five different layers.

The reduced travel-times shown in Figures 6a through 6e were subsequently denuisanced with respect to event hypocenters; assuming prior standard deviations of 4 km on epicenter, 2 km on focal depth and 100 seconds on origin time. The use of prior standard deviations on earthquake location parameters was discussed in Section 2.5 of this report. The resulting denuisanced travel-time data are shown in Figures 7a through 7e. The format of this series of figures is the same as for Figures 6a through 6e. An important point about these data is that the r.m.s. of the observed, denuisanced residuals (i.e., the scatter of the symbols about the theoretical curves in Figures 7a through 7e)

TABLE 3

INITIAL VELOCITY MODEL

Layer	Depth* to Bottom of Layer (km)	Layer Thickness (km)	Velocity (km/s)
1	1.0	1.0	4.5
2	2.0	1.0	5.4
3	3.5	1.5	5.6
4	7.0	3.5	5.75
5	26.0	19.0	6.05

*Measured from datum plane at 2 km above sea level.

TABLE 4

LOCATION INFORMATION FOR FINAL EVENT SET

Event	Date YrMoDy	O-Time Hr	Mn	Sec	Lat(N) Dg	Mn	Sec	Long(W) Dg	Mn	Sec	Depth (km)	m_b
0098	750626	12	30	44.88	38	30	4.8	-113	0	2.4	16.57	4.19
0036	750612	20	44	41.32	38	44	18.0	-112	48	29.4	12.94	2.18
0037	750612	22	58	36.97	38	35	10.2	-112	38	34.2	8.05	1.44
0070	750617	07	29	31.89	38	16	45.6	-112	41	1.2	2.57	1.59
0073	750619	13	00	42.26	38	25	27.4	-113	7	32.4	14.33	3.93
0075	750620	20	55	19.40	38	40	21.0	-112	43	3.6	1.96	2.16
0101	750628	09	48	20.79	38	36	1.9	-113	0	25.8	8.42	3.19
0113	750630	19	48	24.85	38	15	46.2	-112	37	47.4	5.00	2.02
0001	740907	14	32	19.69	38	34	3.6	-112	43	33.0	5.00	1.55
0011	740913	18	19	33.69	38	26	51.0	-113	4	33.0	.67	1.34
0013	740913	19	15	47.86	38	11	46.9	-112	43	7.8	5.00	1.60
0016	740913	21	58	55.40	38	37	1.2	-113	3	1.8	1.80	1.24
0021	740915	17	47	57.16	38	27	9.6	-113	1	45.6	25.58	1.08
0022	740915	18	24	13.50	38	14	36.0	-113	10	34.8	5.00	2.43
0028	740919	19	37	3.76	38	38	3.6	-112	42	17.4	5.00	1.28
0030	740920	23	40	57.84	38	27	17.4	-113	5	26.4	5.00	1.42
0031	740922	10	12	58.51	38	6	55.2	-112	53	30.0	5.00	1.69
0032	740923	13	09	34.86	38	37	38.4	-112	39	48.6	5.00	1.76
0033	740923	20	04	50.95	38	27	46.2	-113	7	3.0	8.37	1.59
0034	740924	00	14	20.54	38	30	37.2	-113	7	44.4	14.50	1.71
0035	750611	21	58	25.81	38	38	22.2	-113	4	19.8	21.13	1.88
0039	750613	02	55	54.89	38	38	57.0	-113	17	14.4	18.06	2.29
0040	750613	08	24	48.20	38	46	20.4	-112	46	12.0	5.00	1.95
0041	750613	08	27	36.36	38	17	31.2	-112	39	35.4	5.00	1.31
0055	750614	22	14	17.08	38	12	51.6	-112	41	2.4	5.00	2.50
0056	750615	08	19	18.46	38	13	45.0	-112	38	50.4	5.00	1.75
0065	750617	00	06	27.04	38	15	31.8	-112	52	34.2	5.00	1.26
0077	750621	16	39	57.44	38	45	20.4	-112	49	31.8	5.00	1.42
0079	750621	21	56	21.36	38	39	28.8	-113	5	25.2	5.00	2.10
0087	750622	19	18	10.62	38	44	45.0	-112	40	17.4	5.00	1.16
0096	750625	23	13	57.50	38	40	36.0	-112	58	55.2	5.00	2.25
0124	750703	02	45	3.03	38	31	58.8	-113	1	27.0	5.00	1.45
0106	750630	04	17	22.24	38	36	9.0	-112	33	21.0	4.75	1.43
0053	750614	12	47	49.78	38	37	13.2	-112	34	27.0	9.58	1.11
0091	750623	18	17	23.56	38	35	38.4	-112	34	9.0	3.16	1.17
0093	750625	04	09	10.23	38	39	13.2	-112	34	27.0	9.15	1.12
0107	750630	04	25	39.73	38	36	4.8	-112	33	17.4	3.02	1.68
0110	750630	04	31	43.99	38	36	4.8	+112	33	36.0	4.70	1.25
0111	750630	04	36	18.31	38	36	3.0	-112	33	27.6	4.79	1.39
0114	750630	22	11	6.45	38	42	37.8	-112	33	6.6	6.55	1.22
0135	750704	08	03	31.03	38	36	27.0	-112	33	43.8	1.69	1.33
0145	750706	01	06	12.61	38	36	17.4	-112	33	50.4	3.95	1.89
0152	750706	16	39	16.10	38	42	20.4	-112	32	22.8	8.01	1.74
0157	750707	09	47	37.32	38	44	34.8	-112	30	32.4	6.28	1.27
0162	750708	15	45	15.02	38	35	54.0	-112	33	33.6	5.63	1.38
0029	740920	14	54	33.46	38	35	9.0	-112	16	39.6	10.00	2.27
0046	750614	04	57	7.46	38	37	40.2	-112	30	28.2	1.02	1.13
0047	750614	05	59	39.97	38	40	43.2	-112	32	12.0	5.00	.93
0049	750614	10	31	32.00	38	36	15.0	-112	34	21.0	5.00	1.95
0051	750614	10	39	46.48	38	36	40.8	-112	32	24.6	3.42	.88
0052	750614	11	16	28.74	38	36	18.6	-112	34	6.0	2.29	.88
0057	750615	09	40	5.19	38	36	38.4	-112	33	3.0	3.38	1.31
0058	750615	09	44	26.26	38	36	29.4	-112	34	6.0	5.00	1.92
0066	750617	03	24	48.38	38	41	41.4	-112	23	54.0	5.00	1.70
0071	750617	13	39	37.40	38	7	46.8	-112	35	1.2	1.17	2.06
0074	750619	13	20	59.43	38	43	42.6	-112	35	48.0	5.00	1.47
0088	750622	19	34	44.11	38	27	37.2	-112	26	37.2	5.00	1.52
0097	750626	12	10	15.11	38	38	46.2	-112	33	2.4	.30	.85
0100	750628	01	58	32.45	38	41	10.2	-112	32	37.2	6.64	.97
0102	750628	16	03	53.94	38	36	17.2	-112	42	57.4	5.00	1.34
0103	750629	02	13	15.39	38	19	46.8	-112	18	11.4	5.90	1.29
0105	750629	14	45	44.77	38	39	6.6	-112	34	36.6	.40	.74
0108	750630	04	29	23.70	38	35	48.6	-112	33	16.8	1.70	.75
0109	750630	04	27	42.45	38	36	17.4	-112	33	14.4	2.90	1.16
0112	750630	06	46	40.67	38	36	3.0	-112	33	35.4	2.72	.75
0115	750701	00	36	14.76	38	35	30.6	-112	33	34.8	5.00	1.40
0116	750701	05	15	44.60	38	35	[illegible]	-112	31	6.0	1.73	.56
0118	750701	17	17	46.45	38	35	60.0	-112	32	49.8	3.67	1.20
0119	750701	17	20	16.20	38	36	16.8	-112	33	25.2	5.00	1.51
0120	750702	01	15	57.92	38	34	18.0	-112	36	39.0	9.66	1.10
0122	750702	05	17	36.36	38	36	39.0	-112	33	[illegible]	.53	.79
0123	750702	06	33	14.61	38	26	[illegible]	-112	16	48.6	5.71	1.80
0126	750703	09	01	39.61	38	36	[illegible]	-112	[illegible]	[illegible]	5.00	1.17

TABLE 4 (continued)

Event	Date YrMoDy	O-Time Hr	O-Time Mn	O-Time Sec	Lat(N) Dg	Lat(N) Mn	Lat(N) Sec	Long(W) Dg	Long(W) Mn	Long(W) Sec	Depth (km)	m_b
0127	750703	07	49	3.90	38	40	51.0	-112	30	45.6	6.02	.63
0128	750703	09	49	22.78	38	38	15.6	-112	30	8.4	2.92	.43
0129	750703	09	49	47.12	38	35	30.0	-112	36	7.8	5.57	.78
0131	750703	13	05	49.98	38	38	57.4	-112	33	27.6	.21	.61
0133	750704	04	04	34.04	38	36	17.4	-112	32	58.2	.38	.97
0136	750704	11	10	40.07	38	36	28.8	-112	33	37.8	1.00	.79
0137	750704	11	24	27.72	38	37	48.0	-112	36	17.4	3.49	.33
0138	750704	12	50	31.71	38	41	17.4	-112	31	29.4	7.55	.40
0140	750704	13	36	37.32	38	36	20.4	-112	33	36.6	2.73	1.17
0141	750704	22	02	43.38	38	41	57.6	-112	33	2.4	5.00	.72
0143	750705	08	12	52.67	38	41	22.2	-112	33	1.2	5.46	.61
0146	750706	01	07	40.81	38	36	12.6	-112	33	42.6	3.43	1.11
0147	750706	02	46	29.34	38	36	20.4	-112	34	12.2	3.89	1.02
0149	750706	06	17	4.46	38	42	17.4	-112	32	30.6	5.00	.76
0151	750706	16	21	41.84	38	44	39.0	-112	33	51.6	6.72	1.06
0153	750707	01	10	19.82	38	36	43.2	-112	34	30.0	5.00	1.18
0154	750707	01	50	33.52	38	36	4.2	-112	33	1.8	5.00	.71
0155	750707	02	56	36.21	38	28	50.4	-112	19	51.0	1.13	1.06
0156	750707	04	22	33.39	38	36	4.8	-112	32	50.4	5.00	.68
0161	750708	03	56	4.27	38	35	53.8	-112	33	27.6	2.50	1.14

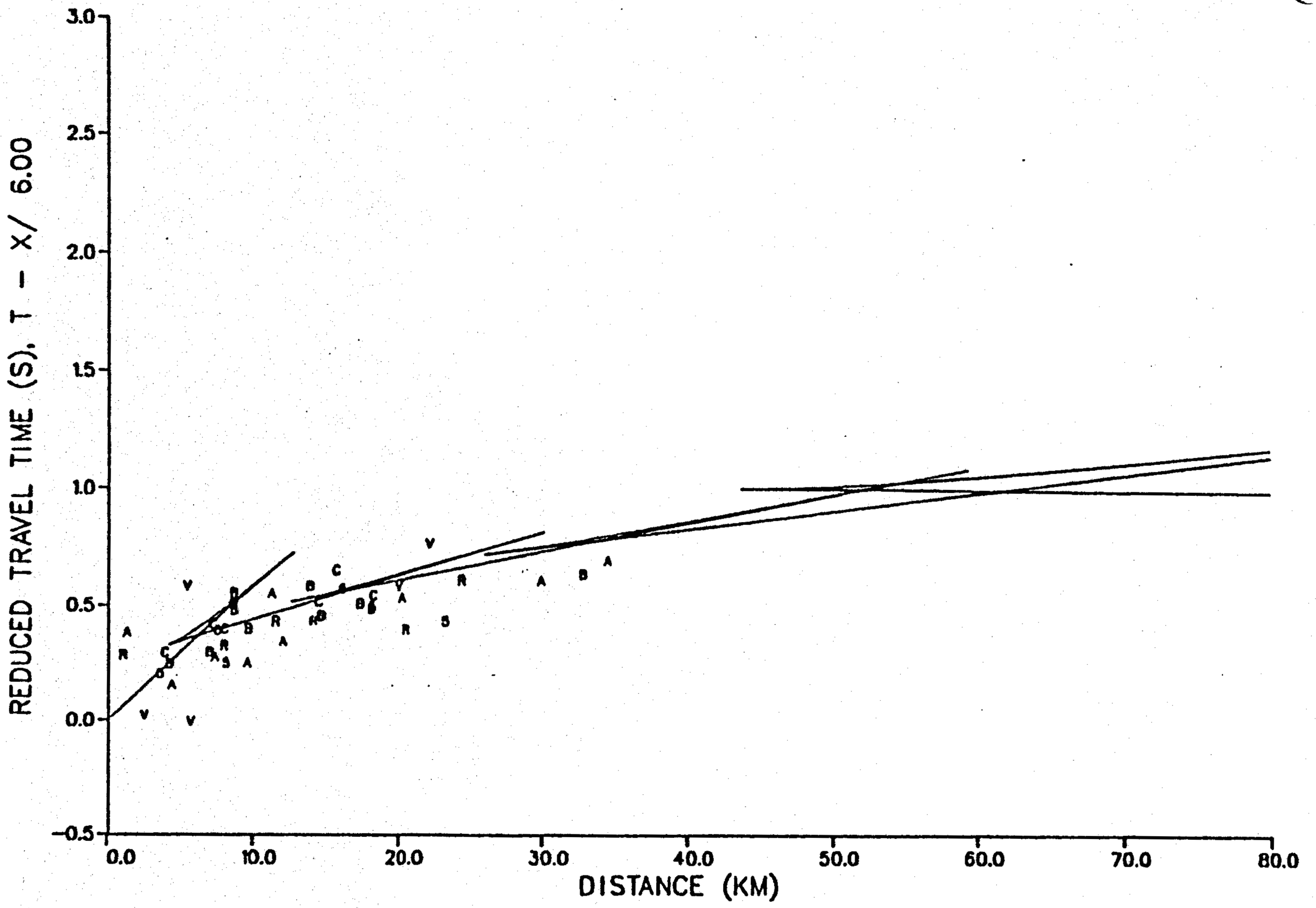

Figure 6a. Observed travel times (symbols) for events with focal depths between 0 and 1 km. Times have been corrected to a common focal depth of 0 km. Theoretical travel-time curve shown (focal depth = 0 km) was computed from initial model in Table 3.

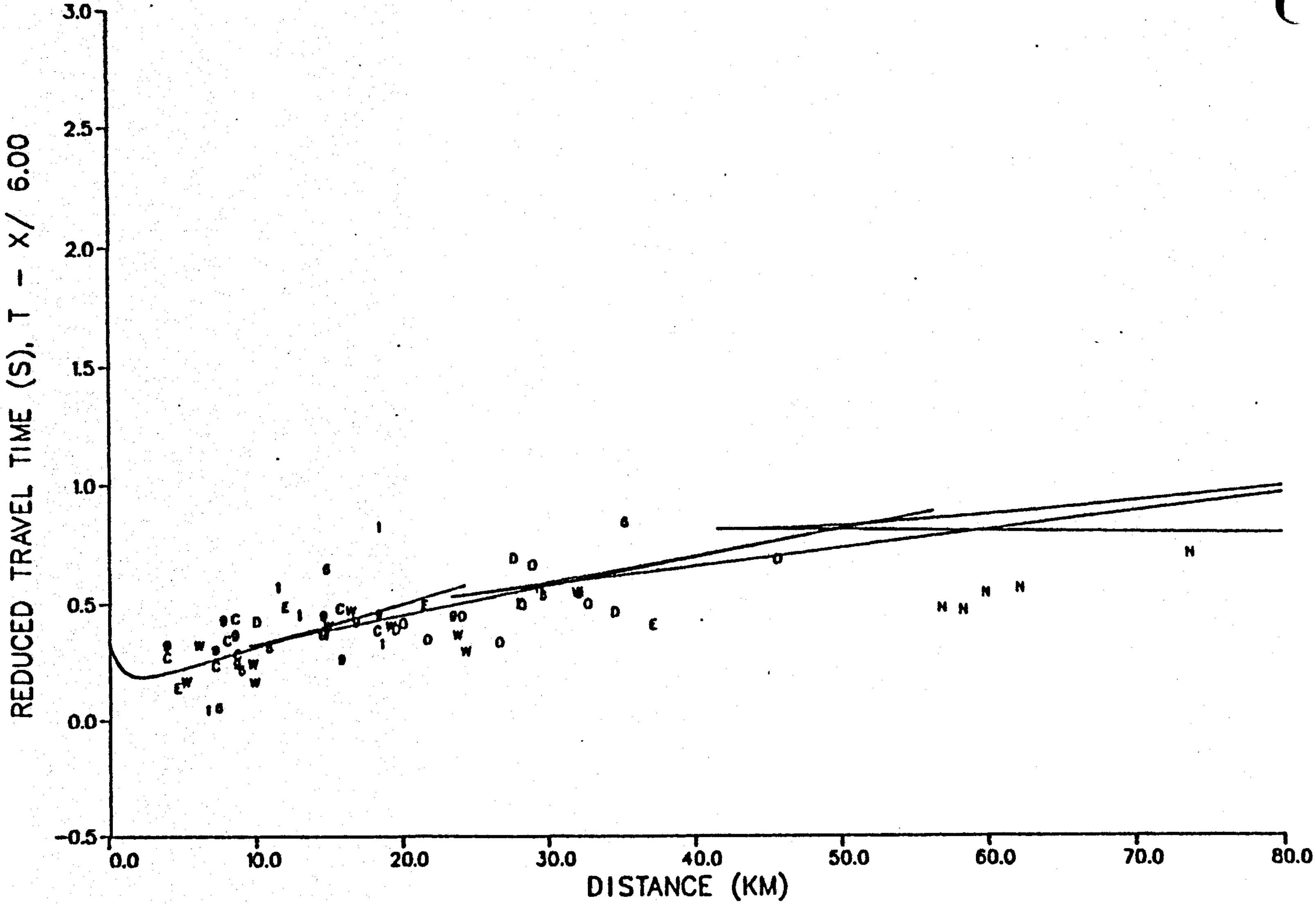

Figure 6b. Observed travel times for events with focal depths between 1 and 2 km. Times have been corrected to a common focal depth of 1.5 km. Theoretical travel-time curve computed for focal depth of 1.5 km.

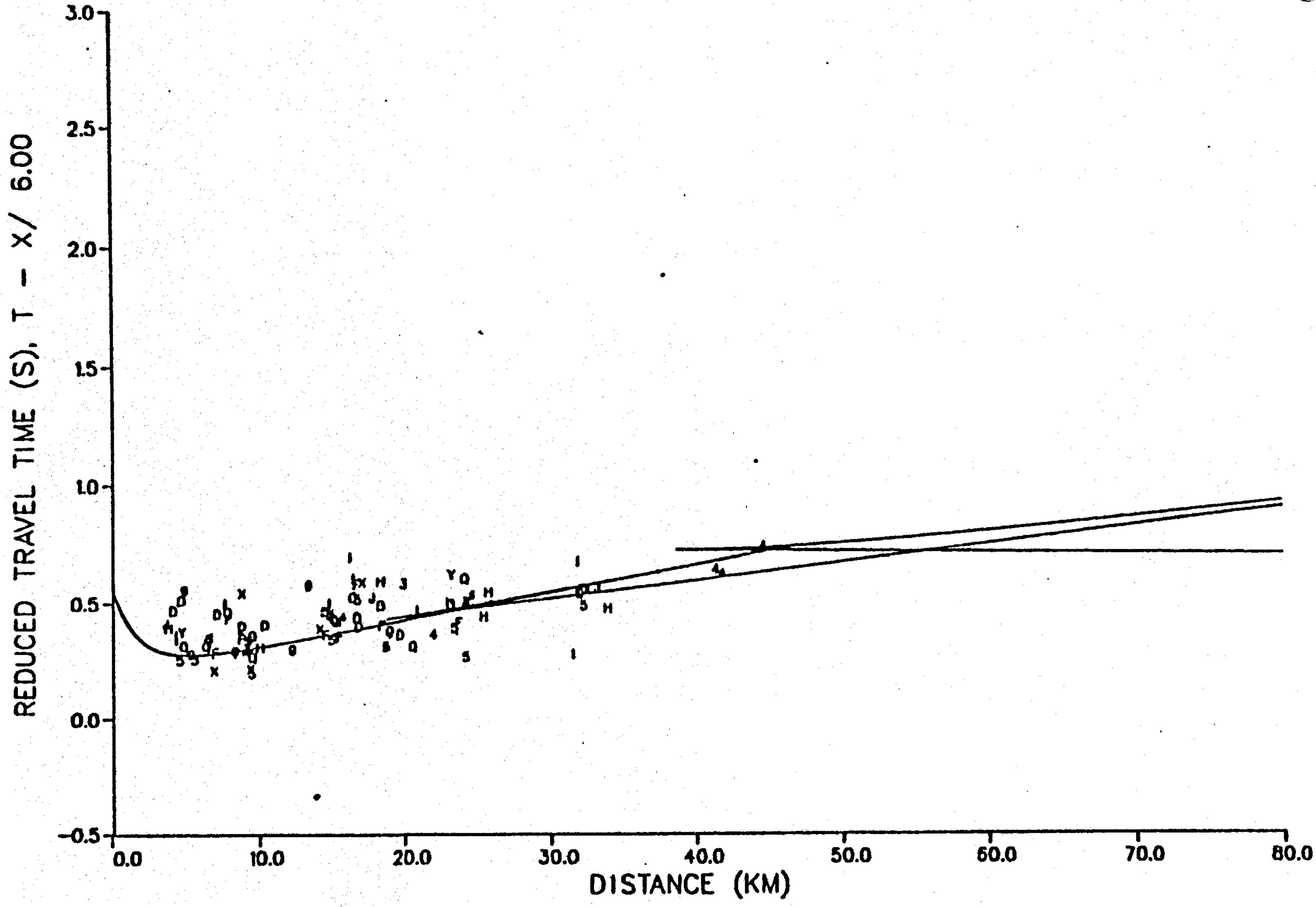

Figure 6c. Observed travel times for events with focal depths between 2.0 and 3.5 km. Times have been corrected to a common focal depth of 2.75 km. Theoretical travel-time curve computed for focal depth of 2.75 km.

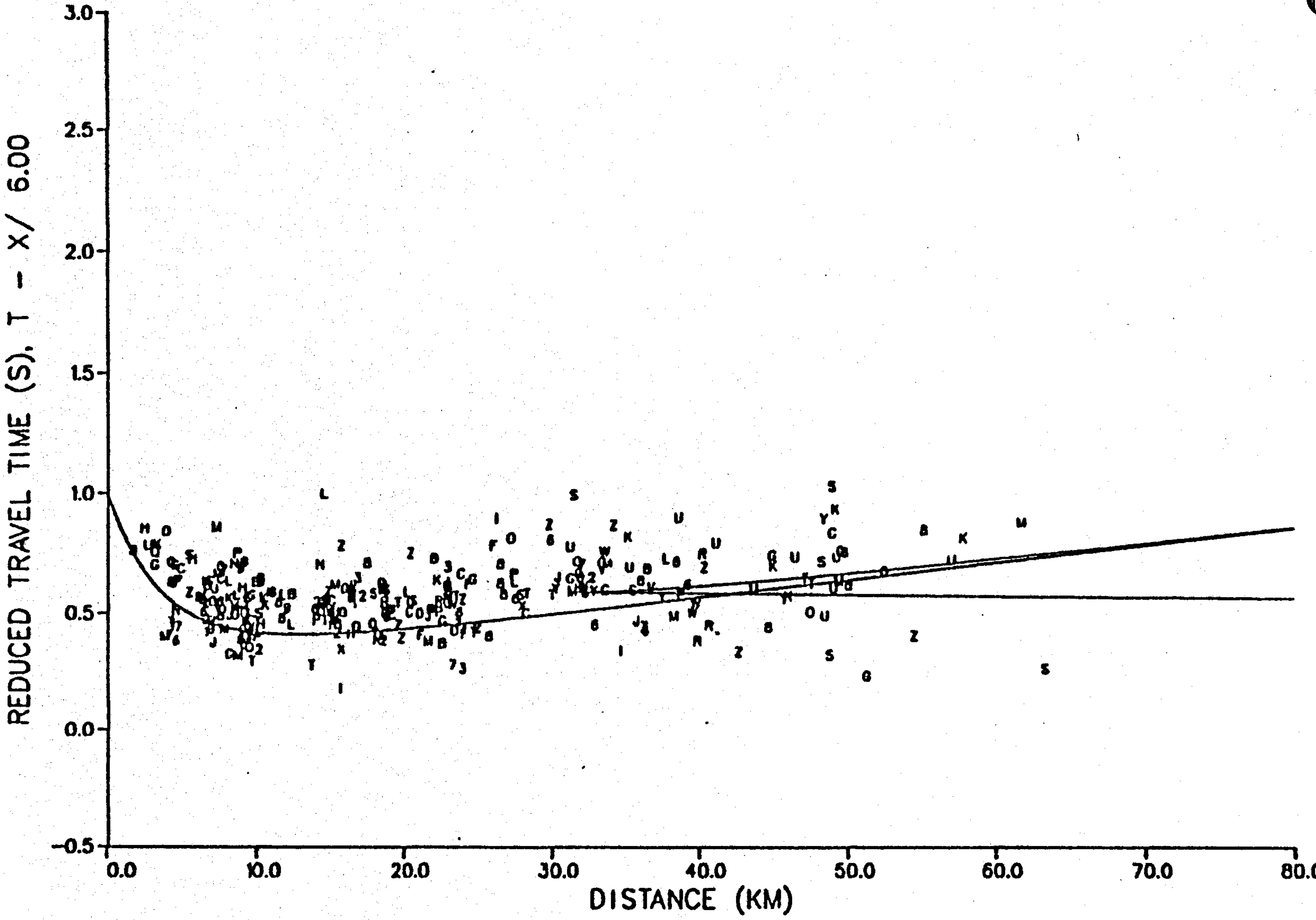

Figure 6d. Observed travel times for events with focal depths between 3.5 and 7.0 km. Times have been corrected to a common focal depth of 5.25 km. Theoretical travel-time curve computed for focal depth of 5.25 km.

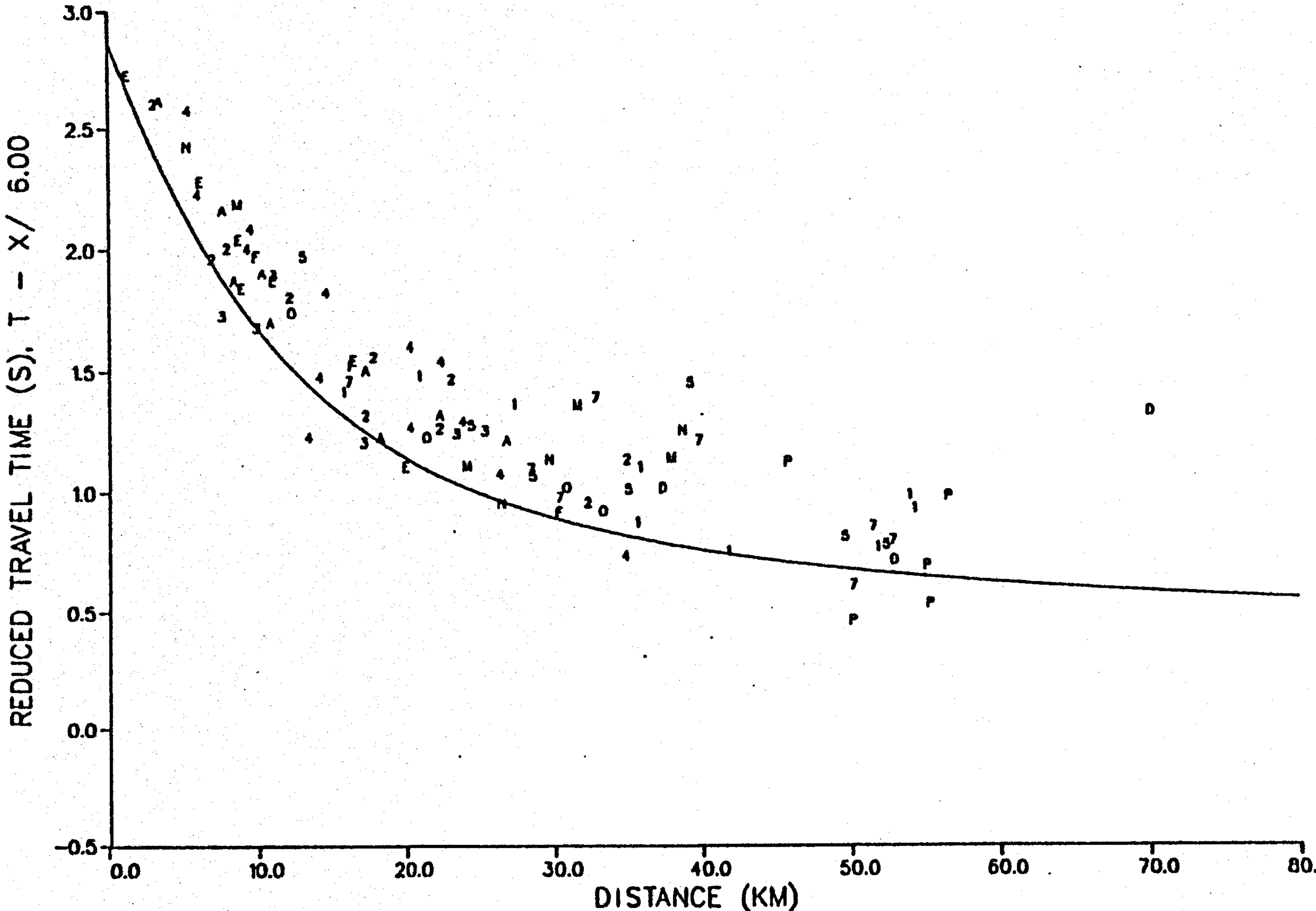

Figure 6e. Observed travel times for events with focal depths between 7.0 and 26.0 km. Times have been corrected to a common focal depth of 16.5 km. Theoretical travel-time curve computed for focal depth of 16.5 km.

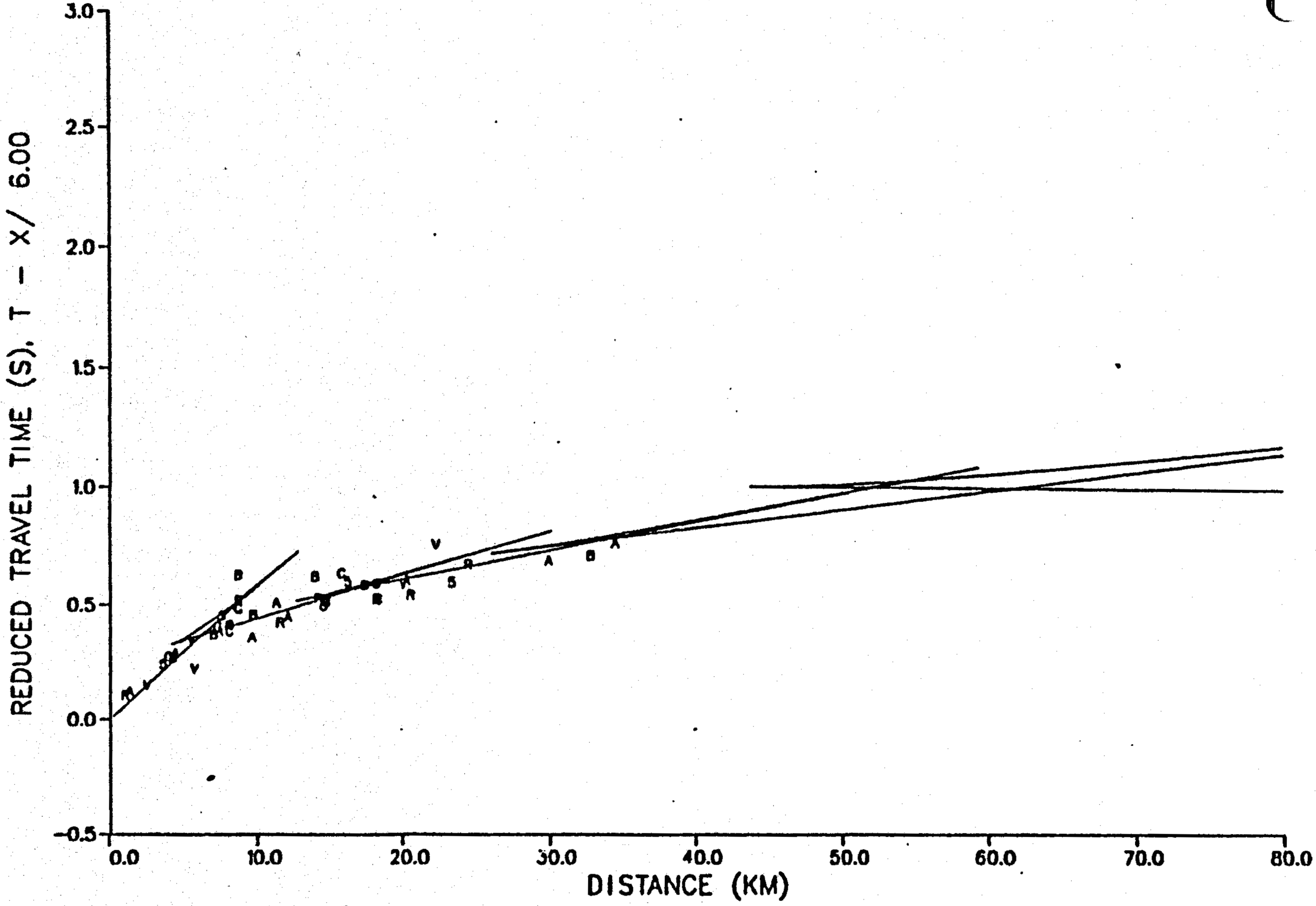

Figure 7a. Observed travel times, denuisanced with respect to event hypocenters (see text). Focal depth range is 0 to 1 km. Focal depth for theoretical curve is 0 km.

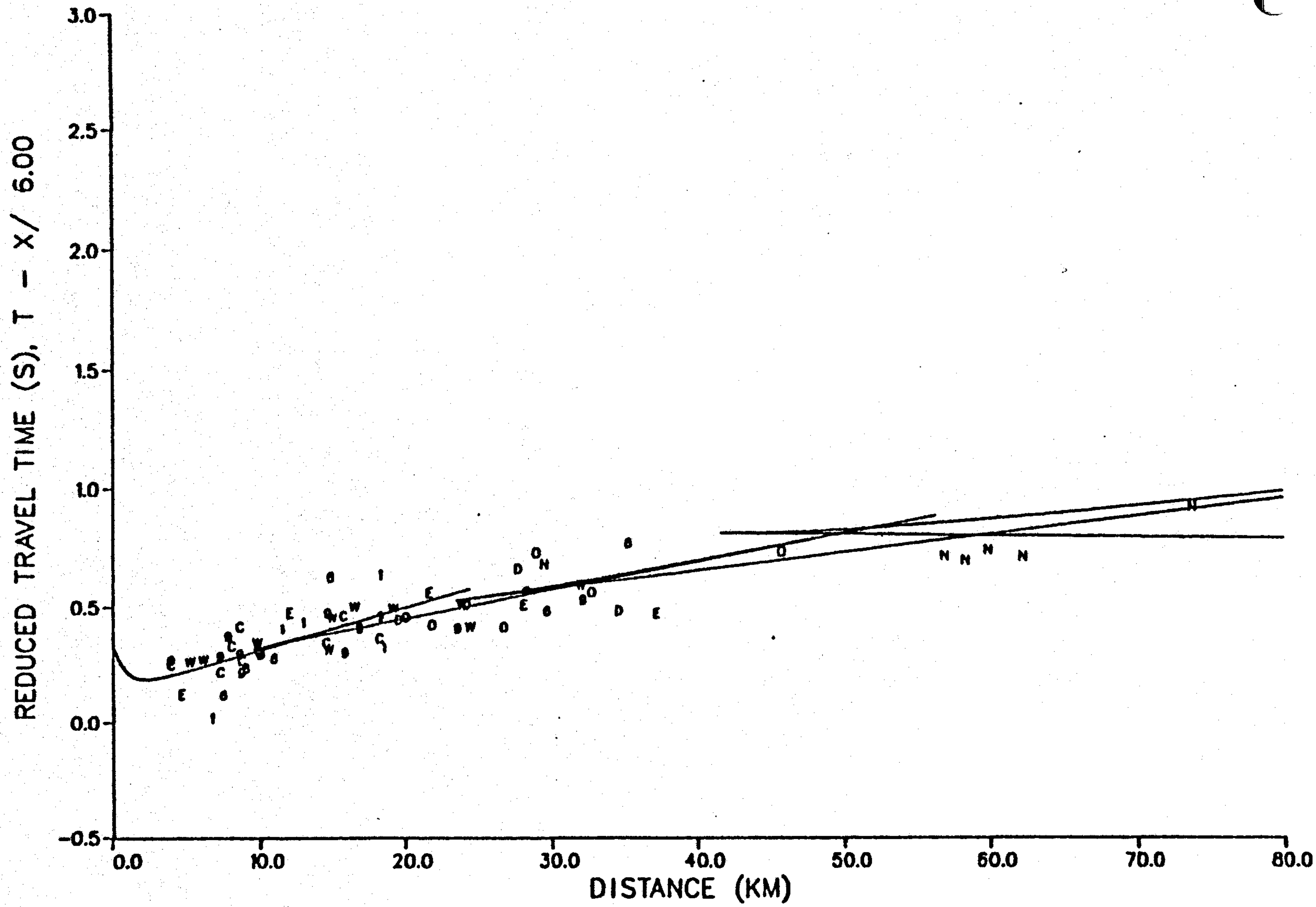

Figure 7b. Observed travel times, denuisanced with respect to event hypocenters. Focal depth range is 1 to 2 km. Focal depth for theoretical curve is 1.5 km.

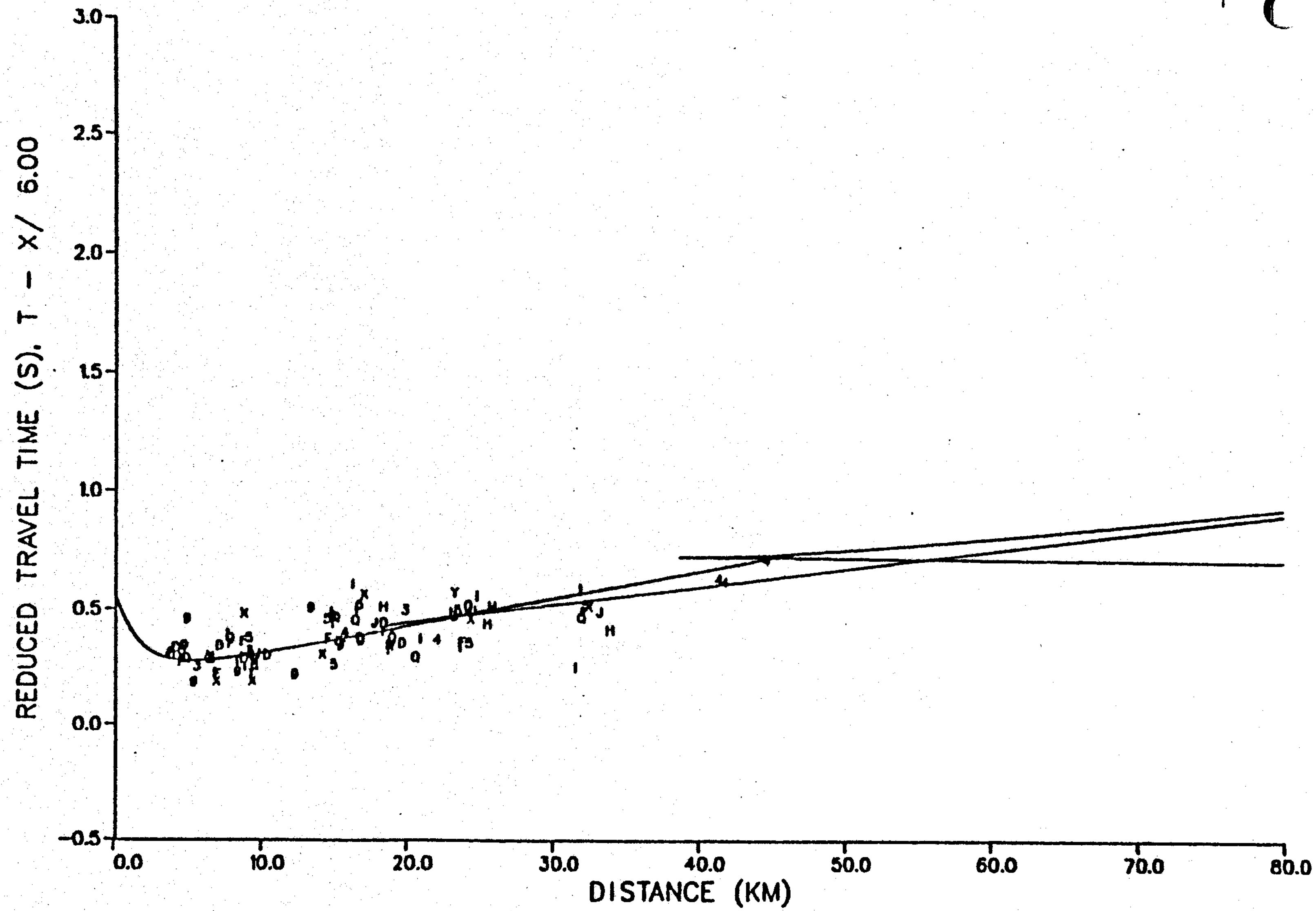

Figure 7c. Observed travel times, denuisanced with respect to event hypocenters. Focal depth range is 2.0 to 3.5 km. Focal depth for theoretical curve is 2.75 km.

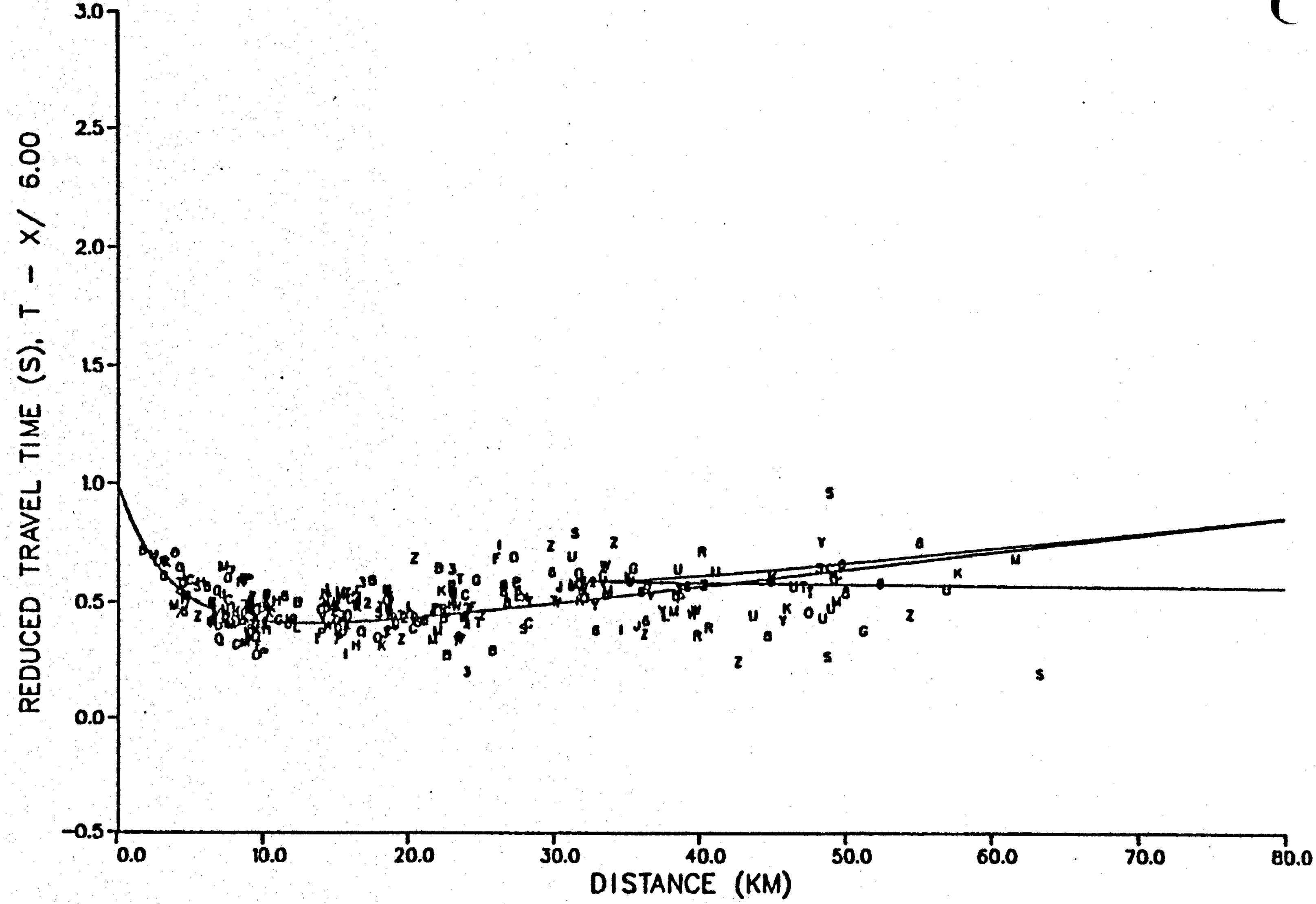

Figure 7d. Observed travel times, denuisanced with respect to event hypocenters. Focal depth range is 3.5 to 7.0 km. Focal depth for theoretical curve is 5.25 km.

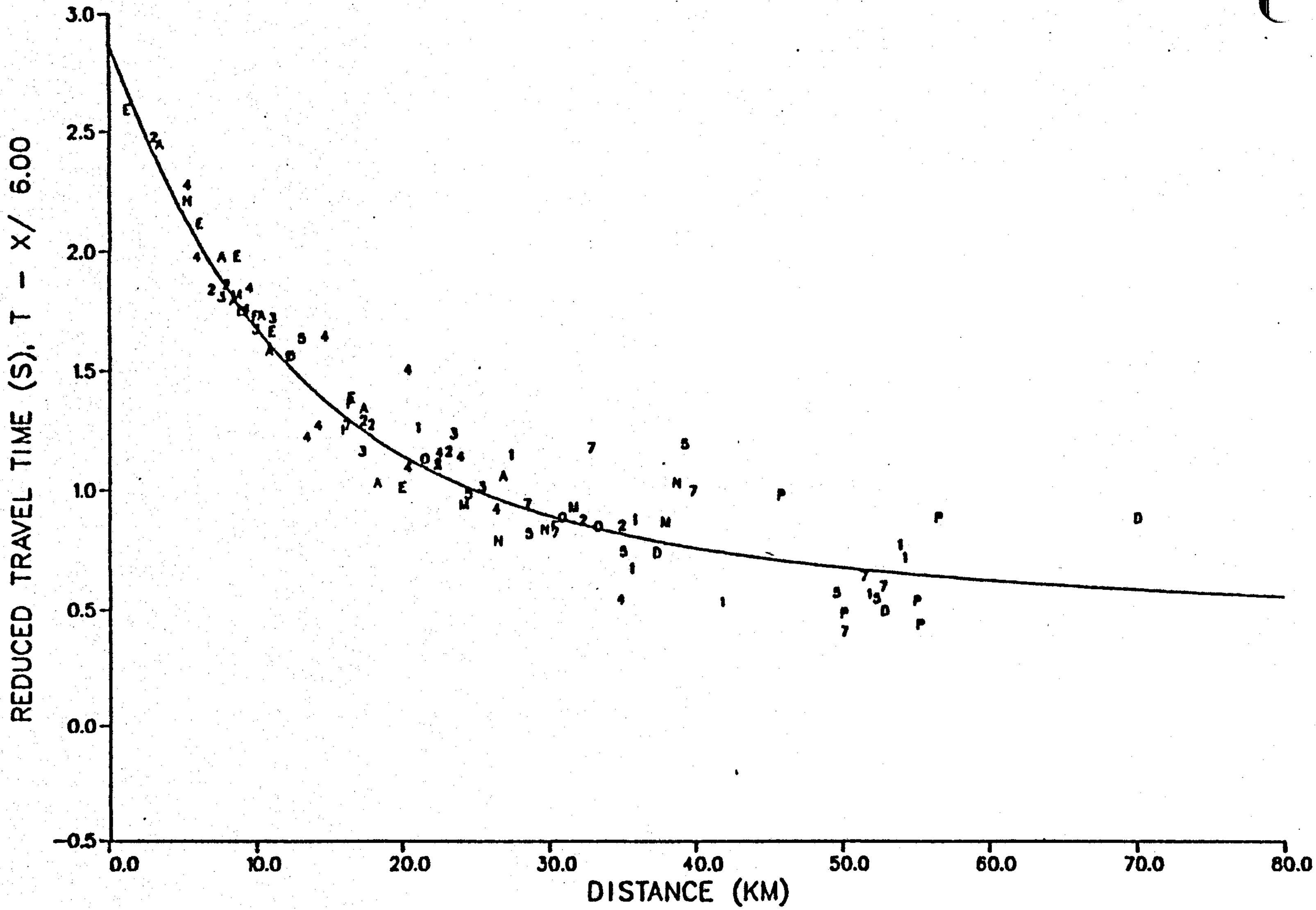

Figure 7e. Observed travel times, denuisanced with respect to event hypocenters. Focal depth range is 7 to 26 km. Focal depth for theoretical curve is 16.5 km.

is only 0.1 seconds. This value is clearly not much greater than the "noise level" associated with these data. The data in Figures 7a through 7e, consisting of 601 arrival times from 93 events, comprise the seismic data set used in subsequent inversions.

The fact that the seismic data mya have a low r.m.s. signal-to-noise ratio suggests the possibility that an inversion model obtained from these data will also have a low signal-to-noise ratio; i.e., the statistical uncertainties in the model velocity perturbations ($\delta\tilde{v}$) will exceed the magnitude of the perturbations themselves, indicating that the model fits primarily the noise. However, because our inversion algorithm is based on the joint optimization of data fit and model smoothness (and of variance and resolution), the signal-to-noise ratio in the inversion model is controllable through the parameter NDF (see Section 2.7). We will see in Section IV that the inversion models for our preferred values of NDF are not seriously contaminated by noise. Assuming the highest reasonable noise level in the data (0.1 s), the model uncertainties are less than one-third the major model perturbations.

3.2 RHS GRAVITY DATA

The gravity data for the RHS study region, consisting of 1468 terrain-corrected Bouguer anomaly values, was obtained from Dr. Kenneth L. Cook of the University of Utah. Figure 8 shows the locations at which the original gravity measurements were taken. The areal extent of the data is approximately 63 km by 43 km and is outlined by the dotted rectangle.

While somewhat premature, in Figure 8 we have superposed the model grid (i.e., the solid intersecting lines) used in the subsequent joint inversion to be discussed in Section IV. Our reasons for including the grid at this time are two-fold. First,

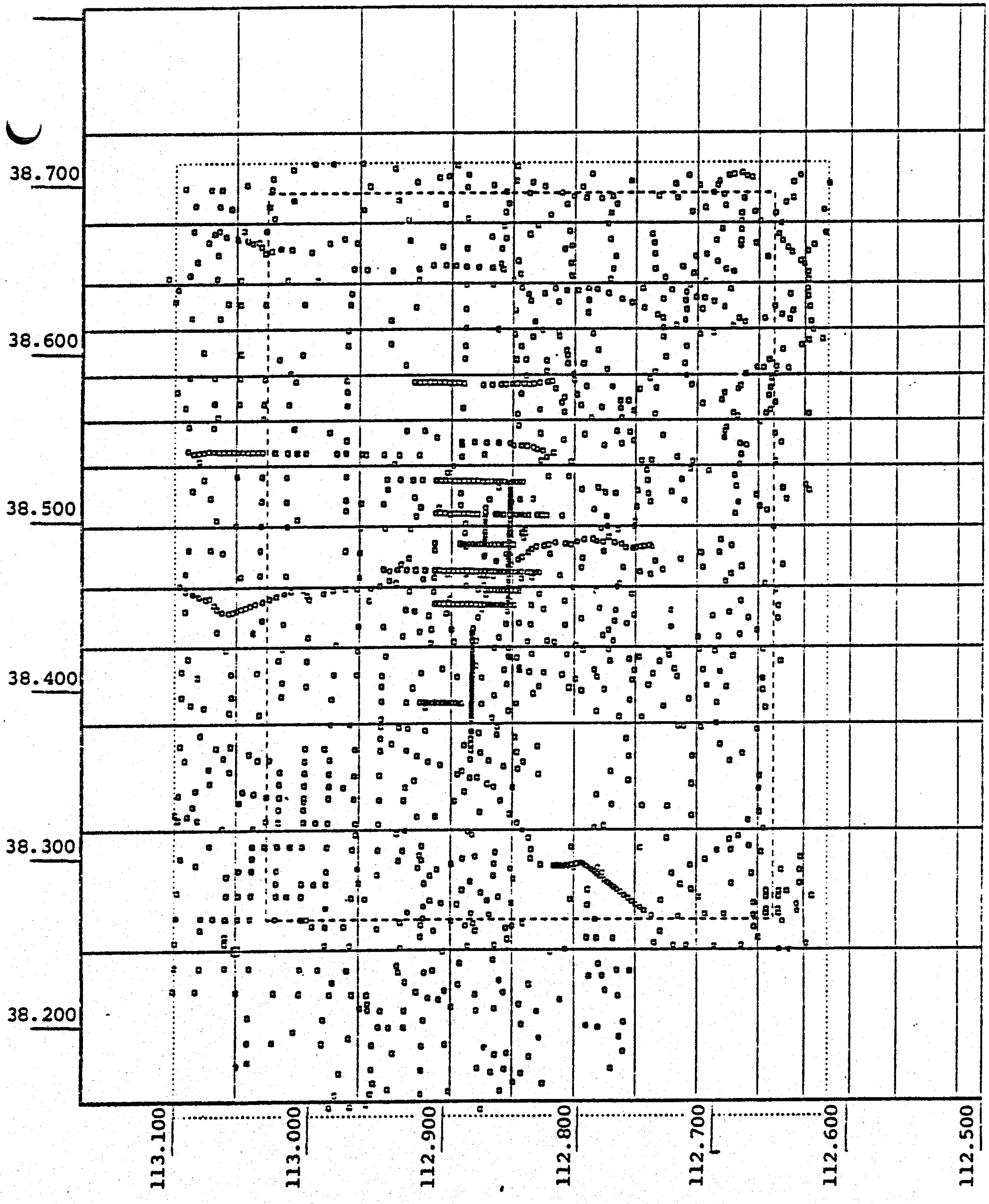

Figure 8. Locations of 1468 gravity stations (boxes) at which observed gravity data used in this study were measured. The solid intersecting lines show the model grid used in the inversion. The dotted box outlining stations is shown for later reference. The dashed box outlines the subset of data inverted.

the grid makes it easier for the reader to ascertain the density of gravity observations. For instance, the smallest grid cells are 3 km by 3 km and in several cases contain as many as ten gravity stations. The second reason is to emphasize a limitation imposed by the areal coverage of the gravity data. Note that the stations cover approximately 60 percent of the intended model grid which was designed to accommodate both seismic and gravity data. The influence of this limitation on the modeling results is discussed in the following section of this report.

3.2.1 Data Processing

The original gravity data were converted to a regular rectangular grid of 2709 values, spaced 1 km apart, by a least-squares quadratic surface interpolation technique (Savino, et al., 1977). A contour map of the interpolated values is shown in Figure 9. The frame of this figure corresponds to the dotted rectangle in Figure 8.

Figures 10 through 12 show the cumulative effects of the remaining series of processing operations that we applied to the gravity data in order to produce a final data vector to be inverted. In Figure 10 we contour the interpolated gravity data after low-pass filtering with a Gaussian filter having a half-width of 1.5 km; i.e., convolution with an operator of the form

$$(\text{const}) \exp \left[- \frac{1}{2} (x^2 + y^2)/(1.5)^2\right] ,$$

where x and y are UTM coordinates. Figure 11 shows the results of decimating the filtered, interpolated data to a 3 km grid spacing and truncating gravity values located on the periphery of the original data grid to conform to the dashed rectangle in Figure 8. Truncating the data was necessary in order to

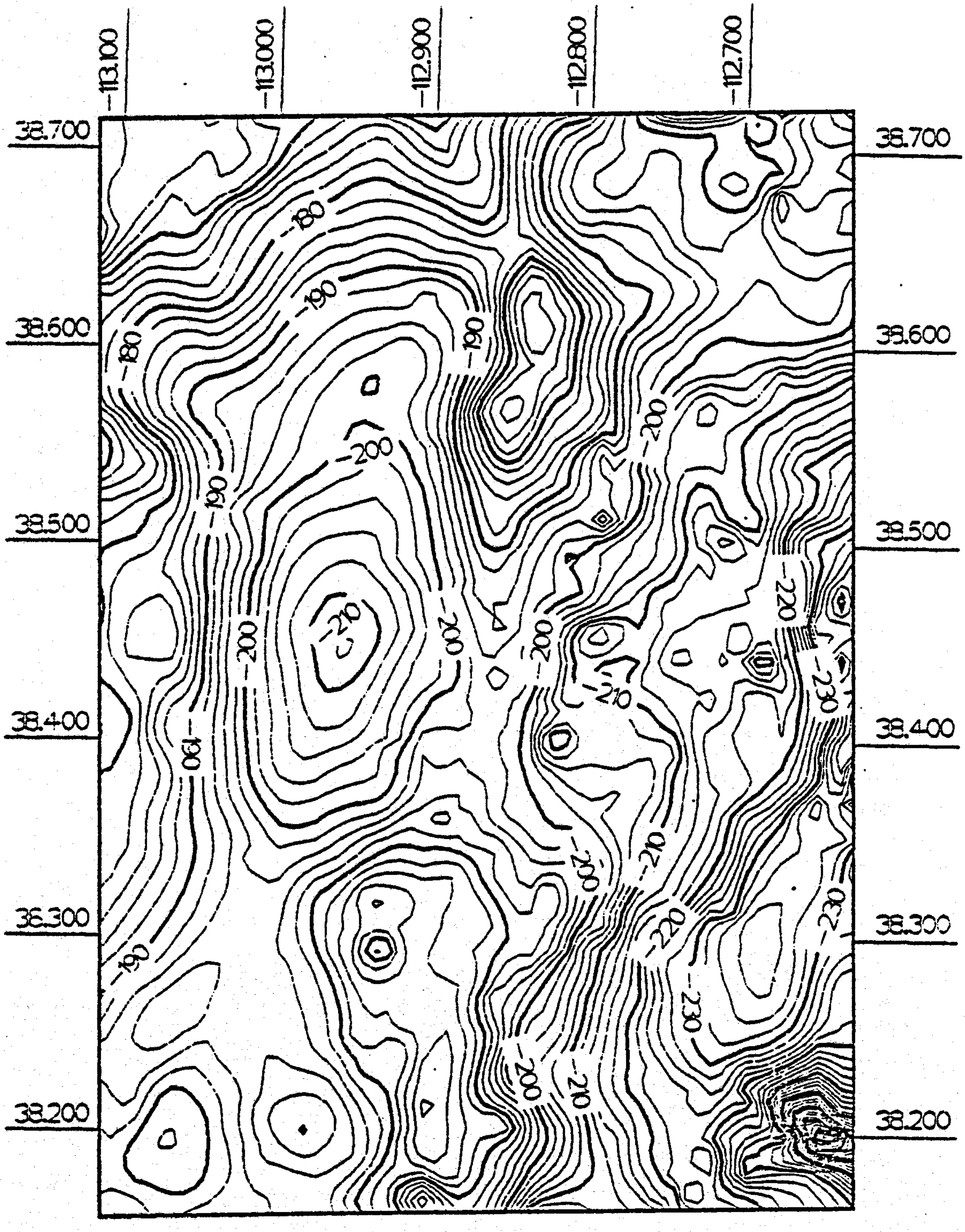

Figure 9. Contours of observed gravity data interpolated to a regular 1 km spaced grid (frame of figure is dotted box in Figure 8). Contour interval is 2 mgals.

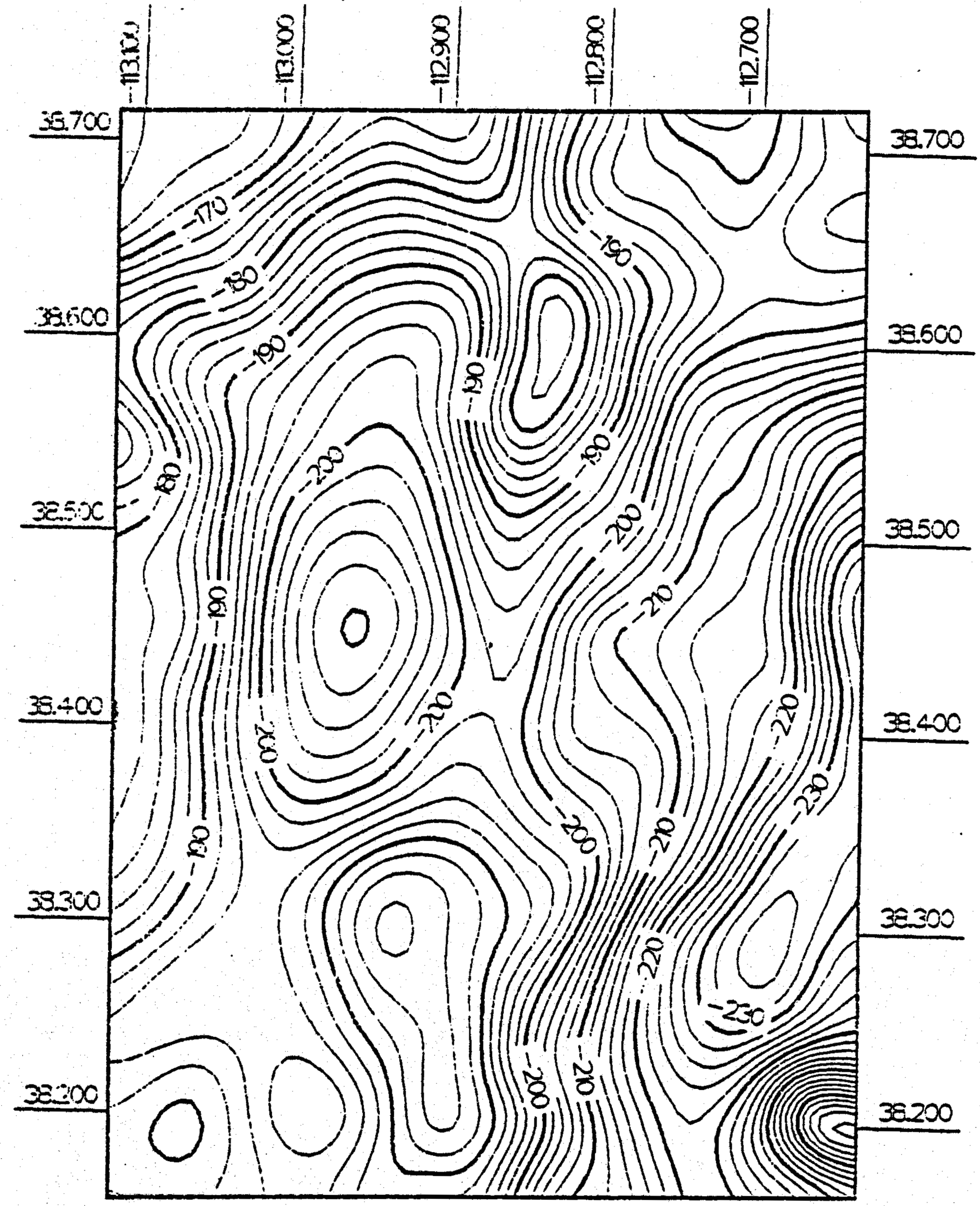

Figure 10. Gravity data, low-pass filtered with a 3.0 km bandwidth Gaussian filter.

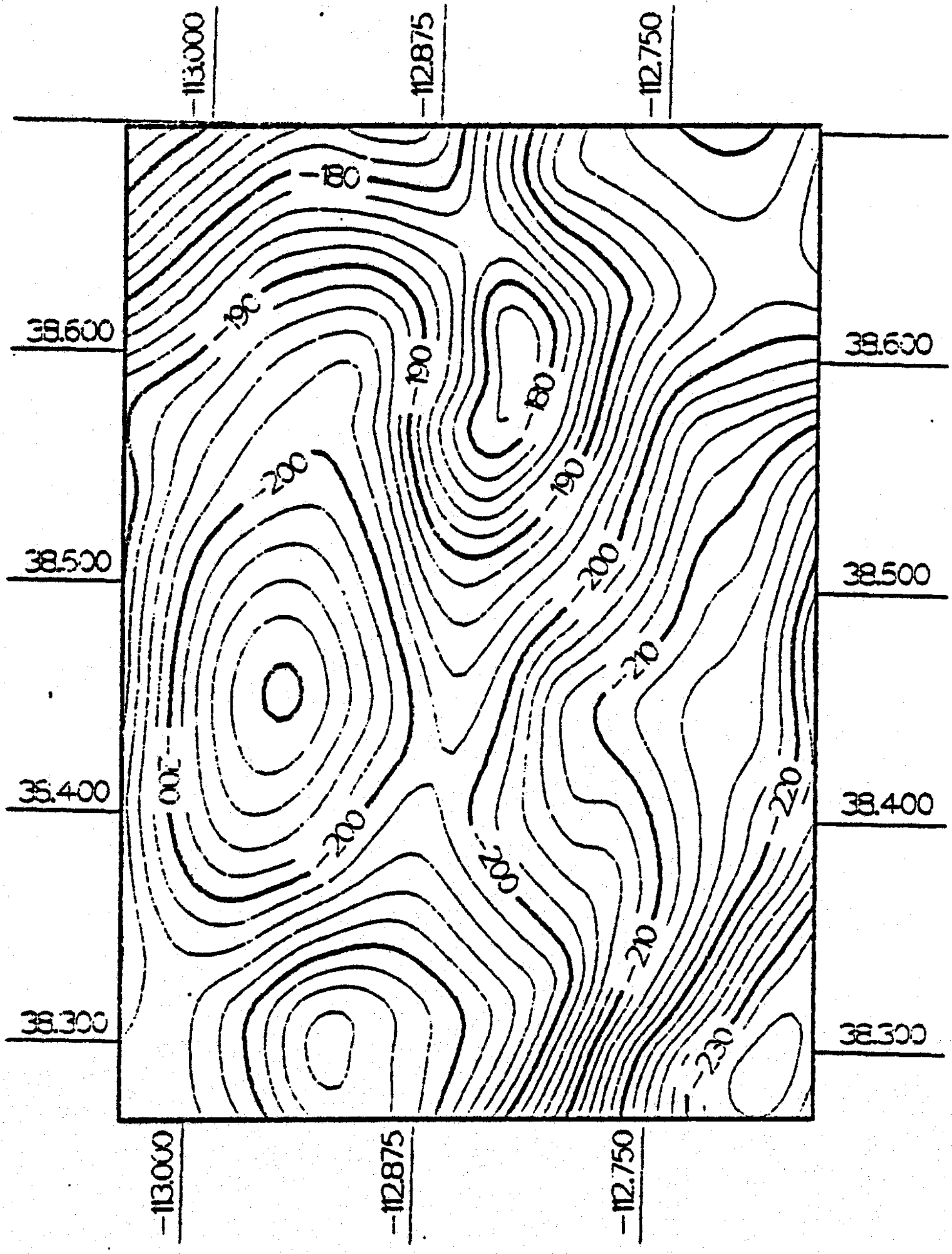

Figure 11. Gravity data, low-pass filtered (same as in Figure 10), decimated to 3 km grid spacing and truncated to limits of the dashed box in Figure 8.

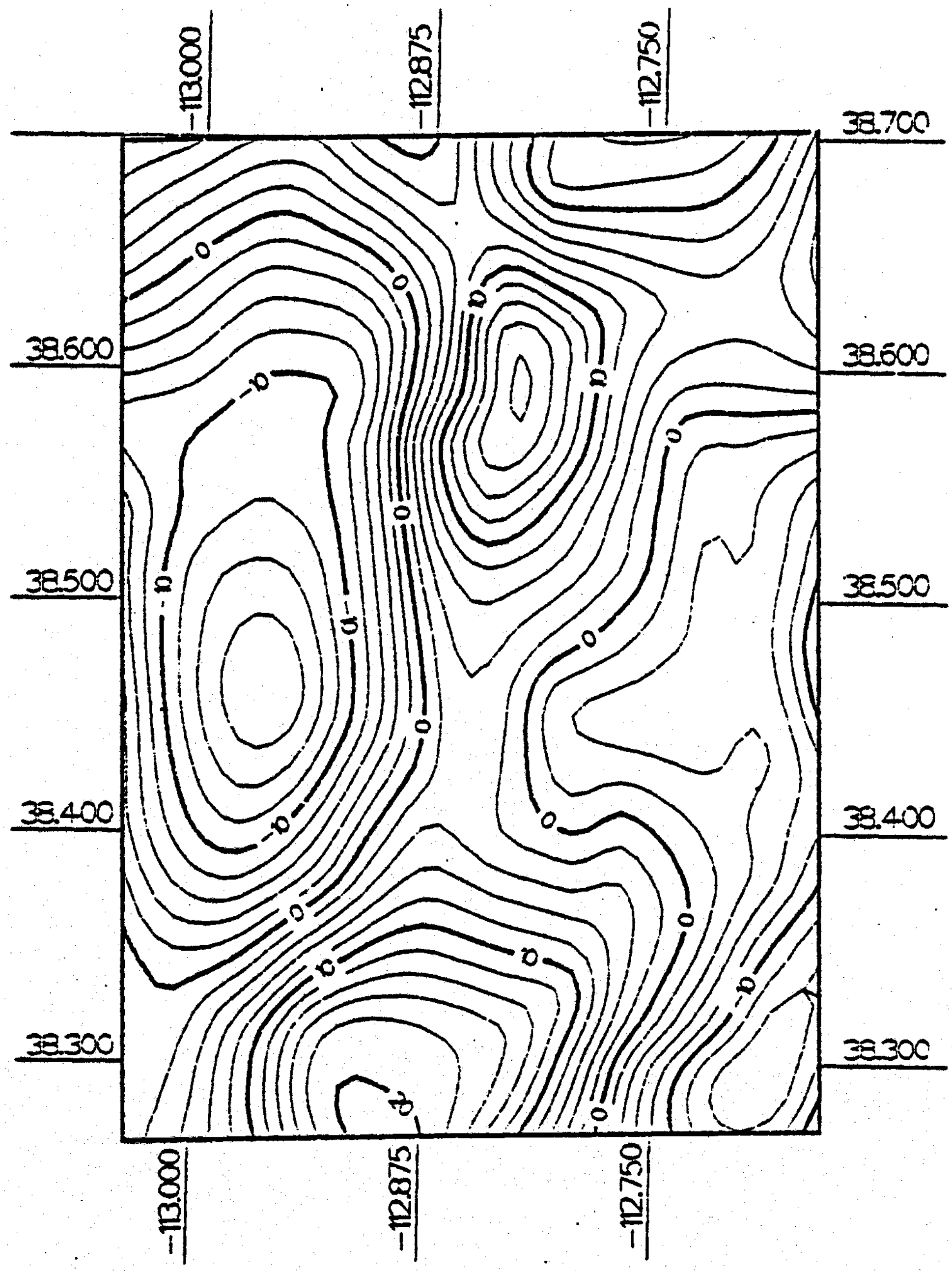

Figure 12. Gravity data (same as in Figure 10) but zero-meaned and detrended for the inversion.

avoid both edge effects and areas of poor data coverage such as the extreme southeastern corner of the region outlined by the dotted box in Figure 8. Given that the minimum horizontal block dimension of our inversion model is 3 km, our choice of filter and decimation parameters probably does not affect our inversion results.

The effects of deep structure on the gravity data (i.e., the regional field due to structure below the model grid) were treated as nuisance parameters. To accomplish this we parameterized the regional field as a constant plus a linear trend given by

$$g_{reg}(x,y) = g_0 + ax + by \quad ,$$

where the constants g_0, a and b are treated as nuisance parameters. Denuisancing the data, then, corresponds to detrending and demeaning the data (Savino, et al., 1977). A contour plot of the detrended and demeaned data is shown in Figure 12. This is the final gravity data set to be used in the inversion and consists of 204 values on a regular spaced grid (spacing equal to 3 km).

3.3 LEACH HOT SPRINGS, NEVADA

As mentioned in the introduction to this report, we were originally interested in applying this modeling approach to seismic and gravity data from a second geothermally active region, namely the Leach Hot Springs area in northwestern Nevada. The data sets for this area were located at the Lawrence Berkeley Laboratory and with the cooperation of several people there, we acquired all the available local earthquake travel-time and Bouguer gravity data.

A comparison of the seismic data sets available for the Roosevelt and Leach Hot Springs areas revealed an insurmountable problem concerning the data set for the latter area. The number of seismic travel-time data available for Roosevelt Hot Springs consisted of 601 arrival times. These data were shown in Figures 7a through 7e. Processing of the available data for Leach Hot Springs, on the other hand, indicated that the final data base was too small to attempt a worthwhile inversion. For instance, during the time period that a 13 station seismic network was operating in the Leach Hot Springs area, only 19 events were recorded at 7 or more stations. This compares with approximately 50 events recorded at 7 or more stations operating in the Roosevelt Hot Springs area. Our modeling experience to date convinced us that the spatial sampling of local earthquake ray paths, one of the most critical aspects of the data, in the Leach Hot Springs area is totally inadequate for inversion modeling. As a result, we placed our emphasis on the Roosevelt area.

IV. MODEL RESULTS

4.1 MODEL GRID

The vertical layering used in all inversions performed in this study was introduced in Section 3.1.1 and listed in Table 3. As noted, it consists of five horizontal layers extending to a depth of 26 km and provides a good fit to the observed travel-time data (Figures 7a through 7e) and an optimal parameterization in terms of the vertical distribution of ray paths.

The next task is to design a horizontal rectangular grid capable of representing lateral velocity and density variations across the region of interest. Our design must meet with the following constraints:

1. The grid samples the entire area covered by both the seismic event and gravity data sets retained for modeling with a minimal waste of unsampled blocks.

2. Grid elements are smaller in areas well sampled by seismic events and gravity data.

3. The grid consists of two parts: an inner grid of finite blocks, containing most of the data, surrounded by a buffer zone of semi-infinite elements (the outer grid), for which structural modeling is necessarily imprecise and unreliable due to poor parameterization.

A 12 by 13 element inner grid was adopted for the inversion modeling. This inner grid, together with the associated outer grid, is shown in Figure 13 on a background of geographical coordinates. Also shown are the 93 local

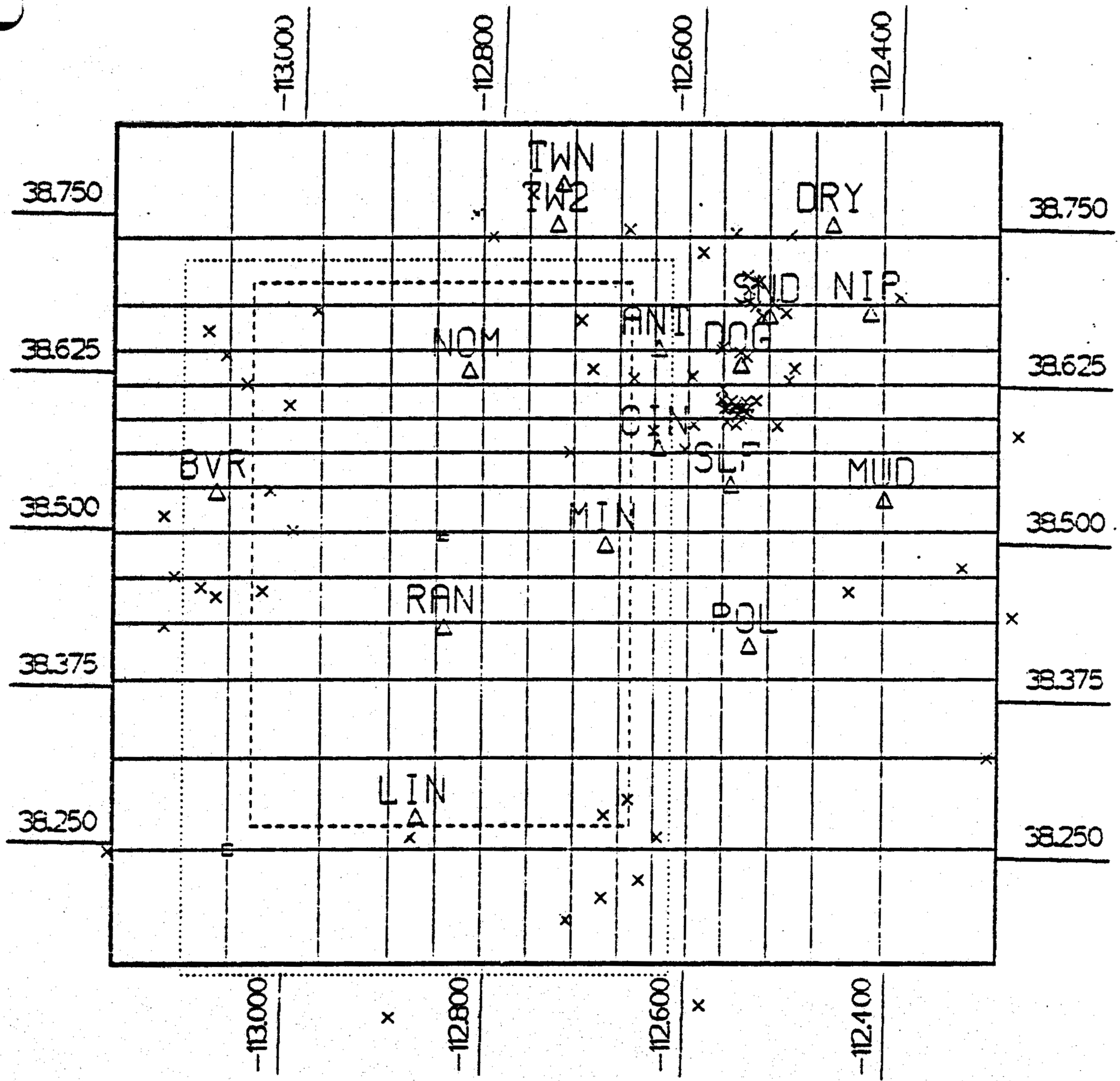

Figure 13. Model grid (intersecting lines), seismic stations (triangles) and earthquake epicenters (crosses). Boundaries of raw gravity data and inverted gravity data are shown by dotted and dashed boxes, respectively.

earthquakes (crosses), 18 seismograph stations (triangles) and the boundaries of the raw gravity data (dotted box) and the final processed gravity data (dashed box). The actual dimensions of the model grid elements are listed in Table 5.

4.2 INVERSION MODELS

Three-dimensional models of the crustal velocity structure in the Roosevelt Hot Springs area were obtained from two inversions: a joint inversion of the seismic travel-time and gravity data (Figures 7 and 12), and an inversion of the travel-time data by themselves. Both inversions solve for a velocity perturbation in each block of the three-dimensional grid described in Section 4.1. The perturbations are with respect to the initial plane-layered velocity model given in Table 3.

In the joint inversion, density perturbations were treated as constrained parameters. The density perturbation, $\delta\rho$, of each block was tied to the velocity perturbation, δv, by

$$\delta\rho = 0.3\ \delta v \quad .$$

This relationship approximates that determined by Birch (1961) for crustal igneous and metamorphic rocks. We note that the density perturbation $\delta\rho$ is defined with respect to a plane-layered model, $\rho_0(z)$, which is not specified. Since the gravity data and their partial derivatives are demeaned as a result of denuisancing (see Section 2.6), $\rho_0(z)$ is inconsequential; i.e., the inversion neither requires ρ_0 as input nor determines ρ_0 from the data.

A constant ratio between velocity and density contrasts, as we have assumed, does not necessarily apply to the variety of subsurface materials encountered throughout our model region (e.g., Gertson and Smith, 1979). For the known hard

TABLE 5

HORIZONTAL GRID DIMENSIONS

Block Index (S-N)	Block Width (km)	Block Index (W-E)	Block Width (km)
1	10*	1	10*
2	8	2	8
3	7	3	6
4	5	4	4
5	4	5	4
6	4	6	4
7	4	7	4
8	3	8	4
9	3	9	3
10	3	10	3
11	3	11	3
12	4	12	4
13	6	13	4
14	10*	14	6
		15	10*

*For plotting only; edge blocks are assumed to be semi-infinite in the actual modeling.

rock geology of the area, the ratio we assumed is reasonable. This includes the granitic rocks of the Mineral Mountains, and the metamorphic rocks believed to underlie the Milford Valley (Ward, et al., 1978). Our ratio may be less appropriate for the contrast of these rocks with the known Quarternary basalts east of the Mineral Mountains, but the gravity data barely extend this far eastward. The only serious question about our assumed velocity-density relation arises with existence of alluvial fill in the Milford and Beaver Valleys. In the case of the Milford Valley, Gertson and Smith (1979) suggest a rather small density contrast between Tertiary sediments and bedrock: ∿ 0.2 gm/cc compared a velocity contrast of ∿ 1.5 km/s. However, they note that a larger sediment-bedrock density contrast might be required by the gravity data, and in fact Ward, et al. (1978) were able to fit the gravity along a profile over Milford Valley by assuming a density contrast of 0.5 gm/cc. This latter value would support our assumed velocity-density ratio.

The only known violation of our density-velocity law, then, occurs with the surface fill of very low velocity (∿ 1.8 km/s) recent sediments in the Milford Valley. For these, in comparison to bedrock, our coefficient 0.3 is too high. But these superficial sediments have limited areal extent over our model and, because of their limited depth extent and expected small density contrast with the underlying Tertiary sediments, probably do not contribute much to the gravity data. We have corrected the travel-time data at station BVR for these sediments; if it could be shown that they have a significant effect on the gravity data, we would prefer to do a gravity correction as well. However, a sufficiently accurate three-dimensional model of the recent sediments is not available.

Both the joint gravity/seismic inversion and seismic-only inversion produced a family of models corresponding to a trade-off between data misfit and model roughness, as described in Section 2.7. The trade-off is parameterized by the scalar parameter θ, or equivalently by the number of degrees of freedom NDF (see Equation (45)). In each inversion, we generated models for six values of θ: 30, 10, 3, 1, 0.3, and 0.1. The corresponding values of NDF ranged from 45 to 259 in the joint inversion, and from 14 to 150 in the seismic only inversion. Figure 14 displays the data misfit/model roughness trade-off curves obtained in the two inversions. The points resulting from the six computed models are labeled on the figure; the curves shown were interpolated between these points. The data misfit plotted is defined as the sum of squared residuals (observed minus predicted data), normalized by the assumed data standard deviations (0.1 second for travel times, 2 mgal for gravity). The squared model norm is the discrete approximation to the integral defined in Equation (20). It measures the average spatial "roughness" of the velocity perturbation, $\delta\tilde{v}(x,y,z)$, as reflected both by the magnitude of $\delta\tilde{v}$ and its wavenumber content; i.e., large variations in $\delta\tilde{v}$ on a small spatial scale imply a high degree of roughness.

A model generated with any NDF is optimal in the sense that the data misfit and model roughness are jointly minimized; i.e., each quantity is minimum given a fixed value of the other (Backus and Gilbert, 1970). However, the models for extreme values of NDF are not very useful representations of the earth. For a too low NDF, the model is so spatially smooth that it does not adequately represent real variations in the earth's velocity which are required by the data. For too high an NDF, the model possesses spurious small-scale variations which attempt to fit the noise in the data.

The parameter NDF also controls a trade-off between the variance of the inversion model and its spatial resolution (see Section 2.7). We examined this trade-off for the joint

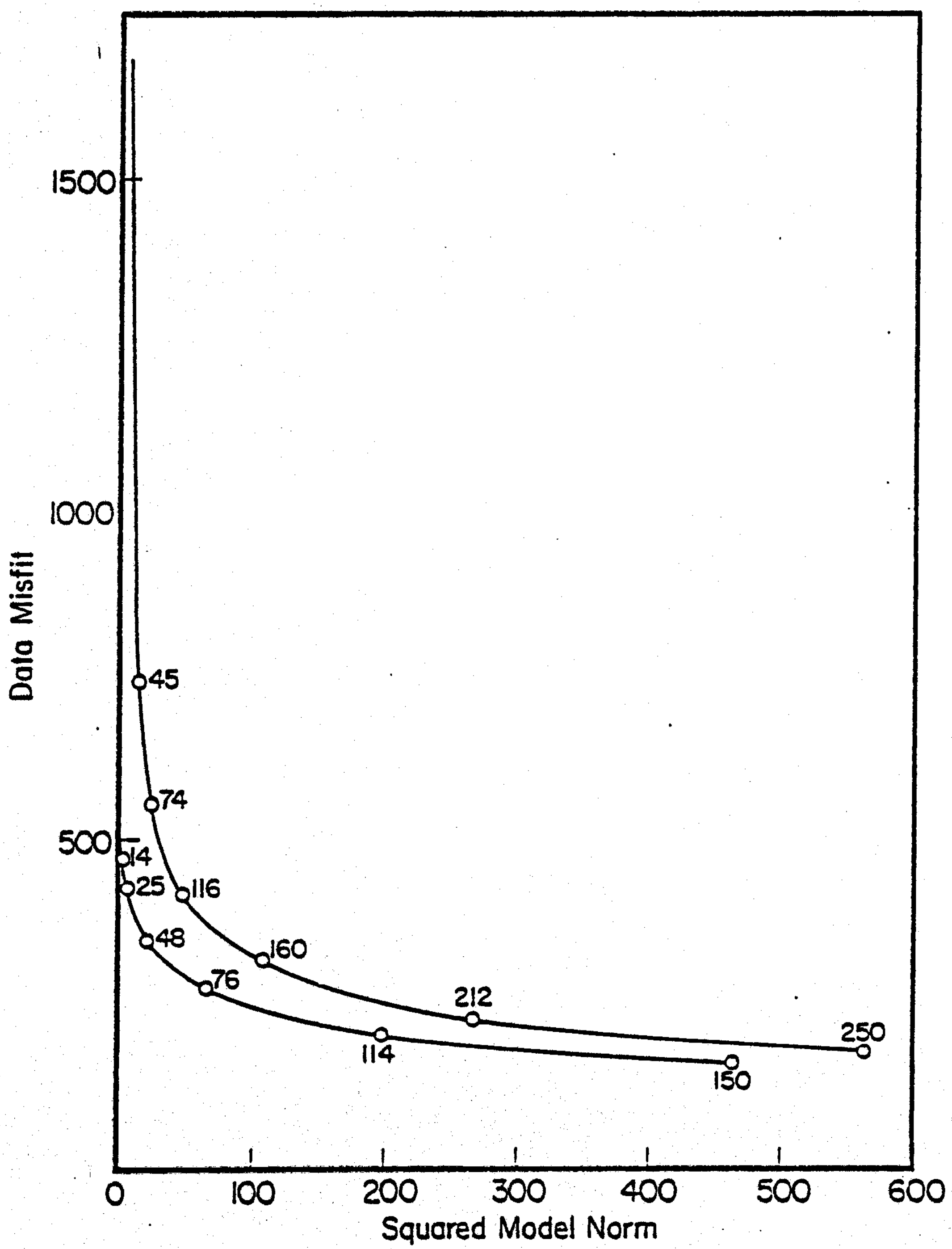

Figure 14. Trade-off curves for travel-time inversion (bottom line) and joint travel-time/gravity inversion (top line). Ordinate ("data misfit") is the sum of squared differences between observed and predicted data (normalized by data variances). Abscissa is a measure of model "roughness." Points on trade-off curves corresponding to various numbers of degrees of freedom (NDF) are labeled.

inversion model family. A separate variance-resolution trade-off curve exists for each block of the model, but our analysis showed that the trade-off curves varied significantly only with depth; for a given NDF, the variance obtained for a block and, to a lesser extent, the resolution did not vary greatly within a given layer (inside the inner grid).

Table 6 shows the trade-off between variance and spatial resolution — determined from the joint seismic/gravity inversion — for the column of model blocks that most nearly lies beneath Roosevelt Hot Springs; i.e., block index (6,5) of each layer (refer to Figure 13). The upper part of the table lists, for each layer and NDF, the standard deviation of the velocity perturbation estimated for the particular block. The "normalized resolution measure" listed in the lower table is a dimensionless quantity which reflects the extent to which the velocity perturbation is spatially averaged over blocks surrounding the target block, (6,5), in a given layer. A value of one for this quantity would imply the best possible spatial resolution — i.e., the velocity in the target block is determined independently of all other blocks — while a value of zero is the worst possible resolution. Since this resolution measure is normalized, it cannot be converted to a measure of "resolving length" as defined by Backus and Gilbert (1970). It can be compared between NDF's, but unfortunately it is difficult to relate its value among different model blocks.

To select a "best" model among the six joint inversion models that we computed, we were swayed to a great extent by the standard deviations in Table 6. It is desirable to have the standard deviation of $\delta\tilde{v}$ in a layer be only a fraction — say, less than one-third — of the principal extrema of $|\delta\tilde{v}|$ in the layer (adjusted for the average $\delta\tilde{v}$ of the layer). Otherwise, the noise-contributed component of $\delta\tilde{v}$ causes a significant distortion in contours of the block velocities and in the location of velocity highs and lows. Only the

TABLE 6

VARIANCE-RESOLUTION TRADE-OFF FOR BLOCK (6,5)
IN FIVE LAYERS OBTAINED FROM THE
JOINT SEISMIC/GRAVITY INVERSION

Standard Deviation of Velocity Perturbation

NDF

Layer	45	74	116	160	212
1	0.06	0.15	0.34	0.60	0.91
2	0.11	0.16	0.22	0.30	0.46
3	0.07	0.09	0.15	0.22	0.31
4	0.04	0.06	0.09	0.13	0.20
5	0.03	0.04	0.05	0.07	0.11

Normalized Resolution Measure (see text)

NDF

Layer	45	74	116	160	212
1	0.39	0.53	0.70	0.82	0.89
2	0.77	0.83	0.86	0.88	0.90
3	0.89	0.92	0.95	0.96	0.97
4	0.90	0.92	0.94	0.95	0.96
5	0.79	0.86	0.89	0.90	0.92

NDF = 45 and 74 models clearly meet a criterion of this type for all five layers. We note that in applying this rule, we are free to scale the model standard deviations up or down by revising the assumed data standard deviations. The fits of the models to the observed data (discussed below) suggest revising our assumed data variances downward, but not by very much.

In Table 6 we see that the model standard deviations tend to decrease with depth (increasing layer number). This is also true of the standard deviations relative to the velocity extrema themselves. Applied on a layer-by-layer basis, our standard deviation criterion would, therefore, accept higher NDF's as we go to deeper layers. For this reason we will later examine the structure in some of the deeper layers of the high NDF models to aid in our interpretation of the inversion results. However, the noisy nature of the shallow layers of these models do not qualify them in our eyes as optimal models. Furthermore, we do not consider a composite model constructed from two or more NDF's to be a valid inversion model since it does not satisfy our data misfit/model norm minimization criterion (Equation (36)).

Between the joint inversion models for NDF = 45 and NDF = 74, we judged the latter to be a better model. Although the former model has smaller standard deviations, it also has poorer spatial resolution (see Table 6, bottom). Furthermore, the data misfit/model norm trade-off curve (Figure 14) shows that the NDF = 74 model provides a significantly improved fit to the data with a relatively minor increase in spatial roughness. We verified this by visually inspecting plots of the data fits and model velocity contours.

The joint inversion model for NDF = 74 is displayed in Figures 15a through 15e as a contour map of velocity perturbations (in km/s) for each of the five model layers. The contours

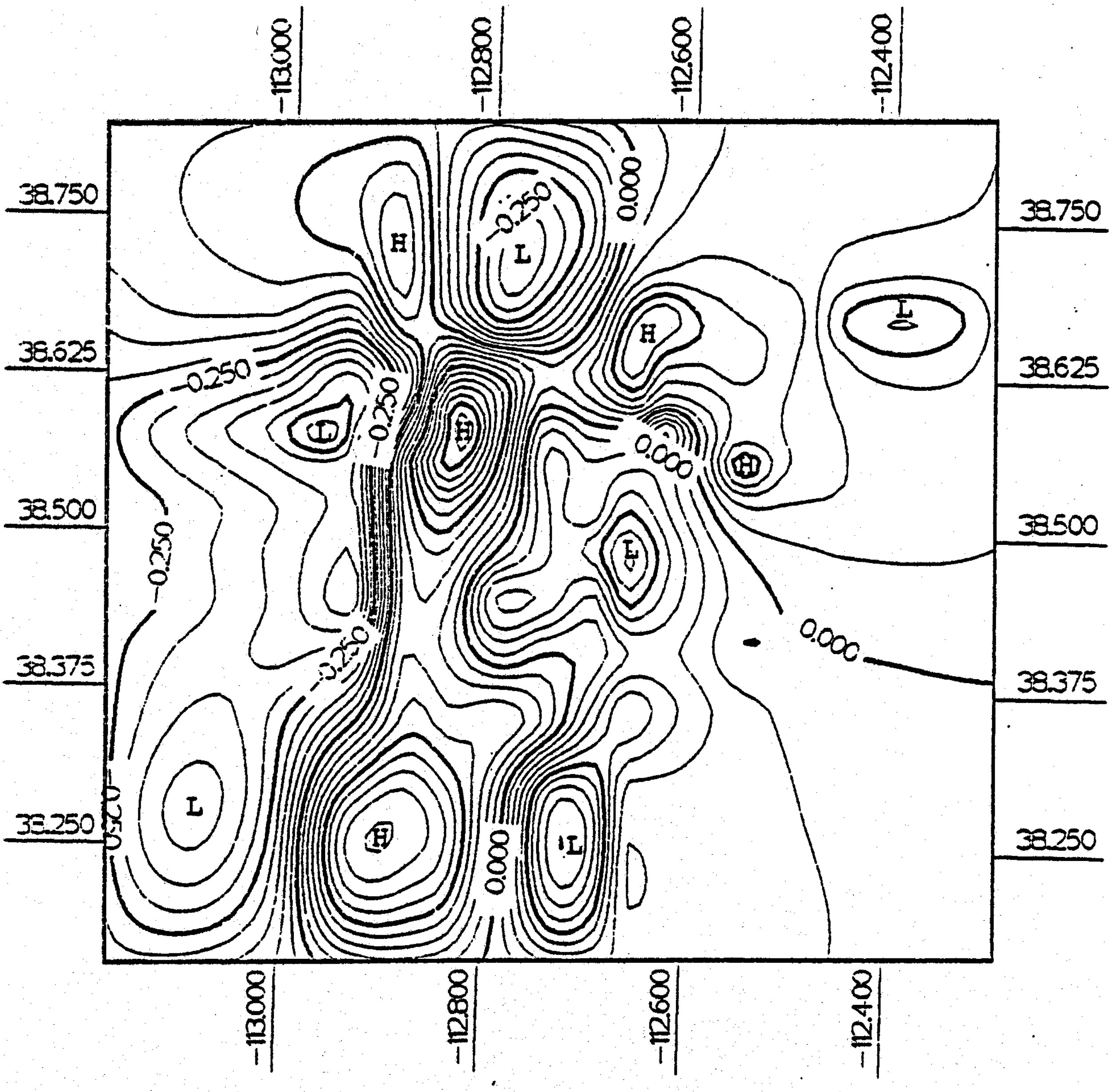

Figure 15a. Contour map of velocity perturbations in Layer 1 (0 - 1 km) of the final joint inversion model for NDF = 74. The contour interval is 0.05 km/s.

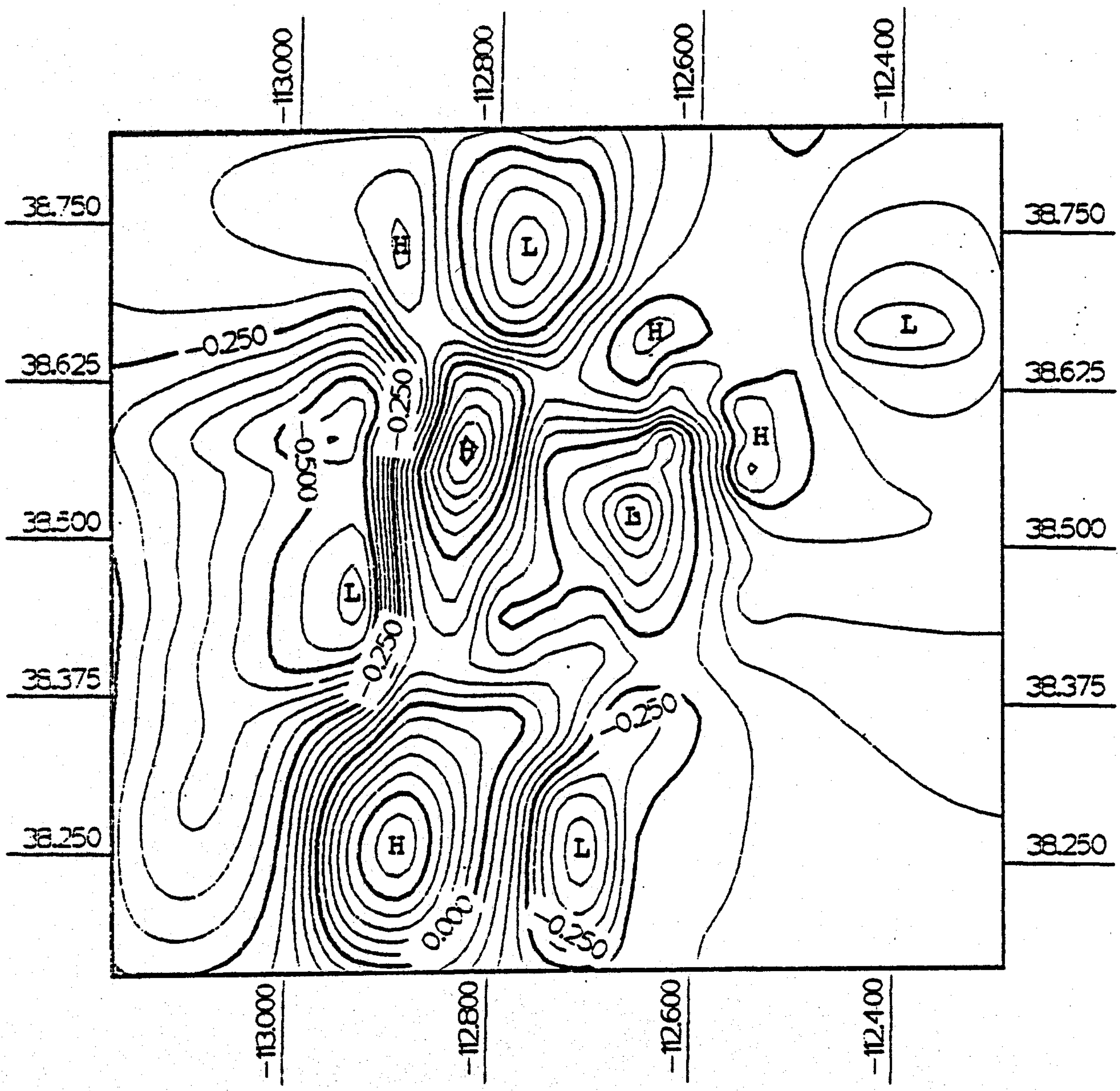

Figure 15b. Layer 2 (1 - 2 km) of joint inversion model for NDF = 74.

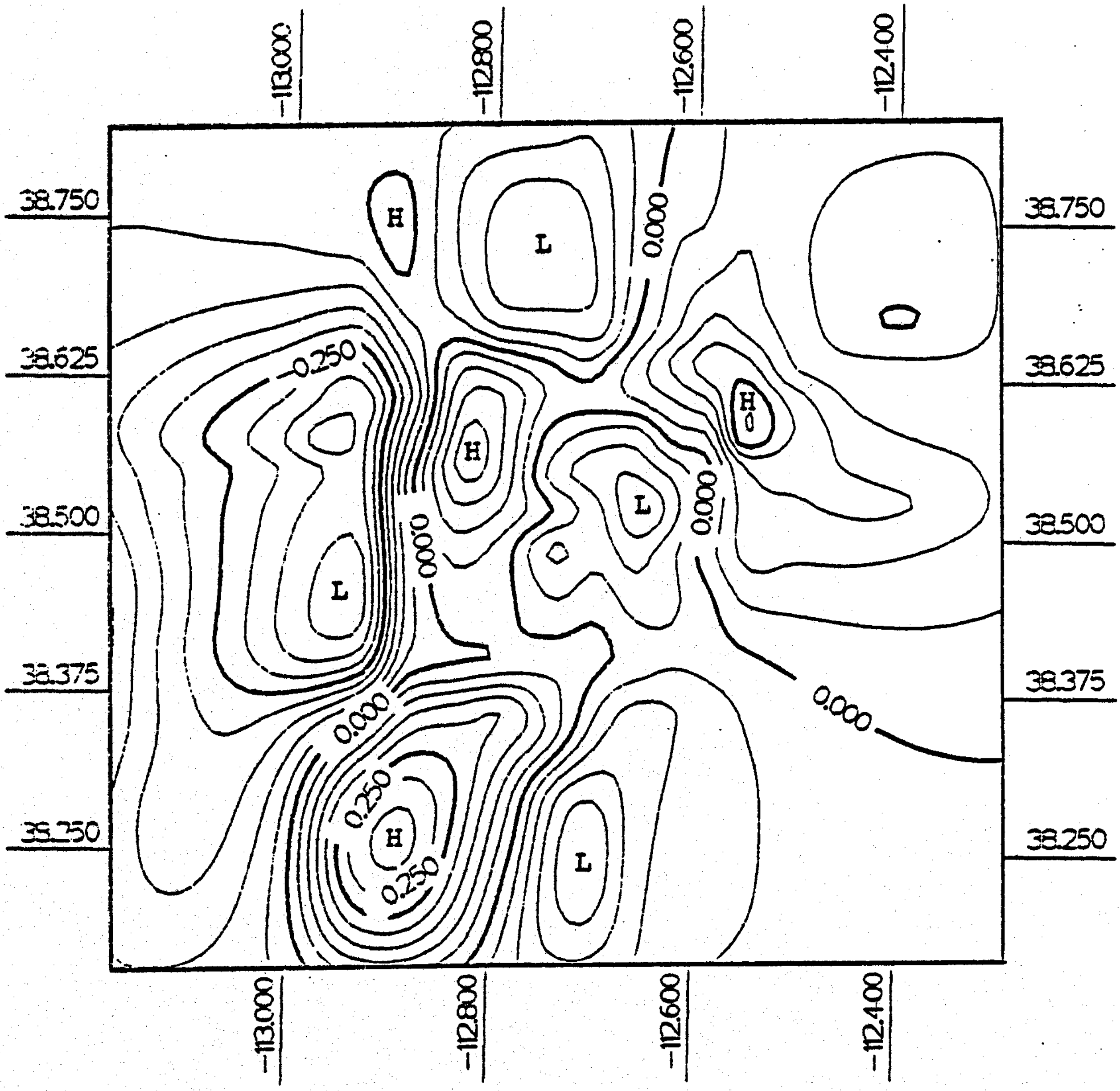

Figure 15c. Layer 3 (2.0 - 3.5 km) of joint inversion model for NDF = 74.

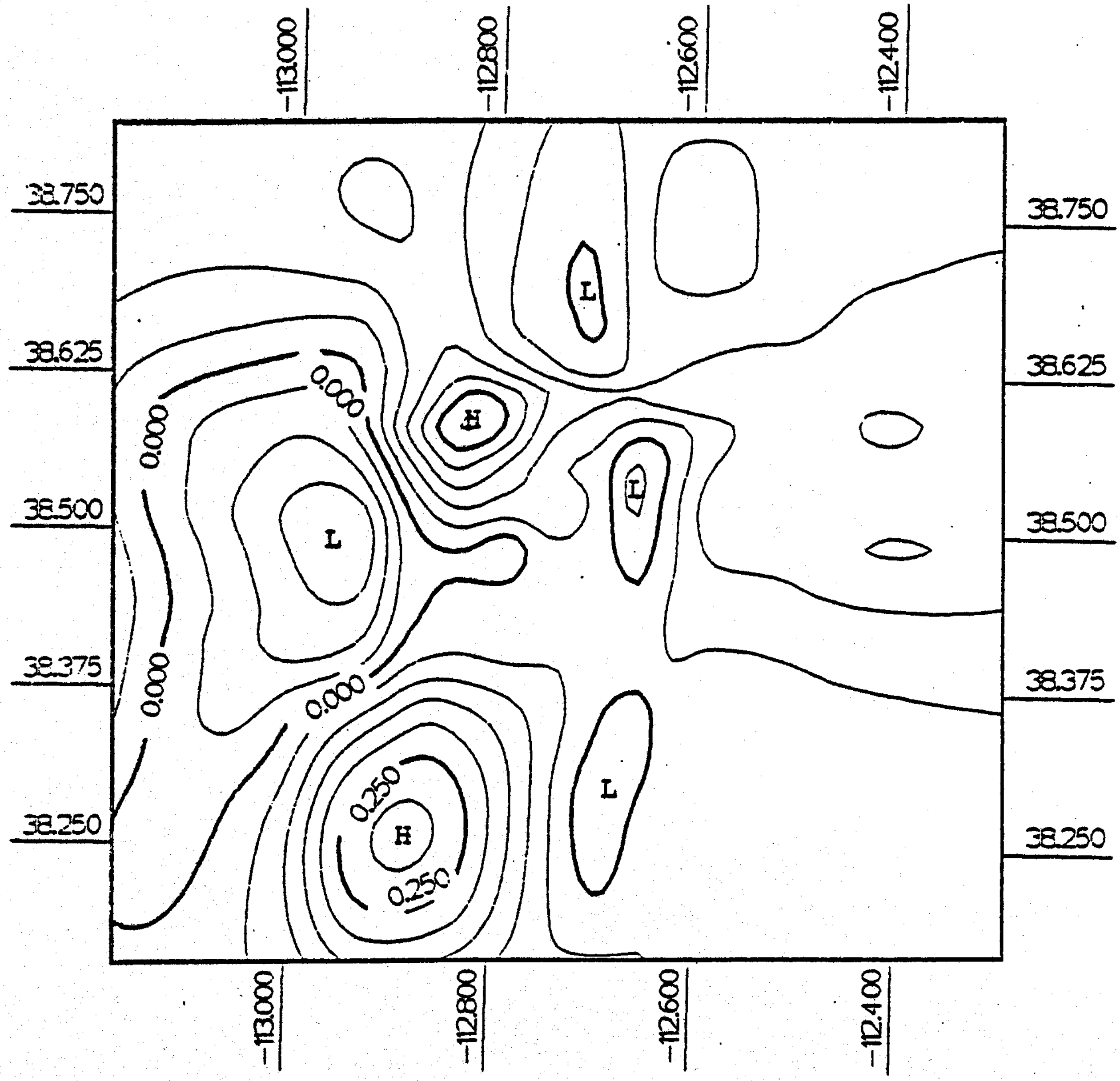

Figure 15d. Layer 4 (3.5 - 7.0 km) of joint inversion model for NDF = 74.

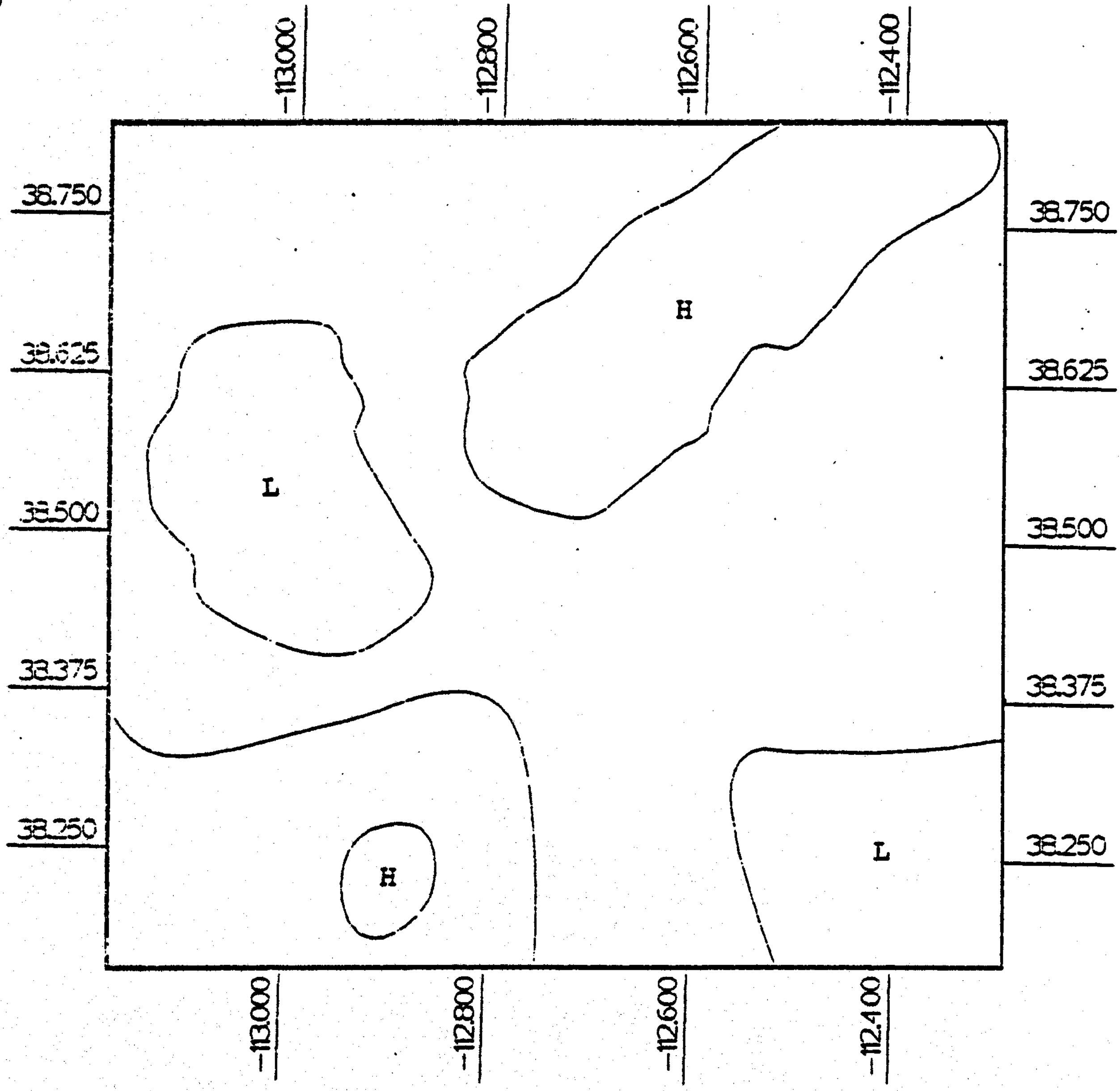

Figure 15e. Layer 5 (7 - 26 km) of joint inversion model for NDF = 74.

are interpolated from the individual block values of velocity. Absolute velocities can be obtained simply by adding the initial velocity of each layer (Table 3) to the velocity perturbations found by the inversion. We note that the contours in Figure 15 are displayed over the 14 by 15 array of "outer grid" blocks defined in Section 4.1.

For completeness, we present in Appendix B the discrete block version of the NDF = 74 joint inversion model. In the appendix, velocity perturbations are given and they are shown for the full 14 by 15 grid including edge blocks.

In the next section, we compare the observed gravity and travel-time data to the data predicted by our preferred joint inversion model (Figure 15), and evaluate the quality of fit. An interpretation of our model follows in the subsequent section. Because of the success of the joint inversion, we consider our inversion of the travel-time data to be a preliminary step in obtaining our final joint inversion model, as well as a corroboration of the assumed velocity-density systematics. We will, however, make use of some of the seismic-only inversion results in our interpretation (Section 4.4).

4.3 DATA FITS

A useful and informative test of our model lies in the comparison of predicted data functionals (namely, travel-time and gravity anomalies) with the observed values. The observed (Figures 7a through 7e) and predicted travel-time data based on the final joint inversion model (Figure 15) are shown in Figure 16. The format used for showing these data is the following. A circle is drawn around the location of each of the 18 seismograph stations used in this study. The circumference of each circle corresponds to a zero travel-time residual. Positive residuals are represented by lines extending out from the circumference at azimuths corresponding

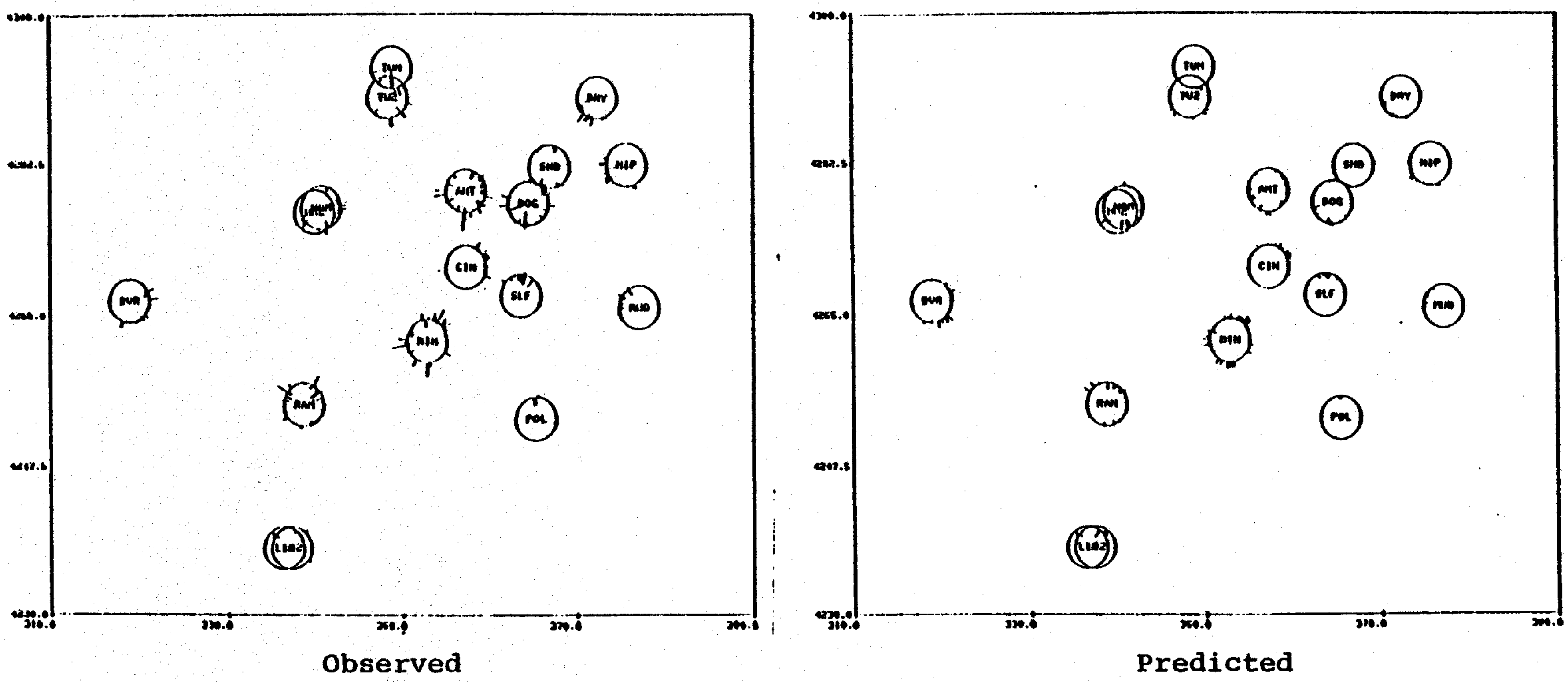

Figure 16. Comparison of observed travel-times (left side) and model-predicted values (right side) for the final joint inversion model (NDF = 74) in Figure 15. Circle radii for observed data are 0.5 seconds, predicted data 0.25 seconds.

to the contributing events. Negative residuals are drawn in toward the center of a circle. The length of any particular line is scaled according to the size, or absolute value, of the residual.

While the form of data representation in Figure 16 has the advantage of showing the behavior — that is the sign, size and azimuthal distribution — of travel-time residuals over the model region, there are two important disadvantages that should be kept in mind when perusing these figures. First, residuals with values near zero seconds (i.e., ± 0.05 seconds) are hard to distinguish and, as a result, fits in this range tend to go unnoticed. Second, the magnitudes of the predicted residuals are in general significantly smaller than the observed values. One reason for this stems from the damping imposed on the inversion procedure which tends to limit the amplitude of lateral variations in the model, and hence to bias predicted residuals toward smaller values. In addition, the high noise level in the observed data acts to create a visual impression that the observations are under-predicted since larger (in general noisy) residuals in the plot of observed data are much more obvious to the eye than those with more average values, so that visual averaging can actually be quite misleading.

With these caveats in mind, we point out that some general features of the observed data set are indeed reflected in the model-predicted values (Figure 16). For instance, the transition from stations with predominantly positive observed residuals (e.g., MIN and CIN) to largely negative residual stations (ANT, DOG and SLF) is reproduced by the predicted residuals. The r.m.s. misfit of the travel-time residuals is 0.085 seconds.

In Figure 17, we compare the observed gravity data (i.e., the zero-meaned and detrended data shown in Figure 12)

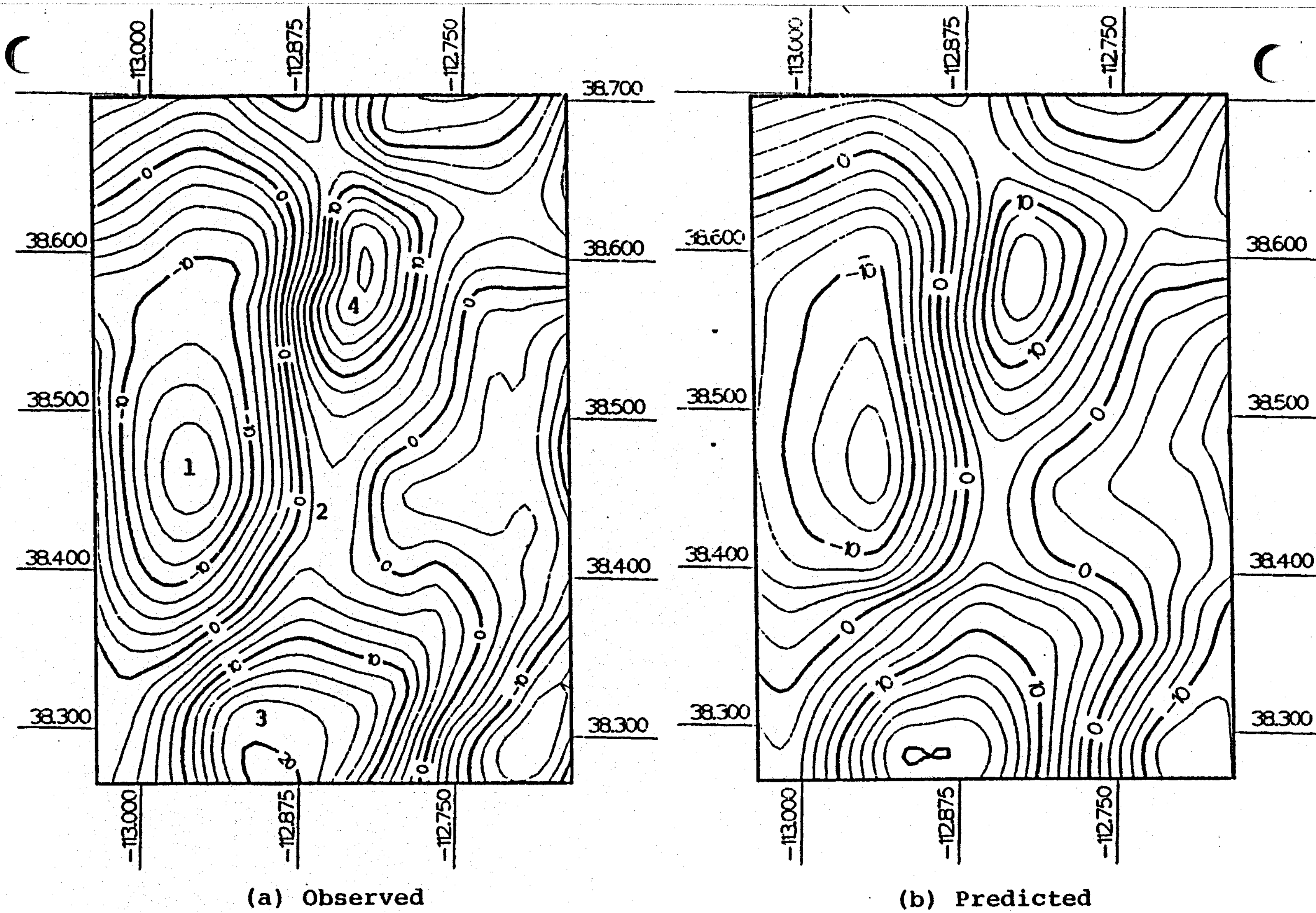

Figure 17. Comparison of observed and predicted gravity data from joint inversion model. Contour interval is 2 mgal.

and the model-predicted data. The data are contoured with a contour interval of 2 mgal. As is obvious the gravity field predicted by the joint inversion model shown in Figure 15 reproduces all of the significant features of the observed field. Of particular note are the Milford Valley gravity low (Number 1 in Figure 17a), the Ranch Canyon gravity saddle (Number 2), the southern Mineral Mountains gravity high (Number 3) and the central Mineral Mountains gravity high (Number 4). These gravity anomalies are identified in the report by Carter and Cook (1978). These patterns are naturally correlated with model features, and we shall discuss them in the framework of model interpretation in the next subsection of this report. Finally, we point out that the r.m.s. misfit to the data is 1.5 mgal.

4.4 DISCUSSION OF MODELING RESULTS

In order to facilitate the discussion of our inversion modeling results we begin this section with a base map of the general model region shown in Figure 18. This map is taken from the study by Robinson and Iyer (1981) and depicts in a simplified manner the major physiographic features of interest in this study. Dominating this region is the Mineral Mountains, a horst composed mainly of Tertiary granitic rocks (10 to 14 m.y. old) and flanked by alluvial valleys typical of the Basin and Range province (Milford Valley and Beaver Valley). Of particular interest in this modeling effort is the Roosevelt Hot Springs geothermal area (the starred symbol in Figure 18) which is located on the western flank of the Mineral Mountains.

The scale of the base map in Figure 18 is equivalent to the scale of all subsequent model plots. This greatly facilitates interpretation of the more robust features in the inversion models.

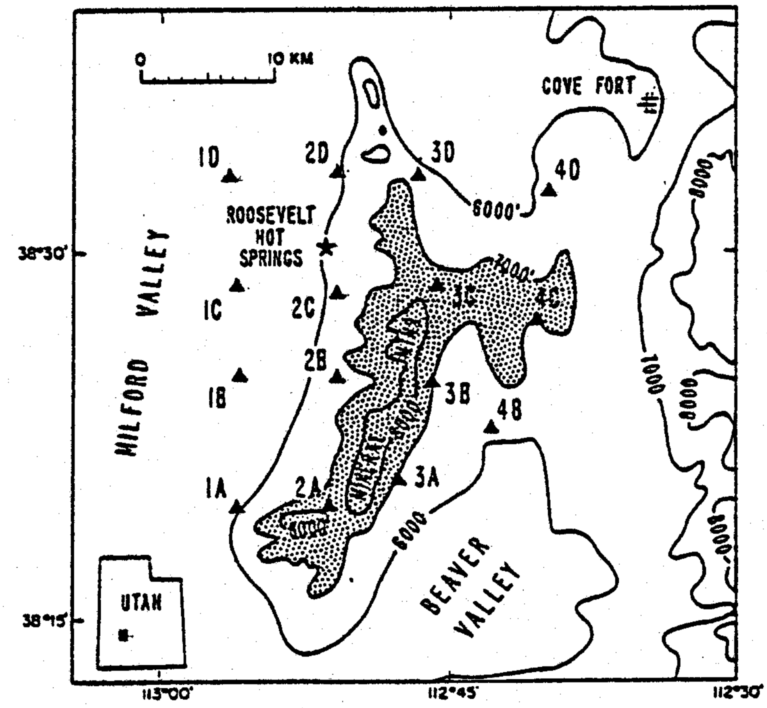

Figure 18. The Mineral Mountains region, southwest Utah. Seismograph stations used in the study by Robinson and Iyer (1981) are shown by triangles. The star indicates the location of the Roosevelt Hot Springs geothermal area. Contour interval is 1000 feet, the shaded region representing the Mineral Mountains. The scale of this map is the same as in Figures 19 through 22.

Before interpreting our model, a few words about resolution are in order. The similarity of the contours in Layers 1, 2 and 3 (Figures 15a, 15b and 15c) suggest that the vertical resolution available from the data in the upper two or three kilometers of the model is relatively poor. Given that Layers 1 and 2 are only 1 km thick, this makes physical sense from the standpoint of both the gravity data, whose horizontal spacing is 3 km, and the travel-times, whose ray paths sample relatively few blocks in Layers 1 and 2. Layer 1, in particular, contains very few horizontal ray paths which intersect two or more blocks. Given the nature of the data, shallow structure in our model may be vertically smeared across Layers 1 and 2 and, to a lesser extent, across Layers 2 and 3 (since some rays do turn in Layer 2; see Figure 7a).

An additional problem with Layer 1 is that the top of this layer is at the approximate mean elevation of the study region (2 km). True ground elevations differ from this datum plane by as much as 500 m, which is half the thickness of Layer 1. Therefore, in addition to modeling geology, Layer 1 has the role of absorbing errors due to elevation corrections made to the seismic data. Of course, such errors have been minimized by our choice of the datum plane. Because of this ambiguity of Layer 1 and the potential problems with depth resolution, we have chosen to ignore this layer in our discussion below.

Vertical resolution may be best in the depth range between Layers 3 and 4. Many rays turn in these layers (Figures 7a, 7b and 7c) and they also contain a large number of earthquake hypocenters (Figures 7c and 7d). Layer 4 is also deep enough to decouple from the highest wavenumber components of the gravity data.

Contour maps of velocity variations in Layers 2 and 3 for the joint inversion model (NDF = 74) and the seismic-only inversion model (NDF = 48) are given in Figures 19 and 20, respectively. (See captions for contour intervals.) The more robust features seen in these layers, particularly in the case of the joint inversion, are the following. A very prominent ridge of high velocities can be seen trending generally northward from the southern limit of the model region between 112.8° and 113°W to as far north as 38.6°N. This ridge is flanked on the west by a narrow zone of steep velocity gradients grading to a pronounced velocity low further to the west.

While these features are probably largely controlled by the terrain-corrected Bouguer gravity data included in the joint inversion (recall the disjoint spatial sampling of the gravity and seismic data in Figure 13 for instance), the local earthquake travel-time data do in fact delineate all three features, especially in Layer 3 (Figure 20, NDF = 48). An interpretation of these model features is taken from a study by Ward, et al. (1978). These authors analyzed a subset of the Bouguer gravity data that we inverted and interpreted the northward-trending gravity contours, with pronounced gradients over the alluvium adjacent to the western margin of the Mineral Mountains as indicating that the mountains are bounded on the west by Basin and Range faults; these faults form the eastern margin of the Milford Valley graben, which is reflected in the gravity low (Figure 17a) along the western portion of this region.

Ward, et al. (1978) further noted two northward-trending, elongate gravity highs extending over the region of interest here and pointed out that the northern gravity high does not coincide with the crest of the Mineral Mountains in this area but rather overlies the western margin of the mountains where granitic rocks are exposed. Referring to our model Layers 2 and 3 in Figures 19 and 20, especially for the joint inversion, we see that the velocity anomalies display a similar behavior;

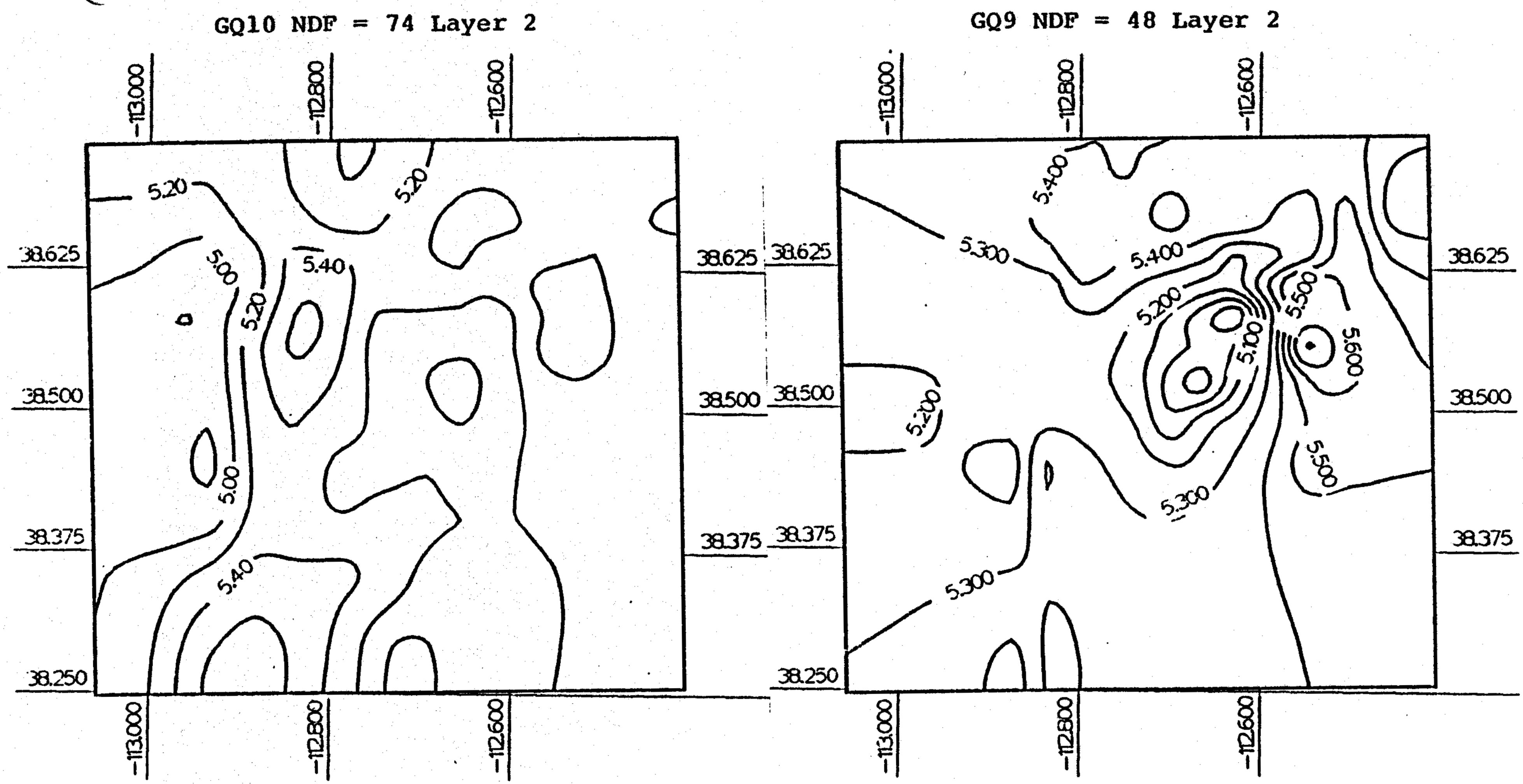

Figure 19. Contour plots of velocity in model Layer 2 of the joint inversion (left) and seismic-only inversion (right). The contour intervals are 0.2 km/s and 0.1 km/s for the joint and seismic-only model layers, respectively.

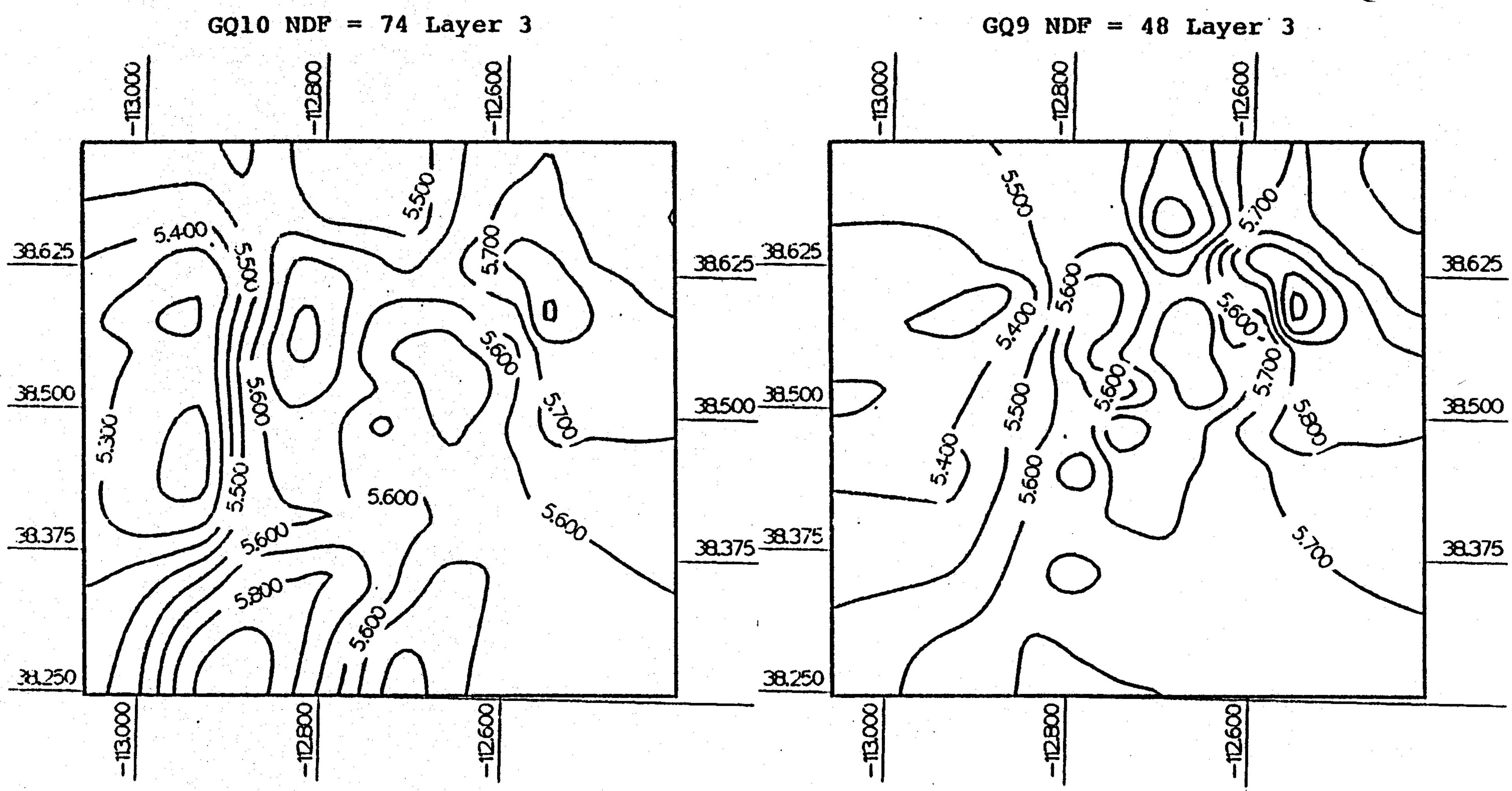

Figure 20. Contour plots of velocity in model Layer 3 of the joint inversion (left) and seismic-only inversion (right). The contour intervals are 0.1 km/s in both plots.

the ridge, with an intervening saddle in the Ranch Canyon area, of high velocity material diverges west of the crest of the mountains going from south to north over the model region.

Additional seismic evidence, supporting the model features in Figures 19 and 20, comes from a study by Robinson and Iyer (1981). These authors inverted teleseismic P-wave travel-times recorded at the stations (solid triangles) depicted in Figure 18 for three-dimensional velocity structure in the crust and upper mantle beneath our general study region. The model obtained by Robinson and Iyer (1981) consisted of four layers extending from 0 to 35 km. The pattern of velocity anomalies determined in their topmost model layer (0 to 5 km) correlates quite well with anomalies in Layers 2 and 3 of our inversion models — and includes the three features discussed above.

The inversion results for the deeper model layers are given in Figures 21 and 22. An extremely interesting feature appears in Layer 4 (Figures 21 and 22), for both the joint and seismic-only inversions, and persists into Layer 5 (Figure 22). The feature of interest is the east-west trending low velocity anomaly centered between approximately 38.45°N and 38.5°N. This anomaly extends beneath the axis of the Mineral Mountains, and, most importantly, underlies the Roosevelt Hot Springs KGRA. Once again, comparing our results with those of Robinson and Iyer (1981) we find that this low velocity anomaly is delineated by the teleseismic travel times between depths of 5 to 25 km, and furthermore is located very nearly in the same place as in our study (i.e., Figure 7b from Robinson and Iyer (1981) shows this anomaly extending beneath the Mineral Mountains just south of 38.5°N).

Robinson and Iyer (1981) stated that their results suggested a pipe-like feature of approximately five to seven

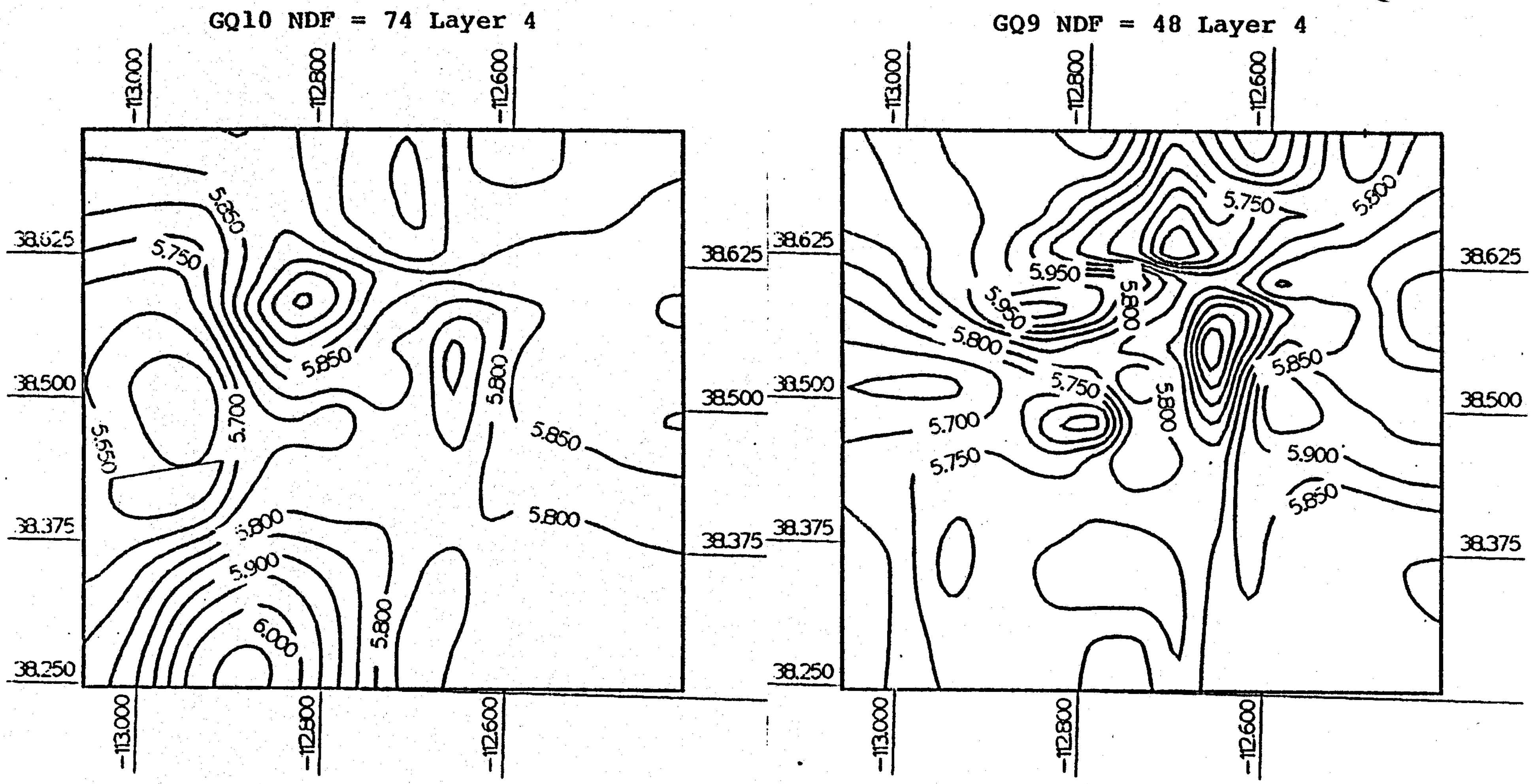

Figure 21. Contour plots of velocity in model Layer 4 of the joint inversion (left) and the seismic-only inversion (right). The contour intervals are 0.05 km/s in both plots.

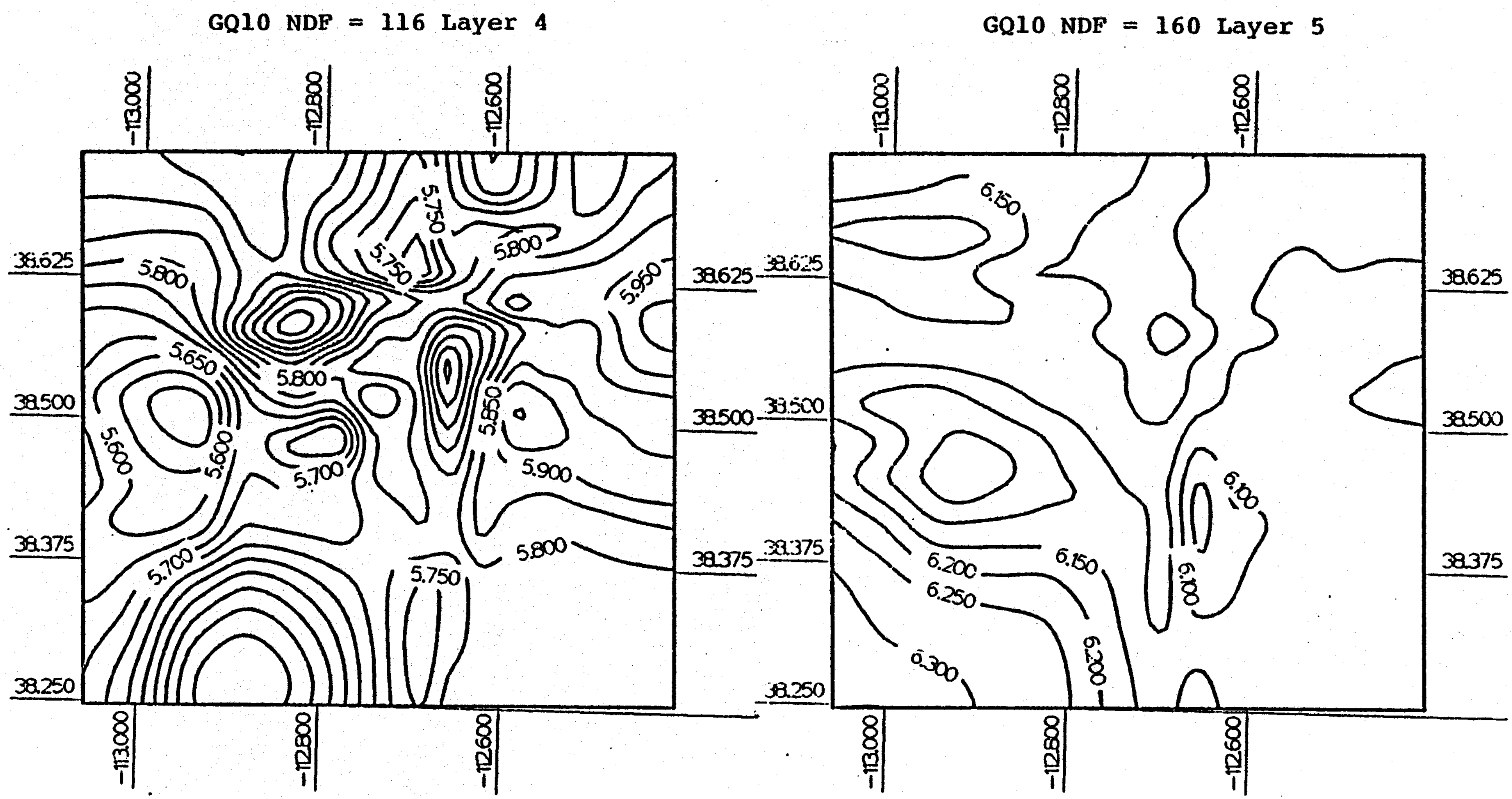

Figure 22. Contour plots of velocity in model Layers 4 (NDF = 116) and 5 (NDF = 160) of the joint inversion. Contour intervals are 0.05 km/s in both plots.

percent velocity contrast extending from about 5 km-depth down at least as far as the uppermost mantle, centered near the Roosevelt Hot Springs geothermal area but extending to the north and south at depth. While our inversion model lacks sufficient resolution in the deepest (i.e., 7 to 26 km) layer (i.e., in terms of defining the depth extent of this anomaly), we note that this low velocity anomaly is well-defined in our Layer 4 (3.5 to 7.0 km) and is thus probably shallower than 5 km.

The similar geological and geophysical picture painted by the various data set considered in this study lends strong support to the joint inversion approach we have described in this report. To a large extent, we were handicapped in this study by the relatively disjoint coverage afforded by the local seismic and gravity data and, in addition, by the poor distribution of seismic events and recording stations, and the small average number of stations recording each event. However, in spite of these circumstances we obtained structure models of considerable merit. Obviously, given a "dedicated" seismic experiment and overlapping gravity coverage, we would expect the joint inversion technique to prove to be a valuable exploration tool.

V. REFERENCES

Aki, K., A. Christoffersson and E. S. Husebye (1977), "Determination of the Three-Dimensional Seismic Structure of the Lithosphere," JGR, 82, pp. 277-296.

Backus, G. and F. Gilbert (1970), "Uniqueness in the Inversion of Inaccurate Gross Earth Data," Phil. Trans. Roy. Soc. (London), Ser. A., 266, pp. 123.

Birch, F. (1961), "The Velocity of Compressional Waves in Rocks to 10 Kilobars, 2," JGR, 66, pp. 2199-2224.

Evoy, J. A. (1978), "Precision Gravity Reobservations and Simultaneous Inversion of Gravity and Seismic Data for Subsurface Structure of Yellowstone," Masters Thesis, University of Utah.

Gertson, R. C. and R. B. Smith (1979), "Interpretation of a Seismic Refraction Profile Across the Roosevelt Hot Springs, Utah and Vicinity," University of Utah, Department of Geology and Geophysics Report IDO/78-1701.a.3 to DOE/DGE, Contract DE-AC07-78ET 28392.

Jordan, T. H. (1973), "Estimation of the Radial Variation of Seismic Velocities and Density in the Earth," Ph.D. Thesis, California Institute of Technology.

Jordan, T. H. (1975), "The Solution of Linear Inverse Problems," Systems, Science and Software Internal Report SSS-IR-75-2590.

Lanczos, C. (1961), Linear Differential Operators, Van Nostrand, New York.

Minster, J. B., J. M. Savino, W. L. Rodi, T. H. Jordan and J. F. Masso (1981), "Three-Dimensional Velocity Structure of the Crust and Upper Mantle Beneath the Nevada Test Site," Systems, Science and Software Final Technical Report submitted to the Advanced Research Projects Agency, SSS-R-81-5138, August.

Olson, T. L. and R. B. Smith (1976), "Earthquake Surveys of the Roosevelt Hot Springs and the Cove Fort Areas, Utah," University of Utah, Department of Geology and Geophysics Final Report to the National Science Foundation, Contract GI-43741.

Pavlis, G. L. and J. R. Booker (1980), "The Mixed Discrete-Continuous Inverse Problem: Application to the Simultaneous Determination of Earthquake Hypocenters and Velocity Structure," JGR, 85, pp. 4801-4810.

V. REFERENCES (continued)

Robinson, R. and H. M. Iyer (1981), "Delineation of a Low-Velocity Body Under the Roosevelt Hot Springs Geothermal Area, Utah, Using Teleseismic P-Wave Data," Geophysics, 46, No. 10, pp. 1456-1466.

Rodi, W. L., T. H. Jordan, J. F. Masso and J. M. Savino (1980a), "Determination of Three-Dimensional Structure of Eastern Washington Based on Inversion of Gravity and Local Earthquake Travel Time Data," Systems, Science and Software Final Report submitted to Weston Geophysical Corporation, SSS-R-80-4431, April.

Rodi, W. L., T. H. Jordan, J. F. Masso and J. M. Savino (1980b), "Determination of Three-Dimensional Structure of Eastern Washington from the Joint Inversion of Gravity and Earthquake Travel Time Data," Systems, Science and Software Final Report submitted to Weston Geophysical Corporation, SSS-R-80-4516, June.

Savino, J. M., W. L. Rodi, R. C. Goff, T. H. Jordan, J. H. Alexander and D. G. Lambert (1977), "Inversion of Combined Geophysical Data for Determination of Structure Beneath the Imperial Valley Geothermal Region," Systems, Science and Software Final Technical Report submitted to the Department of Energy, SSS-R-79-3412, September.

Savino, J. M., W. L. Rodi and J. F. Masso (1979a), "Determination of Three-Dimensional Geophysical and Geological Structure Beneath the Hanford Area of the Central Columbia Plateau," Systems, Science and Software Final Report submitted to Weston Geophysical Corporation, SSS-R-80-4166, September.

Savino, J. M., W. L. Rodi and J. F. Masso (1979), "Determination of Three-Dimensional Geophysical and Geological Structure Beneath the Hanford Area of the Central Columbia Plateau," Systems, Science and Software Interim Report submitted to Weston Geophysical Corporation, SSS-R-80-4300, December.

Spencer, C. and D. Gubbins (1980), "Travel-Time Inversion for Simultaneous Earthquake Location and Velocity Structure Determination in Laterally Varying Media," Geophys. J. R. astr. Soc., 63, pp. 95-116.

Ward, S. H., W. T. Parry, W. P. Nash, W. R. Sill, K. L. Cook, R. B. Smith, D. S. Chapman, F. H. Brown, J. A. Whelan and J. R. Bowman (1978), "A Summary of the Geology, Geochemistry, and Geophysics of the Roosevelt Hot Springs Thermal Area, Utah," Geophysics, 43, No. 7, pp. 1515-1542.

V. REFERENCES (concluded)

Wiggins, R. A. (1972), "The General Linear Inverse Problem: Implication of Surface Waves and Free Oscillations for Earth Structure," Rev. Geophys., 10, pp. 251-285.

APPENDIX A

LISTING OF LOCAL EARTHQUAKE TRAVEL-TIME MODELING PROGRAMS

Program XTP computes local earthquake travel-times for buried sources in a flat-layered one-dimensional velocity model having continuous velocity versus depth and constant velocity gradient in each layer. It is written in ASCII FORTRAN, UNIVAC's version of FORTRAN 77. All input to the program is through NAMELIST reads in the main program (AAMAIN). The program produces printed output and a plot file generated by calls to the DISSPLA graphics library. The program accesses no other tape or disk files. The following program listing is complete except for subroutines in the copyrighted DISSPLA library, which is available from ISSCO, Incorporated, San Diego, California.

```
      FOR    * AAMAIN *

@ELT,LS       XTP.AAMAIN
ELT 8R1-S3C S74Q1C 04/17/82 11:36:40 (19)
      C XTF:
      C
      C  COMPUTE AND PLOT DISTANCE, TRAVELTIME, DELAYTIME, RAYPARAMETER TABLES
      C   FOR MODEL WITH CONTINUOUS VELOCITY AND CONSTANT GRADIENT LAYERS
      C
      C INFUT:
      C
      C   NRTM, ZRTM (1..NRTM), VRTM (1..NRTM) =
      C        VELOCITY-DEPTH MODEL FOR RAYTRACING, ORDERED BY
      C        INCREASING DEPTH (ZRTM(1) IS SURFACE).
      C   NEVT, ZEVT (1..NEVT) = EVENT DEPTHS FOR WHICH TABLES ARE WANTED
      C   VREDUC = VELOCITY FOR REDUCING TRAVELTIMES (T - X/VREDUC)
      C   NTABE = NUMBER OF SAMPLES WANTED IN EMERGING BRANCH TABLES
      C   NTABD = NUMBER OF SAMPLES WANTED IN DIVING BRANCH TABLES
      C   MAXIT = NUMBER OF ITERATIONS ALLOWED FOR FINDING P(X)
      C   LIST = LOGICAL FLAG FOR EXTRA PRINTING
      C   DEBUG = LOGICAL FLAG FOR DEBUG PRINTING
      C   IPRT = PRINT FLAG FOR RAYPATHS
      C        = 0 FOR NO RAYPATHS
      C        > 0 FOR EVERY IPRT'TH RAYPATH
      C   IPLOT = PLOT FLAG
      C         = 0 NO PLOTS
      C         = 1 PRINTER PLOTS
      C         = 2 DISSPLA PLOTS
      C         = 3 BOTH
      C   RUNID = 24 CHARACTER RUN IDENTIFIER
      C
      C RESULTS:
      C
      C   ITABD = INDEX OF FIRST DIVING BRANCH POINT
      C          (EITHER 1 OR 1+NTABD)
      C   NTAB = NUMBER OF TOTAL SAMPLES IN E & D TABLES
      C          (EITHER NTABD OR NTABE+NTABD)
      C   PTAB (1..NTAB) = RAYPARAMETERS
      C   XTAB (1..NTAB) = DISTANCES
      C   TTAB (1..NTAB) = TRAVELTIMES
      C   DTAB (1..NTAB) = DELAY TIMES (TAU)
      C   RTAB (1..NTAB) = REDUCED TIMES (T - X / VREDUC)
      C   NCRIT = NUMBER OF CRITICAL APPARENT VELOCITIES
      C   AVCRIT (1..NCRIT) = CRITICAL APPARENT VELOCITIES
      C   NARR = NUMBER OF ARRIVALS AT DIST
      C   PARR (1..NARR) = RAYPARAMETERS OF ARRIVALS
      C   XARR (1..NARR) = DISTANCES OF ARRIVALS
      C   TARR (1..NARR) = TRAVELTIMES OF ARRIVALS
      C   DXPARR (1..NARR) = DX/DP OF ARRIVALS
      C   AOIARR (1..NARR) = ANGLES OF INCIDENCE OF ARRIVALS
      C   IDVARR (1..NARR) = IDIVE CODES OF ARRIVALS
      C
      C
        INTEGER
       . QRTM,QEVT,QTABE,QTABD,QARR,QDIST,QLAY,QTAB
        PARAMETER
       . QRTM = 31, QEVT = 20, QTABE = 500, QTABD = 500,
       . QARR = 20, QDIST = 101,
       . QLAY = (QRTM+1)/2, QTAB = QTABE + QTABD
        DIMENSION
       . ZRTM(QRTM),VRTM(QRTM),AVCRIT(QRTM), ZEVT(QEVT),
       . HLAY(QLAY),VLAY(QLAY),
       . PTAB(QTAB),XTAB(QTAB),TTAB(QTAB),DTAB(QTAB),RTAB(QTAB),
       . DIST(QDIST), PARR(QARR),
       . XARR(QARR),TARR(QARR),DXPARR(QARR),AOIARR(QARR),IDVARR(QARR)
        CHARACTER
       . H100*100 /' '/, H72*72 /' '/, H24*24 /' '/, RUNID*24 /' '/,
       . PLAB*100 /'RAYPARAMETER (S/KM)$'/, XLAB*100 /'DISTANCE (KM)$'/,
       . TLAB*100 /'TRAVEL TIME (S)$'/, DLAB*100 /'DELAY TIME (S)$'/,
       . RLAB*100,
       . VLAB*100 /'VELOCITY (KM/S)$'/, ZLAB*100 /'DEPTH (KM)$'/
        LOGICAL LIST,DEBUG
      C
      C
        NAMELIST /INPUT/
       . NLAY,HLAY,VLAY, FRACZ,FRACV,
       . VREDUC,NTABE,NTABD,MAXIT, NDIST,DIST,DISERR,
       . NRTM,ZRTM,VRTM,NEVT,ZEVT,LIST,DEBUG,IPRT,IPLOT,RUNID
        NAMELIST /DPLTL/
       .   HLEN,VLEN,
```

```
16            .   VMIN,VMAX,
16            .   ZMIN,ZMAX,
16            .   PMIN,PMAX,
16            .   XMIN,XMAX,
16            .   TMIN,TMAX,
16            .   RMIN,RMAX,
16            .   DMIN,DMAX,
15            .   MARKS
15      C
15      C
15      C READ INPUT & SET UP
15      C
15            RLAB = TLAB
15            CALL S3SET (HLAY,QLAY,-1.)
15            CALL S3SET (VLAY,QLAY,-1.)
15            CALL S3SET (ZRTM,QRTM,-1.)
15            CALL S3SET (VRTM,QRTM,-1.)
15            CALL S3SET (ZEVT,QEVT,-1.)
15            CALL S3SET (DIST,QDIST,-1.)
15            NLAY = 0
15            NRTM = 0
15            NEVT = 1
15            ZEVT(1) = 0.
15            NDIST = 0
15            DISERR = .1
15            VREDUC = 0.
15            NTABE = 50
15            NTABD = 100
15            LIST = .TRUE.
15            DEBUG = .FALSE.
15            IPRT = 0
15            IPLOT = 0
15      C
15            READ (5,INPUT)
15      C
15            CALL FILIST (QLAY,NLAY,HLAY)
15            CALL FILIST (QLAY,NLAY,VLAY)
15            CALL FILIST (QRTM,NRTM,ZRTM)
15            CALL FILIST (QRTM,NRTM,VRTM)
15            CALL FILIST (QEVT,NEVT,ZEVT)
15            CALL FILIST (QDIST,NDIST,DIST)
15      C
15      C INITIALIZE DISSPLA
15      C
15            IF (IPLOT.EQ.2 .OR. IPLOT.EQ.3) THEN
16              HLEN = 9
16              VLEN = 7
16              MARKS = 0
15              READ (5,DPLTL)
15              CALL COMPRS
15              CALL SIMPLX
15              CALL NOCHEK
15              CALL NOBRDR
19              PAGEH = HLEN + 2.
19              PAGEV = VLEN + 2.
15              CALL PAGE(PAGEH,PAGEV)
15              CALL FLATBC
18      C         CALL HWSCAL ('DOWN')
15              CALL INTAXS
15              CALL HEIGHT (.2)
15              IFRAME = 0
15              END IF
15      C
15      C CONVERT LAYERED MODEL TO GRADIENT MODEL, IF NECESSARY
15      C
15            IF (NLAY.GT.0) THEN
15      C
15            NRTM = 2*NLAY
15            DO 20 K = 1,NLAY
15            IF (NLAY.EQ.1) THEN
15              DELV = VLAY(1)
15            ELSE IF (K.EQ.1) THEN
15              DELV = VLAY(2) - VLAY(1)
15            ELSE IF (K.EQ.NLAY) THEN
15              DELV = VLAY(NLAY) - VLAY(NLAY-1)
15            ELSE
15              DELV1 = VLAY(K) - VLAY(K-1)
15              DELV2 = VLAY(K+1) - VLAY(K)
```

```
                IF (DELV1*DELV2.LE.0.) THEN
                  DELV = 0.
                ELSE
                  IF (DELV1.GT.0.) DELV = AMIN1 (DELV1,DELV2)
                  IF (DELV1.LT.0.) DELV = AMAX1 (DELV1,DELV2)
                  END IF
                END IF
              VRTM(2*K-1) = VLAY(K) - FRACV*DELV
              VRTM(2*K)   = VLAY(K) + FRACV*DELV
   20       CONTINUE
C
            ZRTM(1) = 0.
            Z = 0.
            DO 40 K = 1,NLAY-1
            Z = Z + HLAY(K)
            DELZ = AMIN1 (HLAY(K),HLAY(K+1))
            ZRTM(2*K) = Z - FRACZ*DELZ
            ZRTM(2*K+1) = Z + FRACZ*DELZ
   40       CONTINUE
            ZRTM(NRTM) = Z + HLAY(NLAY)
            END IF
C
C PRINT PRELIMINARY INFORMATION
C
            WRITE (6,2100) (L,ZRTM(L),VRTM(L),L=1,NRTM)
 2100       FORMAT ('1RAYTRACING MODEL:'//
           . 1X,'LAYER            DEPTH          VELOCITY'/ (1X,I5,1P2E14.6))
            WRITE (6,2120) NEVT,(ZEVT(I),I=1,NEVT)
 2120       FORMAT (///1X,I4,' EVENT DEPTHS:'/(1X,10G10.3))
C
C DISSPLA PLOT VELOCITY MODEL
C
            IF (IPLOT.EQ.2 .OR. IPLOT.EQ.3) THEN
C
            ENCODE (2400,H100) RUNID
 2400       FORMAT (A24,'$')
C
            CALL TITLE (0,0,ZLAB,100,VLAB,100,HLEN,VLEN)
            CALL HEADIN (H100,100,1.0,1)
            CALL GRACE(0.0)
            CALL YAXANG(0.0)
            CALL GRAF (ZMIN,'SCALE',ZMAX,VMIN,'SCALE',VMAX)
            CALL CURVE (ZRTM,VRTM,NRTM,MARKS)
            IFRAME = IFRAME + 1
            CALL ENDPL (-IFRAME)
            END IF
C
C **** MAIN LOOP OVER EVENT DEPTH **** **** ****
C
            DO 600 IEV = 1,NEVT
C
C GENERATE EMERGING AND DIVING BRANCHES OF X,T,D TABLES
C
            CALL TABXTP
           . (NRTM,ZRTM,VRTM,ZEVT(IEV),NTABE,NTABD,LIST,IPRT,
           .  ITABD,NTAB,PTAB,XTAB,TTAB,DTAB,AVMIN,NCRIT,AVCRIT)
C
C FIND ARRIVALS AT SPECIFIED DISTANCES
C
            IF (NDIST.GT.0) THEN
C
            WRITE (6,2600)
 2600       FORMAT ('1ARRIVALS....'/)
C
            DO 200 IDST = 1,NDIST
C
            CALL GETXTP
           . (NRTM,ZRTM,VRTM, ZEVT(IEV), ITABD,NTAB,PTAB,XTAB,TTAB,AVMIN,
           .  DIST(IDST),DISERR,MAXIT, LIST,DEBUG,
           .  NARR,PARR,XARR,TARR,DXPARR,AOIARR,IDVARR)
C
  200       CONTINUE
            END IF
C
C REDUCE TRAVELTIME TABLES FOR PLOTTING
C
            IF (VREDUC.NE.0.) THEN
              DO 300 I = 1,NTAB
```

```
15   300     RTAB(I) = TTAB(I) - XTAB(I)/VREDUC
15           ENCODE (2700,RLAB) VREDUC
15   2700    FORMAT ('T - X /',F7.3,' (S)S')
15           END IF
15   C
15   C PRINTER PLOT X,T,D TABLES
15   C
15         IF (IPLOT.EQ.1 .OR. IPLOT.EQ.3) THEN
15           ENCODE (2500,H24) RUNID
15   2500    FORMAT (A24)
15           ENCODE (2530,H72) RUNID,ZEVT(IEV),XLAB,PLAB
15   2530    FORMAT (A18,' / EVT DEPTH =',F8.3,' / ',A12,' VS ',A12,1X)
15           CALL  SPLOT (PTAB,XTAB,NTAB,H72,H24,0,NTAB,0,1)
15           ENCODE (2530,H72) RUNID,ZEVT(IEV),TLAB,PLAB
15           CALL  SPLOT (PTAB,TTAB,NTAB,H72,H24,0,NTAB,0,1)
15           ENCODE (2530,H72) RUNID,ZEVT(IEV),DLAB,PLAB
15           CALL  SPLOT (PTAB,DTAB,NTAB,H72,H24,0,NTAB,0,1)
15           ENCODE (2530,H72) RUNID,ZEVT(IEV),RLAB,XLAB
15           CALL  SPLOT (XTAB,RTAB,NTAB,H72,H24,0,NTAB,0,1)
15           END IF
15   C
15   C DISSPLA PLOT X,T,D TABLES
15   C
15         IF (IPLOT.EQ.2 .OR. IPLOT.EQ.3) THEN
15   C
17         ENCODE (2800,H100) ZEVT(IEV),RUNID
18   2800  FORMAT ('EVT DEPTH =',F8.3,' KM  /  ',A24,'S')
15   C
15         CALL TITLE (0,0,PLAB,100,XLAB,100,HLEN,VLEN)
15         CALL HEADIN (H100,100,1.0,1)
15         CALL GRACE(0.0)
15         CALL YAXANG(0.0)
15         CALL GRAF (PMIN,'SCALE',PMAX,XMIN,'SCALE',XMAX)
15         CALL CURVE (PTAB,XTAB,NTAB,MARKS)
15         IFRAME = IFRAME + 1
15         CALL ENDPL (-IFRAME)
15   C
15         CALL TITLE (0,0,PLAB,100,TLAB,100,HLEN,VLEN)
15         CALL HEADIN (H100,100,1.0,1)
15         CALL GRACE(0.0)
15         CALL YAXANG(0.0)
15         CALL GRAF (PMIN,'SCALE',PMAX,TMIN,'SCALE',TMAX)
15         CALL CURVE (PTAB,TTAB,NTAB,MARKS)
15         IFRAME = IFRAME + 1
15         CALL ENDPL (-IFRAME)
15   C
15         CALL TITLE (0,0,PLAB,100,DLAB,100,HLEN,VLEN)
15         CALL HEADIN (H100,100,1.0,1)
15         CALL GRACE(0.0)
15         CALL YAXANG(0.0)
15         CALL GRAF (PMIN,'SCALE',PMAX,DMIN,'SCALE',DMAX)
15         CALL CURVE (PTAB,DTAB,NTAB,MARKS)
15         IFRAME = IFRAME + 1
15         CALL ENDPL (-IFRAME)
15   C
15         CALL TITLE (0,0,XLAB,100,RLAB,100,HLEN,VLEN)
15         CALL HEADIN (H100,100,1.0,1)
15         CALL GRACE(0.0)
15         CALL YAXANG(0.0)
15         CALL GRAF (XMIN,'SCALE',XMAX,RMIN,'SCALE',RMAX)
15         CALL CURVE (XTAB,RTAB,NTAB,MARKS)
15         IFRAME = IFRAME + 1
15         CALL ENDPL (-IFRAME)
15   C
15         END IF
15   C
15   600   CONTINUE
15   C
15   C **** END MAIN LOOP
15   C
15         IF (IPLOT.EQ.2 .OR. IPLOT.EQ.3)
15        *  CALL DONEPL
15         STOP
15         END
```

FOR • FILIST •

```
@ELT,LS     XTP.FILIST
ELT 8R1-S3C S74Q1C 04/17/82 11:36:41 (4)
                     02                   SUBROUTINE  FILIST (M,N,A)
                                          DIMENSION A(M)
                               C
                                          IF (N.LT.1) GO TO 50
                               C
                                          DO 20 I = 1,N
                                          VALUE = A(I)
                                          IF (VALUE.LT.0.) GO TO 30
                     03        C           IF (VALUE.EQ.C.) GO TO 40
                               20         A(I) = VALUE
                               C
                               30         IF (I.GT.1) GO TO 32
                                          A(1) = -VALUE
                                          I = 2
                                          IF (2.GT.N) RETURN
                               32         DO 35 J = I,N
                               35         A(J) = A(J-1) - VALUE
                                          RETURN
                               C
                               40         IF (I.GT.1) GO TO 42
                                          A(1) = 0.
                                          I = 2
                                          IF (2.GT.N) RETURN
                               42         VALUE = A(I-1)
                                          DO 45 J = I,N
                               45         A(J) = VALUE
                                          RETURN
                               C
                     04        50         N = 0
                                          DO 60 I = 1,M
                     04        60         IF (A(I).GE.0.) N = I
                                          RETURN
                               C
                                          END
```

```
@ELT,LS        XTP,GETXTP
ELT 8R1-S3C S74Q1C 04/17/82 11:36:41 (19)
15            SUBROUTINE   GETXTP
15          . (NRTM,ZRTM,VRTM, ZEVT, ITABD,NTAB,PTAB,XTAB,TTAB,AVMIN,
17          .  DIST,DISERR,MAXIT, LIST,DEBUG,
15          .  NARR,PARR,XARR,TARR,DXPARR,AOIARR,IDVARR)
15    C
15    C
15    C FIND THE RAYPARAMETERS AND TRAVELTIMES OF VARIOUS ARRIVALS AT A GIVEN
15    C  DISTANCE.
15    C
15    C ON ENTRY:
15    C
15    C   NRTM, ZRTM (1..NRTM), VRTM (1..NRTM) =
15    C         VELOCITY-DEPTH MODEL FOR RAYTRACING, ORDERED BY
15    C            INCREASING DEPTH (ZRTM(1) IS SURFACE).
15    C   ZEVT = EVENT DEPTH
15    C   ITABD = INDEX OF FIRST POINT IN DIVING BRANCH OF X,T,P TABLES
15    C   NTAB = NUMBER OF POINTS IN X,T,P TABLES
15    C   PTAB (1..NTAB) = TABLE RAYPARAMETERS
15    C   XTAB (1..NTAB) = TABLE DISTANCES
15    C   TTAB (1..NTAB) = TABLE TRAVELTIMES
15    C   AVMIN = MINIMUM APPARENT VELOCITY (HORIZONTAL TAKEOFF)
15    C   DIST = GIVEN EVENT-STATION DISTANCE
15    C   DISERR = ERROR ALLOWED IN DISTANCE (XARR - DIST).
16    C   MAXIT = NUMBER OF ITERATIONS ALLOWED FOR FINDING P(X)
15    C   LIST = PRINT REQUEST (.TRUE. OR .FALSE.)
17    C   DEBUG = DEBUG PRINT REQUEST
15    C
15    C ON RETURN:
15    C
15    C   NARR = NUMBER OF ARRIVALS AT DIST
15    C   PARR (1..NARR) = RAYPARAMETERS OF ARRIVALS
15    C   XARR (1..NARR) = DISTANCES OF ARRIVALS
15    C   TARR (1..NARR) = TRAVELTIMES OF ARRIVALS
15    C   DXPARR (1..NARR) = DX/DP OF ARRIVALS
15    C   AOIARR (1..NARR) = ANGLES OF INCIDENCE OF ARRIVALS
15    C   IDVARR (1..NARR) = IDIVE CODES OF ARRIVALS
15    C
15    C
15            DIMENSION
15          .  ZRTM(NRTM),VRTM(NRTM),
15          .  PTAB(NTAB),XTAB(NTAB),TTAB(NTAB),
15          .  PARR(1),XARR(1),TARR(1),DXPARR(1),AOIARR(1),IDVARR(1)
17            LOGICAL LIST,DEBUG,BRACK
15    C
15    C
15    C **** MAIN LOOP OVER TABLE ENTRIES ****
15    C
15            NARR = 0
15    C
15            DO 500 ITAB = 1,NTAB
15    C
15    C CHECK IF DIST BRACKETED
15    C
15            IF (ITAB.EQ.NTAB) THEN
15              BRACK = XTAB(NTAB).EQ.DIST
15            ELSE
15              BRACK = (DIST.GE.XTAB(ITAB) .AND. DIST.LT.XTAB(ITAB+1))
15          .       .OR. (DIST.LE.XTAB(ITAB) .AND. DIST.GT.XTAB(ITAB+1))
15              END IF
15            IF (.NOT.BRACK) GO TO 500
15    C
15            NARR = NARR + 1
15            PT1 = PTAB(ITAB)
15            PT2 = PTAB(ITAB+1)
15            XT1 = XTAB(ITAB)
15            XT2 = XTAB(ITAB+1)
15            TT1 = TTAB(ITAB)
15            TT2 = TTAB(ITAB+1)
15    C
15            IDV1 = +1
15            IDV2 = +1
15            IF (ITAB.GE.ITABD) IDV1 = -1
15            IF (ITAB+1.GE.ITABD) IDV2 = -1
18    C
18            IF (DEBUG) THEN
18              WRITE (6,3000) NARR,ITAB,PT1,PT2,XT1,XT2,TT1,TT2,IDV1,IDV2
```

```
18   3000    FORMAT ('0++++ GETXTP:  ARRIVAL',I4,' FOUND AFTER TABLE ENTRY',
18         .    I6/ ' PT1,2 XT1,2 TT1,2 IDV1,2 ='/ 5X,3(2E16.9,4X),2I4)
18           END IF
15   C
15   C REFINE BRACKET WITH REGULA-FALSI METHOD
15   C
15         CALL REFINE
17        . (NRTM,ZRTM,VRTM, ZEVT,AVMIN,DIST,DISERR,MAXIT, DEBUG,
15        .  IDV1,IDV2,PT1,PT2,XT1,XT2,TT1,TT2, IERR)
15         IF (IERR.NE.0) THEN
19           WRITE (6,3100) IERR
19   3100    FORMAT ('0???? GETXTP ERROR ???? REFINE RETURNS IERR =',I3/)
15           CALL FTNWB
15           END IF
15   C
15   C PICK FINAL ARRIVAL DATA
15   C
15         IF (ABS(XT1-DIST).LE.ABS(XT2-DIST)) THEN
15           IDVARR(NARR) = IDV1
15           PARR(NARR) = PT1
15           XARR(NARR) = XT1
15           TARR(NARR) = TT1
15         ELSE
15           IDVARR(NARR) = IDV2
15           PARR(NARR) = PT2
15           XARR(NARR) = XT2
15           TARR(NARR) = TT2
15           END IF
15         AOIARR(NARR) = ASIN (PARR(NARR)*VRTM(1))
15         DXPARR(NARR) = 0.
15         IF (IDV1.EQ.IDV2)
15        .  DXPARR(NARR) = (XT2-XT1)/(PT2-PT1)
15   C
15   500   CONTINUE
15   C
15   C **** END MAIN LOOP
15   C
15   C ORCER ARRIVALS IN TRAVELTIME
15   C
15         IF (NARR.GT.1) THEN
15   C
15         DO 600 J = 2,NARR
15         DO 600 I = NARR,J,-1
15         IF (TARR(I).LT.TARR(I-1)) THEN
15           HOLD = PARR(I)
15           PARR(I) = PARR(I-1)
15           PARR(I-1) = HOLD
15           HOLD = XARR(I)
15           XARR(I) = XARR(I-1)
15           XARR(I-1) = HCLC
15           HOLD = TARR(I)
15           TARR(I) = TARR(I-1)
15           TARR(I-1) = HOLD
15           HOLD = DXPARR(I)
15           DXPARR(I) = DXPARR(I-1)
15           CXPARR(I-1) = HCLD
15           HOLD = IDVARR(I)
15           IDVARR(I) = IDVARR(I-1)
15           IDVARR(I-1) = HCLD
15           END IF
15   60C   CONTINUE
15         ENC IF
15   C
15   C PRINT ARRIVAL DATA
15   C
15         IF (LIST.AND.NARR.GT.0) THEN
15   C
15         WRITE (6,2600)
15   2600  FORMAT
15        . ('0        ZEVT       DIST        XARR        TARR       PARR',
15        . '        DARR       DXPARR     AOIARR  IDVARR')
15   C
15         DO 700 I = 1,NARR
15        . DARR = TARR(I) - PARR(I)*XARR(I)
15         AOI = AOIARR(I) * (180./3.141592654)
15         WRITE (6,2640) ZEVT,DIST,
15        .  I,XARR(I),TARR(I),PARR(I),DARR,DXPARR(I),AOI,IDVARR(I)
15   2640  FORMAT (1X,2F1C.3,I4,2F10.3,F10.5,F10.3,E12.4,F10.4,I8)
15   700   CONTINUE
15         ENC IF
15   C
15   800   RETURN
15         END
```

FOR • REFINE •

```
@ELT,LS      XTP.REFINE
ELT 8R1-S3C S74Q1C 04/17/82 11:36:42 (25)
  21              SUBROUTINE  REFINE
  21             . (NRTM,ZRTM,VRTM, ZEVT,AVMIN,DIST,DISERR,MAXIT, DEBUG,
  21             .  IDV1,IDV2,PT1,PT2,XT1,XT2,TT1,TT2, IERR)
  21        C
  21        C
  21        C REFINE A RAYPARAMETER INTERVAL BRACKETING THE RAYPARAMETER
  21        C  BELONGING TO A SPECIFIED DISTANCE, USING REGULA-FALSI ROOT ITERATION
  21        C
  21        C ON ENTRY:
  21        C
  21        C    NRTM, ZRTM (1..NRTM), VRTM (1..NRTM) =
  21        C          VELOCITY-DEPTH MODEL FOR RAYTRACING, ORDERED BY
  21        C          INCREASING DEPTH (ZRTM(1) IS SURFACE).
  21        C    ZEVT = EVENT DEPTH
  21        C    AVMIN = MINIMUM APPARENT VELOCITY (HORIZONTAL TAKEOFF)
  21        C    DIST = DESIRED HORIZONTAL EVENT-STATION DISTANCE
  21        C    DISERR = MAXIMUM DISTANCE-ERROR WANTED
  21        C    MAXIT = MAXIMUM NUMBER OF REFINEMENTS TO MAKE
  21        C    DEBUG = DEBUG PRINT REQUEST (.TRUE. OR .FALSE.)
  21        C    IDV1,2 = DIVING-EMERGING FLAGS BELONGING TO PT1 & PT2
  21        C    PT1,2 = RAYPARAMETERS BRACKETING P(DIST)
  21        C    XT1,2 = DISTANCES BELONGING TO PT1 & PT2
  21        C    TT1,2 = TRAVELTIMES BELONGING TO PT1 & PT2
  21        C
  21        C ON RETURN:
  21        C
  21        C    IDV1,2 = NEW DIVING-EMERGING FLAGS
  21        C    PT1,2 = REFINED RAYPARAMETER BRACKET
  21        C    XT1,2 = DISTANCES BELONGING TO PT1 AND PT2
  21        C    TT1,2 = TRAVELTIMES BELONGING TO PT1 AND PT2
  21        C    IERR = ERROR FLAG (0 NO ERROR, >0 YES ERROR)
  21        C
  21        C
  21              DIMENSION ZRTM(NRTM), VRTM(NRTM)
  21              LOGICAL DEBUG
  21        C
  21        C
  21              IF (DEBUG) THEN
  21                WRITE (6,3100) NRTM,(ZRTM(I),VRTM(I),I=1,NRTM)
  21                WRITE (6,3120) ZEVT,AVMIN,DIST,DISERR,MAXIT
  21        3100    FORMAT ('0++++ REFINE ++++ INPUT ARGUMENTS :'/
  21             .    ' NRTM ZRTM,VRTM(1..NRTM) =',I6/ (1X,5(2E12.6,2X)))
  21        3120    FORMAT (' ZEVT AVMIN DIST DISERR MAXIT =',1X,4E16.9,I8)
  21                END IF
  21        C
  21              IT = 0
  21        C
  21        C DETERMINE DISTANCE ERROR
  21        C
  21        100   DX1 = XT1 - DIST
  21              DX2 = XT2 - DIST
  21              IF (DEBUG) THEN
  21                IF (IT.LT.1) WRITE (6,3000)
  21        3000    FORMAT ('0**** REFINE **** ITERATION DETAILS ****'/
  21             .    1X,T10,'DIST',T27,'XT1',T43,'XT2',T59,'PT1',T75,'PT2',
  21             .    T91,'TT1',T107,'TT2',T118,'IDV1',T126,'IDV2')
  21                WRITE (6,3020) DIST,XT1,XT2,PT1,PT2,TT1,TT2,IDV1,IDV2
  21        3020    FORMAT (1X,7E16.9,2I8)
  21                END IF
  21              IF (DX1*DX2.GT.0.) THEN
  21                IERR = 1
  21                GO TO 950
  21                END IF
  21              ADX = AMIN1 (ABS(DX1),ABS(DX2))
  21        C
  21        C CHECK WHETHER DONE
  21        C
  21              IF (ADX.LE.DISERR) THEN
  21                IERR = 0
  21                RETURN
  21                END IF
  21        C
  21              IF (IT.GE.MAXIT) THEN
  21                IERR = 2
  21                GO TO 950
  21                END IF
```

```
21   C
21   C CALCULATE NEW RAYPARAMETER AND ITS DISTANCE & TIME
21   C
25          IF (ABS(DX1).GT.ABS(DX2)) THEN
25             X1 = (DIST+XT1)/2.
25             X2 = XT2
25          ELSE
25             X1 = XT1
25             X2 = (DIST+XT2)/2.
25             END IF
25          IF (IDV1.EQ.IDV2) THEN
25             IDIVE = IDV1
25             RAYPAR = PT1 + (PT2-PT1) * ((DIST-X1)/(X2-X1))
25             IF (RAYPAR.EQ.PT1 .OR. RAYPAR.EQ.PT2) THEN
25                RAYPAR = (PT1+PT2)/2.
25                IF (RAYPAR.EQ.PT1 .OR. RAYPAR.EQ.PT2) THEN
25                   IERR = 3
25                   GO TO 900
25                   END IF
25                END IF
25          ELSE
25             SN1 = PT1*AVMIN
25             CS1 = -IDV1 * SQRT (1.-SN1**2)
25             SN2 = PT2*AVMIN
25             CS2 = -IDV2 * SQRT (1.-SN2**2)
25             COSE = CS1 + (CS2-CS1) * ((DIST-X1)/(X2-X1))
25             IF (COSE.EQ.CS1 .OR. COSE.EQ.CS2) THEN
25                COSE = (CS1+CS2)/2.
25                END IF
25             EPS = .0001
25             IF (COSE.LT.0.) THEN
25                IDIVE = +1
25                COSE = AMIN1 (-EPS,COSE)
25             ELSE
25                IDIVE = -1
25                COSE = AMAX1 (EPS,COSE)
25                END IF
25             SINE = SQRT (1.-COSE**2)
25             RAYPAR = SINE / AVMIN
25             IF (RAYPAR.EQ.PT1 .OR. RAYPAR.EQ.PT2) THEN
25                IERR = 4
25                GO TO 900
25                END IF
25             END IF
21   C
21          CALL TRACE3
21        . (NRTM,ZRTM,VRTM, IDIVE,ZEVT,RAYPAR,
21        .  NPRAY,XTOT,ZTOT,STOT,TTOT, JERR)
21   C
21          IF (JERR.NE.0) THEN
25             IERR = 5
21             GO TO 900
21             END IF
21          IF ((XTOT.LT.XT1 .AND. XTOT.LT.XT2) .OR.
21        .     (XTOT.GT.XT1 .AND. XTOT.GT.XT2)) THEN
21             WRITE (6,2100) ZEVT,DIST,XTOT,XT1,XT2,PT1,PT2,IDV1,IDV2,IT
22   2100      FORMAT ('0???? REFINE WARNING ???? XTOT OUTSIDE BRACKET'/
21        .     ' ZEVT DIST XTOT XT1,2 PT1,2 IDV1,2 IT ='/
21        .     3X,3E15.8,2(2X,2E15.8),2I4,I8/)
21             END IF
21          IF ((XT1.LT.DIST .AND. XTOT.LE.DIST) .OR.
21        .     (XT1.GT.DIST .AND. XTOT.GE.DIST)) THEN
21             IDV1 = IDIVE
21             PT1 = RAYPAR
21             XT1 = XTOT
21             TT1 = TTOT
21          ELSE
21             IDV2 = IDIVE
21             PT2 = RAYPAR
21             XT2 = XTOT
21             TT2 = TTOT
21             END IF
21   C
21          IT = IT+1
21          GO TO 100
21   C
21   900    WRITE (6,2050) IDIVE,ZEVT,RAYPAR, NPRAY,XTOT,ZTOT,JERR
21   2050   FORMAT ('0???? REFINE ????'/
21        .  ' TRACE3 INPUT:  IDIVE ZEVT RAYPAR =',I6,2E16.9/
21        .  ' TRACE3 OUTPUT: NPRAY,XTOT,ZTOT,JERR =',I6,2E16.9,I6)
21   950    WRITE (6,2000) IERR,IDIVE,ZEVT,DIST,DISERR,MAXIT,IT,
21        .  PT1,PT2,XT1,XT2,TT1,TT2,IDV1,IDV2
21   2000   FORMAT ('0???? REFINE ???? ERROR CODE =',I3/
21        .  'CIDIVE ZEVT DIST DISERR =',I3,3E16.9/
21        .  ' MAXIT IT =',2I4/
21        .  ' PT1,2 XT1,2 TT1,2 IDV1,2 =' / 5X,3(2E16.9,4X),2I4/)
21          RETURN
21          END
```

FOR * RPGEN *

```
BELT,LS     XTP.RPGEN
ELT 8R1-S3C S74Q1C 04/17/82 11:36:43 (33)
29          SUBROUTINE  RPGEN
29         . (NRTM,ZRTM,VRTM,ZEVT,NTABE,NTABD,
29         .  AVMIN,NCRIT,AVCRIT, PTABE,PTABD, IERR)
29    C
29    C
29    C GENERATE ARRAYS OF GOOD RAYPARAMETERS AT WHICH TO
29    C  COMPUTE DISTANCE AND TRAVELTIME TABLES.
29    C
29    C ON ENTRY:
29    C
29    C   NRTM = NUMBER OF POINTS IN RAYTRACING MODEL (1 + NO. LAYERS)
29    C   ZRTM (1..NRTM) = DEPTHS IN RAYTRACING MODEL
29    C   VRTM (1..NRTM) = VELOCITIES IN RAYTRACING MODEL
29    C   ZEVT = DEPTH OF EVENT (SOURCE DEPTH)
29    C   NTABE = NUMBER OF WANTED SAMPLE POINTS IN EMERGING BRANCH
29    C           OF DISTANCE AND TIME VS RAYPARAMETER TABLES
29    C   NTABD = NUMBER OF WANTED SAMPLE POINTS IN DIVING BRANCH OF TABLES
29    C
29    C ON RETURN:
29    C
29    C   AVMIN = MINIMUM APPARENT VELOCITY (HORIZONTAL TAKEOFF)
29    C   NCRIT = NUMBER OF CRITICAL APPARENT VELOCITIES (=< NRTM)
29    C   AVCRIT (1..NCRIT) = CRITICAL APPARENT VELOCITIES
29    C   PTABE (1..NTABE) = RAYPARAMETER ARRAY FOR EMERGING BRANCH
29    C   PTABD (1..NTABD) = RAYPARAMETER ARRAY FOR DIVING BRANCH
29    C   IERR = ERROR FLAG (0 FOR NO ERROR, >0 FOR ERROR)
29    C
29    C
29          DIMENSION
29         . ZRTM(NRTM), VRTM(NRTM), AVCRIT(NRTM), PTABE(NTABE), PTABD(NTABD)
29          DATA  PI /3.141592654/
29    C
29    C FIND MINIMUM APPARENT VELOCITY AND SOURCE (EVENT) LAYER
29    C
29          AVMIN = 0.
29          VBIG = VRTM(1)
29          LGO = 0
29          DO 100 L = 2,NRTM
29          IF (ZRTM(L).GE.ZEVT) THEN
29           IF (LGO.EQ.0) THEN
29            DVDZ = (VRTM(L) - VRTM(L-1)) / (ZRTM(L) - ZRTM(L-1))
29            VEVT = VRTM(L) + DVDZ * (ZEVT - ZRTM(L))
29            AVMIN = AMAX1 (VEVT,VBIG)
29            LGO = L
29            END IF
29           END IF
29    100   VBIG = AMAX1 (VRTM(L),VBIG)
29    C
29          IF (LGO.EQ.0) THEN
29           IERR = 1
29           RETURN
29           END IF
29    C
29    C FIND CAUSTIC AND LVZ-LID APPARENT VELOCITIES
29    C
29          IC = 1
29          AVCRIT(1) = AVMIN
29    C
29          DO 150 L = LGO,NRTM
29          IF (VRTM(L).GT.AVCRIT(IC)) THEN
29           IC = IC + 1
29           AVCRIT(IC) = VRTM(L)
29          ELSE IF (IC.GT.1) THEN
29           IF (AVCRIT(IC).NE.AVCRIT(IC-1)) THEN
29            IC = IC + 1
29            AVCRIT(IC) = AVCRIT(IC-1)
29            END IF
29           END IF
29    150   CONTINUE
29    C
29          IF (AVCRIT(IC).EQ.AVCRIT(IC-1)) IC = IC - 1
29          NCRIT = IC
29          IF (NCRIT.LT.2) THEN
29           IERR = 2
29           RETURN
29           END IF
```

```
29   C
29   C ADJUST CRITICAL VELOCITIES TO AVOID PATHOLOGIES.
29   C  FIND AND FLAG POINTS OF DISCONTINUITY IN DIST AND TIME.
29   C
33         EPS = 1.E-4
29         NDISC = 0
29         AVIM1 = 0.
29         AVI = AVCRIT(1)
29         AVCRIT(1) = (1.-EPS) * AVCRIT(1) + EPS * AVCRIT(2)
29   C
29         DO 200 I = 2,NCRIT
29         AVIM1 = AVI
29         AVI = AVCRIT(I)
29         IF (AVI.EQ.AVIM1) THEN
29           AVCRIT(I) = (1.-EPS) * AVI + EPS * AVCRIT(I+1)
29           AVCRIT(I) = -AVCRIT(I)
29           NDISC = NDISC + 1
29         ELSE
29           AVCRIT(I) = (1.-EPS) * AVI + EPS * AVIM1
29           END IF
29   200   CONTINUE
29   C
29   C CALCULATE ARRAY OF RAYPARAMETERS FOR EMERGING RAYS
29   C
29         IF (NTABE.LT.2) THEN
29          IERR = 3
29          RETURN
29          END IF
29         PTABE(NTABE) = 1. / AVCRIT(1)
29         DANG = PI / (2.*(NTABE-1))
29   C
29         DO 300 I = 1,NTABE-1
29         ANG = (I-1)*DANG
29   300   PTABE(I) = SIN (ANG) / AVCRIT(1)
29   C
29   C CALCULATE ARRAY OF RAYPARAMETERS FOR DIVING RAYS
29   C
29         IF (NTABD.LT.NCRIT) THEN
29          IERR = 4
29          RETURN
29          END IF
29         NPERC = (NTABD-NDISC-1) / (NCRIT-NDISC-1)
29         NXTRA = NTABD-NDISC-1 - NPERC*(NCRIT-NDISC-1)
29         IGO = 1
29         PMIN = 1. / AVCRIT(1)
29         PTABD(1) = PMIN
29   C
29         DO 400 IC = 2,NCRIT
29         PMAX = PMIN
29         PMIN = 1. / AVCRIT(IC)
29         IF (PMIN.LT.0.) THEN
29          PMIN = -PMIN
29          N = 1
29         ELSE
29          IF (NXTRA.GT.0) THEN
29           N = NPERC + 1
29           NXTRA = NXTRA - 1
29          ELSE
29           N = NPERC
29           END IF
29          END IF
29         DP = (PMAX - PMIN) / N
29   C
29         DO 350 I = 1,N
29   350   PTABD(IGO+I) = PMIN + (N-I)*DP
29         IGO = IGO + N
29   400   CONTINUE
29   C
29   C FINAL ERROR CHECK
29   C
29         IF (IGO.NE.NTABD) THEN
29          IERR = 5
29          RETURN
29          END IF
29   C
29         IERR = 0
29         RETURN
29         END
```

FOR • TABXTP •

```
ELT,LS      XTP.TABXTP
ELT 8R1-S3C S74Q1C 04/17/82 11:36:43 (9)
            05              SUBROUTINE TABXTP
            05             . (NRTM,ZRTM,VRTM, ZEVT, NTABE,NTABD, LIST,IPRT,
            05             .  ITABD,NTAB,PTAB,XTAB,TTAB,DTAB, AVMIN,NCRIT,AVCRIT)
            05        C
            05        C  COMPUTE DISTANCE, TRAVELTIME, DELAYTIME, RAYPARAMETER TABLES
            05        C   FOR MODEL WITH CONTINUOUS VELOCITY AND CONSTANT GRADIENT LAYERS
            05        C
            05        C ON ENTRY:
            05        C
            05        C    NRTM, ZRTM (1..NRTM), VRTM (1..NRTM) =
            05        C          VELOCITY-DEPTH MODEL FOR RAYTRACING, ORDERED BY
            05        C          INCREASING DEPTH (ZRTM(1) IS SURFACE).
            05        C    ZEVT = EVENT DEPTH
            05        C    NTABE = NUMBER OF SAMPLES WANTED IN EMERGING BRANCH TABLES
            05        C    NTABD = NUMBER OF SAMPLES WANTED IN DIVING BRANCH TABLES
            07        C    LIST = PRINT REQUEST FLAG
            05        C    IPRT = PRINT FLAG FOR RAYPATHS
            05        C           = 0 FOR NO RAYPATHS
            05        C           > 0 FOR EVERY IPRT'TH RAYPATH
            05        C
            05        C ON RETURN:
            05        C
            05        C    ITABD = INDEX OF FIRST DIVING BRANCH POINT
            05        C           (EITHER 1 OR 1+NTABD)
            05        C    NTAB = NUMBER OF TOTAL SAMPLES IN E & D TABLES
            05        C          (EITHER NTABD OR NTABE+NTABD)
            05        C    PTAB (1..NTAB) = RAYPARAMETERS
            05        C    XTAB (1..NTAB) = DISTANCES
            05        C    TTAB (1..NTAB) = TRAVELTIMES
            05        C    DTAB (1..NTAB) = DELAY TIMES (TAU)
            05        C    AVMIN = MINIMUM APPARENT VELOCITY (HORIZONTAL TAKEOFF)
            05        C    NCRIT = NUMBER OF CRITICAL APPARENT VELOCITIES
            05        C    AVCRIT (1..NCRIT) = CRITICAL APPARENT VELOCITIES
            05        C
            05        C
            05              DIMENSION
            05             . ZRTM(NRTM),VRTM(NRTM),
            05             . PTAB(1),XTAB(1),TTAB(1),DTAB(1), AVCRIT(1)
            05        C
            05              LOGICAL LIST
            05        C
            05        C
            05        C GENERATE ARRAY OF GOOD RAYPARAMETERS
            05        C
            05              CALL  RPGEN
            05             . (NRTM,ZRTM,VRTM,ZEVT,NTABE,NTABD,
            05             .  AVMIN,NCRIT,AVCRIT,PTAB,PTAB(NTABE+1),IERR)
            05              IF (ZEVT.LE.ZRTM(1)) THEN
            05               ITABD = 1
            05               NTAB = NTABD
            05               DO 100 I = 1,NTABD
            05        100    PTAB(I) = PTAB(NTABE+I)
            05              ELSE
            05               ITABD = NTABE + 1
            05               NTAB = NTABE + NTABD
            05               END IF
            05        C
            05              IF (LIST) THEN
            05        C
            05              WRITE (6,230C) ZEVT
            09        2300  FOFMAT ('1**** **** EVENT DEPTH =',1PE12.5)
            05              WRITE (6,232C) NCRIT,(AVCRIT(I),I=1,NCRIT)
            05        2320  FOFMAT ('0',I4,' CRITICAL APPARENT VELOCITIES:'//
            05             .    (1X,1P1CG13.3))
            05              WRITE (6,2340) NTAB
            05        2340  FORMAT ('0',I5,' GENERATED RAY PARAMETERS:'/)
            09              NPERLN = 8
            05              NLINES = MAXC (1+(NTAB-1)/NPERLN, 20)
            C5              DO 120 J = 1,NLINES
            05        120   WRITE (6,236C) (PTAB(I),I=J,NTAB,NLINES)
            09        2360  FOFMAT (1X,1P8E16.8)
            05              IF (IERR.NE.C) THEN
            08                WRITE (6,3100) IERR
            08        3100    FORMAT ('0???? TABXTP ERROR ???? RPGEN RETURNS IERR =',I3/)
            08                CALL FTNWB
            08                END IF
```

FOR   * TABXTP *

```
08      C
05            WRITE (6,2210)
05      2210  FORMAT ('0       RAY PARAM    APPAR VEL    DISTANCE   TRAVELTIME',
05          . '   DELAY TIME   NPRAY'/)
05            END IF
05      C
05      C GENERATE EMERGING AND DIVING BRANCHES OF X,T,D TABLES
05      C
05            DO 200 I = 1,NTAB
05      C
05            IF (I.LT.ITABD) THEN
05              IDIVE = +1
05            ELSE
05              IDIVE = -1
05              END IF
05            CALL   TRACE3
05          . (XRTM,ZRTM,VRTM,IDIVE,ZEVT,PTAB(I),
05          .   NPRAY,XTOT,ZTOT,STOT,TTOT, IERR)
05            IF (IERR.NE.0) THEN
08              WRITE (6,3200) IERR
08      3200    FORMAT ('0???? TABXTP ERROR ???? TRACE3 RETURNS IERR =',I3/)
08              CALL FTNWB
08              END IF
05            XTAB(I) = XTOT
05            TTAB(I) = TTOT
05            DTAB(I) = TTAB(I) - PTAB(I) * XTAB(I)
05      C
05      C PRINT X,T,D & MAYBE RAYPATH
05      C
05            IF (LIST) THEN
05            AV = 1./PTAB(I)
05            WRITE (6,2220) I,PTAB(I),AV,XTAB(I),TTAB(I),DTAB(I),NPRAY, ZEVT
09      2220  FORMAT (1X,I4,1P5E12.5,I7, T101,'ZEVT =',1PE12.5)
05            END IF
05      C
05      200   CONTINUE
05      C
05            RETURN
05            END
```

FOR * TRACE3 *

```
@ELT,LS     XTP.TRACE3
ELT 8R1-S3C S74Q1C 04/17/82 11:36:46 (8)
      04              SUBROUTINE  TRACE3
      04            . (NRTM,ZRTM,VRTM, IDIVE,ZEVT,RAYPAR,
      06            .  NPRAY,XTOT,ZTOT,STOT,TTOT, IERR)
      04      C
      04      C
      04      C       WRITTEN 2-18-80 BY W. L. RODI
      04      C
      04      C TRACE A RAY FROM A STATION AT SURFACE (Z=0.) TO AN EVENT AT
      04      C  DEPTH ZEVT THROUGH A ONE-D VELOCITY MODEL
      04      C  HAVING CONTINUCUS VELOCITY WITH CONSTANT GRADIENT LAYERS.
      04      C
      04      C INPUT:
      04      C
      04      C    NRTM = NUMBER OF POINTS IN RAYTRACING MODEL (1 + NO. LAYERS)
      04      C    ZRTM (1..NRTM) = DEPTHS IN RAYTRACING MODEL
      04      C    VRTM (1..NRTM) = VELOCITIES IN RAYTRACING MODEL
      04      C    IDIVE = CODE INDICATING WHETHER RAY IS DIVING OR EMERGING
      04      C          = +1, EMERGING (TAKEOFF ANGLE > 90)
      04      C          =  0, TAKEOFF ANGLE = 90
      04      C          = -1, DIVING (TAKEOFF ANGLE < 90)
      04      C    ZEVT = DEPTH OF EVENT
      04      C    RAYPAR = RAY PARAMETER (INVERSE OF APPARENT VELOCITY)
      04      C
      04      C OUTPUT:
      04      C
      04      C    NPRAY = NO. OF POINTS IN TRACED PATH (NO. OF SEGMENTS + 1)
      04      C    XTOT = HORIZONTAL DISTANCE OF ENDING POINT OF RAY
      04      C    ZTOT = DEPTH OF ENDING POINT OF RAY
      04      C    STOT = TOTAL LENGTH OF RAY
      04      C    TTOT = TOTAL TRAVEL TIME ALONG RAY
      04      C    IERR = ERROR FLAG
      04      C         = 0, NO ERROR
      07      C         > 0, ERROR
      05      C
      05      C       TELESEISMIC RAYS ARE SIMULATED (DEFINED) BY ...
      05      C       1) IDIVE = +1   AND   2) ZEVT  >  ZRTM(NRTM)
      04      C
      04      C
      04              DIMENSION ZRTM(NRTM),VRTM(NRTM)
      04              LOGICAL ERROR
      08              DATA PI /3.141592654/, EPS /1.E-4/
      04      C
      04      C
      04      C        PRINT *,'TRACE3 ARGS = ' ,NRTM,ZRTM,VRTM, IDIVE,ZEVT,RAYPAR
      04      C
      04              CALL TRACE4
      04            . (NRTM,ZRTM,VRTM, 0.,0.,ZEVT, RAYPAR,
      04            .  NPRAY,XTOT,ZTOT,STOT,TTOT, ISTAT)
      04      C
      04              ERROR = ISTAT.LE.-1
      04            .     .OR. (ISTAT.EQ.0 .AND. ZEVT.GT.0.0)
      04            .     .OR. (ISTAT.EQ.2 .AND. IDIVE.LE.0)
      07              IF (ERROR) THEN
      07                IERR = 1
      07                GO TO 90
      07                END IF
      08              ZERR = ZTOT - ZEVT
      08              ERROR = ISTAT.EQ.3 .AND. ABS(ZERR).GT.EPS*ZEVT
      08              IF (ERROR) THEN
      08                IERR = 2
      08                GO TO 90
      08                END IF
      04      C
      04              IF (ISTAT.GT.1) GO TO 60
      04              IF (ISTAT.EQ.1 .AND. IDIVE.GE.0) GO TO 60
      04      C
      04              ERROR = (ISTAT.EQ.0.AND.IDIVE.GE.0) .OR. ZEVT.GE.ZRTM(NRTM)
      07              IF (ERROR) THEN
      08                IERR = 3
      07                GO TO 90
      07                END IF
      08      C
      04              NPRAY1 = NPRAY
      04      C
      04              CALL TRACE4
      04            . (NRTM,ZRTM,VRTM, 0.,ZTOT,ZRTM(NRTM), RAYPAR,
```

```
04              .  NPRAY2,XTOT2,ZTOT2,STOT2,TTOT2, ISTAT)
04        C
04              NPRAY = NPRAY1 + NPRAY2 - 1
04              ERROR = ISTAT.NE.1
07              IF (ERROR) THEN
08                IERR = 4
07                GO TO 90
07                END IF
04        C
04              NPRAY = NPRAY1 + 2*(NPRAY2 - 1)
04              XTOT = XTOT + 2.*XTOT2
04              STOT = STOT + 2.*STOT2
04              TTOT = TTOT + 2.*TTOT2
04              ZTOT = ZTOT2
04        C
04        60    IERR = 0
04              RETURN
04        C
07        90    PRINT *, '*TRACE3* ERROR : IERR,ISTAT,IDIVE,ZEVT,RAYPAR,NPRAY = '
07              PRINT *, IERR,ISTAT,IDIVE,ZEVT,RAYPAR,NPRAY
04        C
04              RETURN
04              END
```

FOR * TRACE4 *

```
@ELT,LS        XTP.TRACE4
ELT 8R1-S3C S74Q1C 04/17/82 11:36:47 (5)
         01              SUBROUTINE  TRACE4
         01             . (NRTM,ZRTM,VRTM, X1,Z1,Z2,RAYPAR,
         01             .  NPRAY,XTOT,ZTOT,STOT,TTOT, ISTAT)
         01        C
         01        C
         01        C     WRITTEN 2-16-80 BY W. L. RODI
         01        C
         01        C TRACE A RAY FROM DEPTH Z1 TO Z2 THROUGH A ONE-D VELOCITY MODEL
         01        C  HAVING CONTINUOUS VELOCITY WITH CONSTANT GRADIENT LAYERS.
         01        C
         01        C INPUT:
         01        C
         01        C   NRTM = NUMBER OF POINTS IN RAYTRACING MODEL (1 + NO. LAYERS)
         01        C   ZRTM (1..NRTM) = DEPTHS IN RAYTRACING MODEL
         01        C   VRTM (1..NRTM) = VELOCITIES IN RAYTRACING MODEL
         01        C   X1 = HORIZONTAL DISTANCE OF STARTING POINT OF RAY
         01        C   Z1 = DEPTH OF STARTING POINT OF RAY
         01        C   Z2 = DEPTH TO TRACE TO, UNLESS RAY TURNS SHALLOWER (Z2 >= Z1)
         01        C   RAYPAR = RAY PARAMETER (INVERSE OF APPARENT VELOCITY)
         01        C
         01        C OUTPUT:
         01        C
         01        C   NPRAY = NO. OF POINTS IN TRACED PATH (NO. OF SEGMENTS + 1)
         01        C   XTOT = HORIZONTAL DISTANCE OF ENDING POINT OF RAY
         01        C   ZTOT = DEPTH OF ENDING POINT OF RAY
         01        C   STOT = TOTAL LENGTH OF RAY
         01        C   TTOT = TOTAL TRAVEL TIME ALONG RAY
         01        C   ISTAT = STATUS FLAG
         01        C         = -1, INVALID INPUT
         01        C         =  0, TRIVIAL RAY (Z1=Z2 OR VRTM(Z1)=1./RAYPAR)
         01        C         =  1, RAY TRACED TO Z2
         01        C         =  2, RAY HITS BOTTOM OF MODEL (EQUIV. TO Z2 = ZRTM(NRTM))
         01        C         =  3, RAY TURNS AT OR ABOVE Z2
         01        C
         01        C
         01              DIMENSION ZRTM(NRTM),VRTM(NRTM)
         01              LOGICAL  LINEAR, HOMOG, INIT
         05              DATA  EPS1 /1.E-5/, EPS2 /1.E-5/
         03              DATA  ZB,VB,SNB,CSB,TFACB,ANGB /6*0./
         01        C
         01              ISTAT = -1
         01              NPRAY = 1
         01              XTOT = X1
         01              ZTOT = Z1
         01              STOT = 0.
         01              TTOT = 0.
         01        C
         01              IF (Z1.GT.Z2 .OR. Z1.LT.ZRTM(1) .OR. Z1.GE.ZRTM(NRTM)) GO TO 91
         01              IF (RAYPAR.LT.0.) GO TO 91
         01              NM1 = NRTM - 1
         01              INIT = .FALSE.
         01        C
         01        C MAIN LOOP OVER LAYERS
         01        C
         01              DO 60 L = 1,NM1
         01        C
         01              ZBOT = ZRTM(L+1)
         01              IF (Z1.GE.ZBOT) GO TO 60
         01              VBOT = VRTM(L+1)
         01              DVDZ = (VRTM(L) - VBOT) / (ZRTM(L) - ZBOT)
         01              IF (INIT) THEN
         01                ZA = ZB
         01                VA = VB
         01                SNA = SNB
         01                CSA = CSB
         01                TFACA = TFACB
         03                ANGA = ANGB
         01              ELSE
         01                INIT = .TRUE.
         01                ZA = Z1
         01                VA = VBOT + DVDZ * (ZA - ZBOT)
         01                SNA = RAYPAR * VA
         01                IF (SNA.GT.1.) GO TO 91
         01                CSA = SQRT (1. - SNA**2)
         01                TFACA = (1. + CSA) / VA
         01                ANGA = ASIN (SNA)
```

```
            IF (SNA.EC.1.) THEN
             IF (DVDZ.EQ.0.) GO TO 91
             IF (DVDZ.GT.0.) GO TO 92
             END IF
            IF (Z1.EQ.Z2) GO TO 92
            END IF
C
      NPRAY = NPRAY + 1
      ZB = AMIN1 (ZBOT,Z2)
      VB = VBOT + DVDZ * (ZB - ZBOT)
      SNB = RAYPAR * VB
      IF (SNB.GE.1.) THEN
       ISTAT = 3
       VB = 1./RAYPAR
       ZB = ZBOT + (VB - VBOT) / DVDZ
       SNB = 1.
       END IF
      CSB = SQRT (1. - SNB**2)
      TFACB = (1. + CSB) / VB
C
      LINEAR = ABS (SNB-SNA) .LT. EPS1*CSB
      IF (LINEAR) THEN
       SNB = SNA
       CSB = CSA
       ANGB = ANGA
       DZ = ZB - ZA
       DS = DZ / CSA
       DX = DS * SNA
       HOMOG = ABS (VB-VA) .LT. EPS2*VB
       IF (HOMOG) THEN
        DT = DS / VA
       ELSE
        DT = ALOG (TFACA/TFACB) / DVDZ
        END IF
      ELSE
       ANGB = ASIN (SNB)
       CRV = DVDZ * RAYPAR
       RADIUS = 1. / CRV
       DX = RADIUS * (CSA - CSB)
       DS = RADIUS * (ANGB - ANGA)
       DT = ALOG (TFACA/TFACB) / DVDZ
       END IF
C
      XTOT = XTOT + DX
      STOT = STOT + DS
      TTOT = TTOT + DT
      ZTOT = ZB
      IF (ISTAT.EQ.3) GC TO 80
      IF (ZB.GE.Z2) THEN
       ISTAT = 1
       GO TO 80
       END IF
C
60    CONTINUE
C
C ENC MAIN LOOP
C
      IF (.NOT.INIT) GO TO 91
      ISTAT = 2
80    RETURN
C
91    ISTAT = -1
      RETURN
C
92    ISTAT = 0
      RETURN
C
C      PPINT *,'TRACE4 RETURNED, ARGS  .. X1,Z1,Z2,RAYPAR =',
C     .  X1,Z1,Z2,RAYPAR
C      PRINT *, 'NPRAY,XTOT,ZTOT,STOT,TTOT,ISTAT=',
C     .  NPRAY,XTOT,ZTOT,STOT,TTOT, ISTAT
C      RETURN
      END
```

```
FOR   * XTSET *

@ELT,LS      XTP.XTSET
ELT 8R1-S3C S74Q1C 04/17/82 11:36:47 (0)
      SUBROUTINE XTSET (NTAB,XTAB,TTAB,XMIN,XMAX, NPLOT,XPLOT,TPLOT)
C
C SET UP PLOT ARRAYS OF DISTANCE (X) AND TRAVELTIME (T) FROM
C  DISTANCE-TRAVELTIME TABLES.  INCLUDE ONLY POINTS WITH DISTANCES
C  BETWEEN XMIN AND XMAX.
C
      DIMENSION XTAB(NTAB),TTAB(NTAB), XPLOT(1),TPLOT(1)
C
      NPLOT = 0
      IF (NTAB.LT.1) RETURN
C
      DO 100 I = 1,NTAB
      IF (XTAB(I).GE.XMIN .AND. XTAB(I).LE.XMAX) THEN
        NPLOT = NPLOT + 1
        XPLOT(NPLOT) = XTAB(I)
        TPLOT(NPLOT) = TTAB(I)
        END IF
100   CONTINUE
C
      RETURN
      END
```

APPENDIX B

VELOCITY PERTURBATIONS IN FINAL JOINT INVERSION MODEL (NDF = 74)

Figures B.1 through B.5 show the velocity perturbations in each grid cell of the final joint inversion model. The number in a cell is δv in units of 0.01 km/s. Both outer grid and inner grid can be compared with corresponding figures in the text.

-113.000 -112.800 -112.600 -112.400

38.750 38.625 38.500 38.375 38.250

−7	−5	−4	−4	−7	−9	−5	−2	3	6	9	11	12	13	10
−10	−4	−4	12	−13	−36	−33	−15	9	15	16	15	14	8	8
−15	−13	−23	4	−3	−23	−15	3	30	33	25	21	19	−1	7
−19	−26	−42	−13	24	18	5	15	33	21	20	23	16	6	7
−22	−39	−51	−10	47	32	2	10	21	9	12	17	15	9	7
−23	−45	−48	9	55	30	−11	−3	−3	−2	2	17	15	10	7
−22	−39	−42	22	51	23	−16	−11	−14	−12	3	28	15	10	7
−20	−34	−42	19	32	12	−14	−11	−24	−15	−3	9	10	9	7
−21	−36	−46	14	18	−1	−14	−22	−35	−21	−10	0	4	5	5
−21	−35	−49	13	9	−21	−19	−9	−28	−19	−10	−3	1	3	3
−22	−36	−32	15	7	−8	−2	−2	−11	−11	−8	0	−1	0	1
−23	−30	−4	22	16	19	9	−12	−24	−17	−12	−7	−4	−2	−1
−23	−28	33	42	30	4	−35	−35	−7	−8	−7	−6	−5	−4	−3
−17	−11	6	9	5	−2	−10	−11	−9	−8	−7	−7	−6	−5	−4

38.750 38.625 38.500 38.375 38.250

-113.000 -112.800 -112.600 -112.400

Figure B.1. Model Layer 1 (0 - 1 km).

−113.000 −112.800 −112.600 −112.400

Latitude labels (left and right edges): 38.750, 38.625, 38.500, 38.375, 38.250

−17	−16	−16	−16	−18	−19	−15	−18	−13	−9	−5	−2	2	−3	−6
−19	−17	−17	−7	−23	−39	−36	−22	−8	−4	−3	−3	−4	−14	−10
−22	−26	−34	−14	−13	−25	−21	−5	5	5	0	−3	0	−20	−11
−26	−37	−50	−25	5	1	−9	−2	3	−7	−7	−2	0	−11	−10
−29	−46	−57	−25	13	9	−12	−10	−7	−14	−6	7	2	−7	−9
−30	−50	−56	−13	23	7	−22	−24	−27	−36	−19	5	2	−5	−8
−28	−45	−53	−4	22	2	−27	−33	−36	−33	−17	10	2	−4	−7
−26	−47	−54	−7	9	−5	−26	−38	−50	−35	−20	−4	−2	−3	−7
−24	−50	−60	−12	−1	−14	−24	−30	−40	−32	−21	−11	−7	−6	−7
−23	−51	−62	−14	−6	−25	−25	−22	−31	−27	−19	−8	−9	−9	−9
−24	−50	−50	−14	−14	−20	−14	−14	−21	−22	−19	−14	−13	−12	−11
−25	−35	−13	7	5	3	−8	−25	−33	−28	−24	−20	−17	−15	−13
−28	−28	19	28	12	−8	−38	−42	−26	−23	−22	−20	−18	−17	−15
−24	−19	−5	−3	−9	−17	−23	−24	−22	−21	−20	−19	−18	−17	−16

−113.000 −112.800 −112.600 −112.400

Figure B.2. Model Layer 2 (1 - 2 km).

Longitude: −113.000, −112.800, −112.600, −112.400

Latitude: 38.750, 38.625, 38.500, 38 375, 38.250

−5	−5	−5	−4	−5	−5	−6	−8	−4	0	3	7	8	7	6
−6	−7	−7	0	−9	−18	−19	−15	−3	5	9	11	6	3	5
−9	−15	−21	−6	−3	−10	−12	−13	0	8	16	13	8	2	6
−12	−24	−33	−12	9	7	1	−2	7	16	22	22	10	6	7
−13	−30	−39	−6	14	15	4	2	5	10	14	29	18	9	8
−14	−33	−40	−8	19	15	−2	−7	−7	2	5	30	20	13	9
−12	−29	−37	−2	21	14	−6	−13	−14	−8	−2	15	17	15	9
−9	−31	−38	−2	14	9	0	−9	−19	−13	−1	12	14	16	9
−6	−33	−42	−5	6	2	−11	−7	−12	−6	3	12	11	11	7
−4	−34	−43	−6	3	1	−5	−2	−7	−6	−1	6	6	7	5
−5	−33	−35	−4	−1	0	2	1	−2	−4	−3	0	2	3	4
−6	−18	−1	17	20	20	8	−6	−12	−10	−7	−4	−2	0	1
−11	−8	27	34	23	7	−14	−20	−12	−9	−7	−5	−4	−2	−1
−9	−5	7	7	1	−8	−14	−13	−9	−6	−5	−4	−4	−3	−2

Figure B.3. Model Layer 3 (2.0 - 3.5 km).

−113.000 −112.800 −112.600 −112.400

38.750 38.625 38.500 38.375 38.250

13	13	13	14	12	8	5	4	6	7	8	9	9	9	10
11	10	12	14	11	6	1	0	8	13	13	10	7	9	10
9	4	4	13	13	6	1	0	7	7	7	7	9	11	11
6	−1	0	11	17	12	5	1	7	9	11	12	12	13	12
4	−6	−2	14	25	23	15	11	11	12	14	13	13	14	12
4	−9	−4	18	29	23	11	7	2	3	7	12	12	15	12
4	−11	−10	10	21	14	7	3	−5	1	9	11	12	14	12
5	−14	−17	2	11	8	9	3	−5	4	12	13	11	11	11
7.	−13	−18	−2	0	−3	4	3	−3	4	11	12	11	10	11
8	−12	−15	−1	1	1	4	4	1	5	7	8	10	11	11
8	−11	−9	2	4	3	4	4	2	6	5	5	6	7	8
5	−3	10	18	17	12	7	0	−1	2	2	3	4	4	5
1	5	26	30	26	16	4	−3	0	2	3	3	4	4	4
1	7	16	16	13	9	5	5	5	4	4	4	4	4	4

Figure B.4. Model Layer 4 (3.5 - 7.0 km).

Longitude: −113.000, −112.800, −112.600, −112.400

Latitude: 38.750, 38.625, 38.500, 38.375, 38.250

9	8	8	8	8	7	8	8	9	9	10	10	10	10	10
8	7	8	8	9	9	9	10	11	11	11	10	10	10	10
6	5	5	7	9	10	11	11	11	11	11	10	10	10	9
6	4	5	8	10	11	11	11	11	11	10	10	10	9	9
6	4	5	8	10	11	12	12	11	11	10	10	9	9	9
6	4	5	8	10	11	12	12	11	10	10	9	8	8	8
6	3	4	7	10	11	11	11	10	9	9	8	8	8	8
7	2	3	6	9	10	10	10	9	8	8	8	8	8	7
8	3	2	4	7	8	9	9	7	7	7	7	7	7	7
8	3	2	4	6	7	8	8	6	6	6	6	6	6	6
9	6	5	7	8	8	8	7	5	6	5	5	5	5	6
10	9	10	11	12	10	8	7	5	5	5	5	5	5	5
11	12	14	15	14	12	9	7	6	5	5	5	5	5	5
10	12	14	14	13	11	9	8	7	6	6	5	5	5	4

Figure B.5. Model Layer 5 (7.0 - 26.0 km).